Vol. 57 MAY, 1953 No. 5

THE JOURNAL OF PHYSICAL CHEMISTRY

(Registered in U. S. Patent Office)

Founded by Wilder D. Bancroft

WILDER DWIGHT BANCROFT

1867–1953

FOUNDER OF THE JOURNAL OF PHYSICAL CHEMISTRY

EDITOR, 1896–1932

PRESIDENT OF THE AMERICAN CHEMICAL SOCIETY, 1910

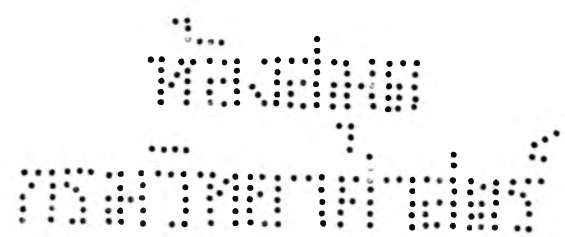

Founded by Wilder D. Bancroft

THE JOURNAL OF PHYSICAL CHEMISTRY

(Registered in U. S. Patent Office)

Published monthly (except July, August and September) by the American Chemical Society at 20th and Northampton Sts., Easton, Pa.

Entered as second-class matter at the Post Office at Easton, Pennsylvania.

The *Journal of Physical Chemistry* is devoted to the publication of selected symposia in the broad field of physical chemistry and to other contributed papers.

Manuscripts originating in the British Isles, Europe and Africa should be sent to F. C. Tompkins, The Faraday Society, 6 Gray's Inn Square, London W. C. 1, England.

Manuscripts originating elsewhere should be sent to W. Albert Noyes, Jr., Department of Chemistry, University of Rochester, Rochester 3, N. Y.

Correspondence regarding accepted copy, proofs and reprints should be directed to Assistant Editor, Allen D. Bliss, Department of Chemistry, Simmons College, 300 The Fenway, Boston 15, Mass.

Business Office: American Chemical Society, 1155 Sixteenth St., N. W., Washington 6, D. C.

Advertising Office: American Chemical Society, 332 West 42nd St., New York 36, N. Y.

Articles must be submitted in duplicate, typed and double spaced. They should have at the beginning a brief Abstract, in no case exceeding 300 words. Original drawings should accompany the manuscript. Lettering at the sides of graphs (black on white or blue) may be pencilled in, and will be typeset. Figures and tables should be held to a minimum consistent with adequate presentation of information. Photographs will not be printed on glossy paper except by special arrangement. All footnotes and references to the literature should be numbered consecutively and placed on the manuscript at the proper places. Initials of authors referred to in citations should be given. Nomenclature should conform to that used in *Chemical Abstracts*, mathematical characters marked for italic, Greek letters carefully made or annotated, and subscripts and superscripts clearly shown. Articles should be written as briefly as possible consistent with clarity and should avoid historical background unnecessary for specialists.

Symposium papers should be sent in all cases to Secretaries of Divisions sponsoring the symposium, who will be responsible for their transmittal to the Editor. The Secretary of the Division by agreement with the Editor will specify a time after which symposium papers cannot be accepted. The Editor reserves the right to refuse to publish symposium articles, for valid scientific reasons. Each symposium paper may not exceed four printed pages (about sixteen double spaced typewritten pages) in length except by prior arrangement with the Editor.

Remittances and orders for subscriptions and for single copies, notices of changes of address and new professional connections, and claims for missing numbers should be sent to the American Chemical Society, 1155 Sixteenth St., N. W., Washington 6, D. C. Changes of address for the *Journal of Physical Chemistry* must be received on or before the 30th of the preceding month.

Claims for missing numbers will not be allowed (1) if received more than sixty days from date of issue (because of delivery hazards, no claims can be honored from subscribers in Central Europe, Asia, or Pacific Islands other than Hawaii), (2) if loss was due to failure of notice of change of address to be received before the date specified in the preceding paragraph, or (3) if the reason for the claim is "missing from files."

Subscription Rates: to members of the American Chemical Society, $8.00 for 1 year, $15.00 for 2 years, $22.00 for 3 years; to nonmembers, $10.00 for 1 year, $18.00 for 2 years, $26.00 for 3 years. Postage free to countries in the Pan American Union; Canada, $0.40; all other countries, $1.20. Single copies, $1.25; foreign postage, $0.15; Canadian postage, $0.05.

The American Chemical Society and the Editors of the *Journal of Physical Chemistry* assume no responsibility for the statements and opinions advanced by contributors to THIS JOURNAL.

The American Chemical Society also publishes *Journal of the American Chemical Society, Chemical Abstracts, Industrial and Engineering Chemistry, Chemical and Engineering News, Analytical Chemistry*, and *Journal of Agricultural and Food Chemistry*. Rates on request.

SYMPOSIUM ON NUCLEAR AND PARAMAGNETIC RESONANCE, ATLANTIC CITY, N. J., SEPTEMBER, 1952

WILDER DWIGHT BANCROFT

1867–1953

FOUNDER OF THE "JOURNAL OF PHYSICAL CHEMISTRY"

EDITOR, 1896–1932

PRESIDENT OF THE AMERICAN CHEMICAL SOCIETY, 1910

THE JOURNAL OF PHYSICAL CHEMISTRY

(Registered in U. S. Patent Office) (Copyright, 1953, by the American Chemical Society)

Founded by Wilder D. Bancroft

VOLUME 57 MAY 21, 1953 NUMBER 5

ELECTRON DISTRIBUTION IN MOLECULES. II. PROTON AND FLUORINE MAGNETIC RESONANCE SHIFTS IN THE HALOMETHANES[1]

BY L. H. MEYER[2] AND H. S. GUTOWSKY

Contribution from the Noyes Chemical Laboratory, University of Illinois, Urbana, Illinois

Received January 19, 1953

Experimental chemical shifts in the proton and fluorine magnetic resonances are reported for the simple halomethanes and the chlorofluoromethanes. An analysis of the shifts and their relation to other electron-dependent parameters, such as bond distance and chlorine quadrupole coupling, demonstrates qualitatively the importance of both ionic and double-bonded electron distributions in these compounds. The electron distributions in the halomethanes are related to the electronic effects of the halogens as substituents in benzene. The proton and fluorine resonances in the fluoromethanes were multiplets, the structure arising from indirect coupling of the nuclear spins by the valence electrons. Fluorine chemical shifts were measured in a number of substituted fluorobenzenes, including the *o*-, *m*- and *p*-benzaldehydes, benzyl and benzal chlorides; the corresponding Hammett σ-values, estimated from the chemical shifts, are given.

Introduction

The basic aspects of nuclear magnetic resonance absorption have been reviewed in some preceding papers.[3] The principle underlying the present research is that the magnetic field at a nucleus is in general not the same as that in the bulk sample, the difference arising from interactions between the applied field and the motions of the electrons in the sample.[4] Explicitly, $H_0 = H_b(1 - \chi_s)$, where H_0 is the field at the nucleus; H_b, that in the bulk sample; and $H_b\chi_s$ is an internal diamagnetism, or a nuclear magnetic shielding field. Differences in electronic environment cause easily measurable differences in χ_s for a magnetic nucleus in different substances or even in structurally non-equivalent positions in the same molecule.

These differences are often called "chemical shifts" because they reflect the chemical state of the system. They are measured conveniently at a fixed resonance frequency as $\delta = 10^5 \times (H_r - H_c)/H_r$, where H_r is the applied magnetic field for the given nuclear resonance in some parent, reference compound, and H_c is the resonance field for the compound in question. Thus δ is a quantitative measure of the differences in the electron distribution about the nuclei in the two compounds. But, unfortunately, the complexity of the effect restricts theoretical calculations[4] and the interpretation of experimental data is in terms of simplified, qualitative concepts.

In the first paper[5] of this series it was shown that chemical shifts in the magnetic shielding of fluorine nuclei in substituted fluorobenzenes could be used to analyze the effects of the substituents upon the electron distribution in the benzene ring. In this article, similar data are reported for the fluorine and proton resonances in many of the halogen substituted methanes. Multiplet resonance lines of the type described elsewhere[6] were observed in the fluoromethanes. In addition, some further chemical shifts data are given for the fluorine resonances in substituted fluorobenzenes.

Experimental

Apparatus and Procedure.—In these experiments, the apparatus and procedure were somewhat different from the previous work.[5] A detailed description of the changes is

(1) Supported in part by ONR.

(2) AEC Predoctoral Fellow.

(3) Some earlier reviews have been given under the title "Nuclear Moments" in "Annual Reviews of Nuclear Science," Annual Reviews, Inc., Stanford, Calif., N. F. Ramsey, Vol. 1, 1952, p. 97; B. T. Feld, Vol. 2, 1953, p. 239. See also G. E. Pake, *Am. J. Phys.*, **18**, 438, 473 (1950).

(4) N. F. Ramsey, *Phys. Rev.*, **78**, 699 (1950); *ibid.*, **86**, 243 (1952).

(5) H. S. Gutowsky, D. W. McCall, B. R. McGarvey and L. H. Meyer, *J. Am. Chem. Soc.*, **74**, 4809 (1952). Prior work is cited there in detail.

(6) H. S. Gutowsky, D. W. McCall and C. P. Slichter, *J. Chem. Phys.*, **21**, 279 (1953).

being published.[7] Improved resolution, which was essential for measuring the proton shifts, was obtained mainly by using smaller samples. The magnetic field was that of a permanent magnet of about 4180 gauss. In the experiments, a direct observation is made of the difference required in the applied magnetic field for the resonance, at fixed frequency, in the compound and in some reference. For ease of comparison, a different reference was chosen within each class of compound investigated. Each of these class references has been established on a general scale with an arbitrarily chosen primary reference, trifluoroacetic acid for fluorine and distilled water for the proton. All measurements were made on samples in the liquid state, usually at room temperature except for low boiling gases which were condensed in a simple cryostat.[7] Solids were dissolved in solvents of similar chemical constitution.

Materials.—Highly purified samples are not required for this type of measurement; the only critical factor is that there be no question about the identity of the constituent giving the measured resonance line. In most cases, commercial materials were used, without purification. The fluorobenzaldehydes, benzyl chlorides, and benzal chlorides were purchased from Custom Chemical Laboratories; the methyl fluoride from Beta Research Laboratory, Chicago, Illinois; the methyl chloride from Ohio Chemical and Surgical Equipment Co.; and the methyl bromide and methane from The Matheson Company, Inc. The methylene chloride, bromide and iodide, the bromoform and methyl iodide were purchased from Eastman Kodak Company; the chloroform from Merck and Company; and the iodoform from Mallinckrodt Chemical Works. The remainder of the compounds were donated by the Jackson Laboratory, E. I. du Pont de Nemours and Company.

Results and Discussion

A. Substituted Benzene Derivatives.—In Table I there are listed fluorine δ-values for a number of substituted fluorobenzenes, referred to fluorobenzene.[8] In the previous research,[5] a comparison of the observed δ-values with the corresponding Hammett[9] σ-constants for about thirty other substituents gave separate linear least squares relations for meta and for para substituents[10]: $\sigma_m = 1.69\,\delta_m$ and $\sigma_p = 0.560\,\delta_p + 0.271$. It was concluded that the separate curves are a direct demonstration of the different character of the principal mechanism by which substituents affect the electron distribution at the meta and at the para positions. The relations themselves are of use in predicting σ-values from δ-values and thereby estimating the effect of the substituent on chemical reactivity, *via* the Hammett σρ method.[9]

The prediction of σ from δ is an attractive procedure since a δ-value can be obtained in less than a half hour with an operating high resolution spectrometer, while the evaluation of σ by the usual kinetic or equilibrium study is a much longer process. So, σ-values have been computed from the δ-values for substituents for which no direct σ-values are available. These include several of the substituents examined earlier[5] as well as most of those reported now. The σ-values predicted are included in Table I.

Some of the δ-values in Table I are particularly interesting. From chemical evidence, the aldehyde group, CHO, is classed usually as a +E substituent in the effects ascribed to the resonance or electromeric mechanism. Previously,[5] an intercomparison of the *o*-, *m*- and *p* δ-values of different substituents confirmed their division into +E and −E classes. A similar comparison of the δ-values for CHO places it in the +E class, which includes those substituents with π-electrons on the atom attached to the benzene ring. The δ-values for CH_2Cl and $CHCl_2$ and those reported before for CH_3 and CCl_3 show an interesting intermediate character going toward +E in the sequence $CH_3, \ldots, CCl_3$. This seems reasonable since the greater electronegativity of Cl compared to H would make electron distributions of the form $^+\phi{=}C{=}Cl_3^-$ more stable than $^+\phi{=}C{=}H_3^-$.

TABLE I

δ-VALUES AND PREDICTED σ-VALUES FOR MONOSUBSTITUTED BENZENE DERIVATIVES

Substituent	δ_F	σ_{pred}	Substituent[a]	δ_F	σ_{pred}
o-CHO	−0.96	...	*m*-NHCOCH₃	+0.10	+0.17
m-CHO	+0.10	+0.17[b]	*p*-NHCOCH₃	−0.57	−0.05
p-CHO	+0.98	+0.82[b]	*p*-SO_2Cl	+1.26	+0.98
o-CH_2Cl	−0.54	...	*p*-CCl_3	+0.26	+0.42
m-CH_2Cl	+0.02	+0.03	*m*-O—C_6H_4—F(p)	−0.05	−0.08
p-CH_2Cl	−0.07	+0.23	*p*-O—C_6H_4—F(p)	−0.67	−0.10
o-$CHCl_2$	−0.51	...	*p*-NH—C_6H_5	−0.94	−0.26
m-$CHCl_2$	+0.14	+0.24	*m*-CH(OH)CH_3	0.00	0.00
p-$CHCl_2$	+0.25	+0.41			

[a] δ-values in this column are taken from ref. 5. [b] In ref. 7, p. 188, experimental σ-values of +0.381 and +1.126, respectively, are reported for *m*- and *p*-CHO. The poor agreement with the predicted σ-values is typical of +E substituents.

B. Halogen Substituted Methanes.—In Table II there are listed the δ_H and δ_F-values for the simple halomethanes, and also the δ_F-values for the chlorofluoromethanes. The proton δ-values are given with respect to methane and the fluorine with respect to carbon tetrafluoride.[11] The proton and fluorine resonances in the fluoromethanes exhibited a fine structure of the electron nuclear-spin-coupling type[6]; these results are given and discussed in the second section following. Also included in Table II are the chlorine quadrupole coupling constants[12] of the chloromethanes and chlorofluoromethanes, and the available more precisely known C–H and C–F bond distances in the various halomethanes. All of these parameters have magnitudes determined in one way or another by the electron distribution in the molecule. Interrelations are to be expected, therefore, and comparisons of the various parameters in homologous series should be valuable in assessing the nature of the corresponding changes in electron distribution.

Proton and Fluorine Chemical Shifts.—Figure 1 presents graphically the dependence of the δ_H-values upon the extent of halogenation in the halomethanes; and Fig. 2, that of δ_F in the fluoro- and chlorofluoromethanes. In Fig. 1 it is seen that δ_H increases quite uniformly in the series CH_4, CH_3X, CH_2X_2 and CHX_3 for each of the halogens F,

(7) H. S. Gutowsky, L. H. Meyer and R. C. McClure, *Rev. Sci. Instruments*, **24**, in press (1953).

(8) Fluorobenzene has a δ_F-value of −3.56 referred to trifluoroacetic acid.

(9) L. P. Hammett, "Physical Organic Chemistry," 1st Ed., McGraw-Hill Book Co., Inc., New York, N. Y., 1940.

(10) The σ-values are not defined ordinarily for ortho substituents because steric as well as electronic factors can affect reaction rates at the ortho position.

(11) Methane has a δ_H-value of −0.94 referred to distilled water, and carbon tetrafluoride a δ_F-value of +1.24 referred to trifluoroacetic acid.

(12) A review of quadrupole spectroscopy and discussions of current work were given at the symposium by B. P. Dailey, THIS JOURNAL, **57**, 490 (1953), and in the two papers following it.

TABLE II

δ-VALUES FOR HYDROGEN AND FLUORINE IN HALOMETHANES

Compound	δ_H	δ_F	$\lvert eqQ \rvert_{av}$-(Cl^{35}),[c] Mc.	d_{C-H}, Å.	a_{C-F}, Å.
CH_4	0.00	...			
CH_3F	+0.71	−21.00		1.109[d]	1.385[d]
CH_2F_2	+0.88	− 8.09[b]		1.092[e]	1.358[e]
CHF_3	+1.03	− 1.82[b]		1.098[f]	1.332[f]
CF_4	...	0.00[b]			1.322[g]
CH_3Cl	+0.71		68.40	1.109[h]	
CH_2Cl_2	+0.99		72.47	1.068[i]	
$CHCl_3$	+1.18		76.98	1.073[f]	
CCl_4	...		81.85		
CH_3Br	+0.73			1.104[h]	
CH_2Br_2	+1.01				
$CHBr_3$	+1.24			1.068[j]	
CH_3I	+0.75			1.100[h]	
CH_2I_2	+0.99				
CHI_3[a]	+0.65				
CF_3Cl		+ 3.68	77.58		1.323[k]
CF_2Cl_2		+ 6.04	78.16		
$CFCl_3$		+ 7.67	79.63		

[a] In CCl_4 solution. [b] Approximate values for these compounds were reported by H. S. Gutowsky and C. J. Hoffman, *Phys. Rev.*, **80**, 110 (1950). [c] R. Livingston, This Journal, **57**, 496 (1953). [d] O. R. Gilliam, H. D. Edwards and W. Gordy, *Phys. Rev.*, **75**, 1014 (1949). [e] D. R. Lide, *J. Am. Chem. Soc.*, **74**, 3548 (1952). [f] S. N. Ghosh, R. Trambarulo and W. Gordy, *J. Chem. Phys.*, **20**, 605 (1952). [g] L. O. Brockway, private communication. This is a recent electron diffraction result; C–F distances determined in the other fluoromethanes are in good agreement with the microwave results. [h] W. Gordy, J. W. Simmons and A. G. Smith, *Phys. Rev.*, **74**, 243 (1948). [i] R. J. Meyers and W. D. Gwinn, *J. Chem. Phys.*, **20**, 1420 (1952). [j] Q. Williams, J. T. Cox and W. Gordy, *ibid.*, **20**, 1524 (1952). [k] D. K. Coles and R. H. Hughes, *Phys. Rev.*, **76**, 858 (1949).

Cl and Br, with relatively much smaller increases in δ_H for a given type of molecule in the sequence F, Cl and Br. Of the iodides, methyl iodide is "normal"; the δ_H-value in methylene iodide is somewhat small compared to the other methylene halides; and the iodoform δ_H-value is even lower than that of methyl iodide. The fact that the δ_H-values are pretty nearly the same for all halides of a given molecular type, as for example CH_3X, suggests that the changes associated with halogenation are not caused in a simple manner by electronegativity differences, but the effects of the latter are balanced partially by an opposing mechanism.

Similarly complex results were found for the proton resonance shifts in the binary covalent hydrides[13] and for the fluorine resonance shifts in the halogen substituted fluorobenzenes.[5] In the hydrogen halides δ_H increased[14] in the sequence HI, HBr, HCl and HF, with HI anomalously low. The bare proton has the largest δ-value, so this trend may be ascribed to increasing ionic character of the H–X bond. But as one goes from the group 7 to the group 4 hydrides, the dependence reverses. Thus δ_H for CH_4 is less than for SiH_4 even though carbon is more electronegative than silicon, suggesting that bond hybridization as well as ionic

(13) H. S. Gutowsky and C. J. Hoffman, *J. Chem. Phys.*, **19**, 1259 (1951).

(14) The original data are given in terms of magnetic shielding of the proton, referred to the bare proton as the scale zero; the δ-scale used here reverses the sign.

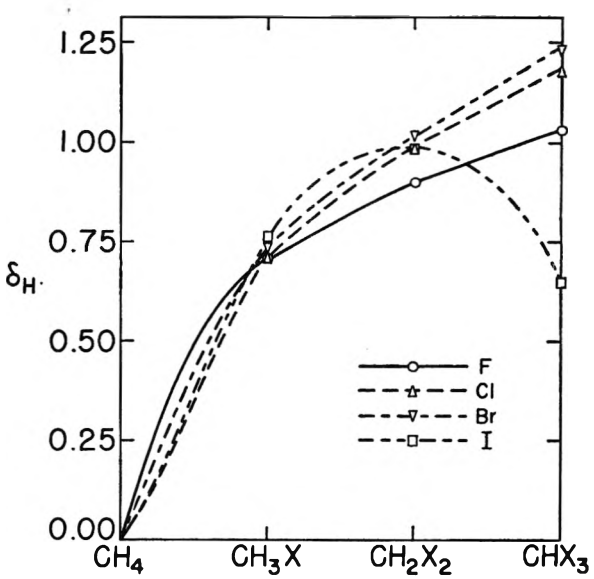

Fig. 1.—The dependence of the proton magnetic resonance shift upon extent of halogenation in the simple halomethanes.

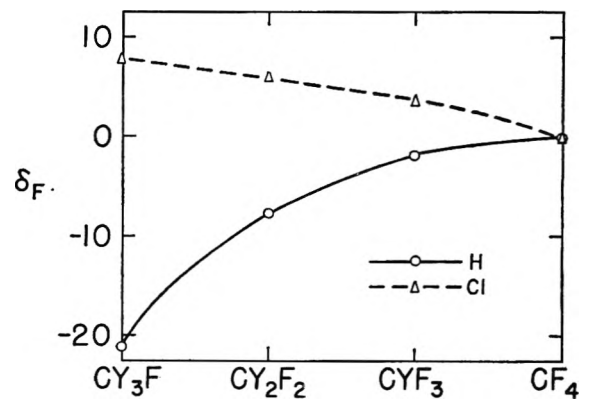

Fig. 2.—The dependence of the fluorine magnetic resonance shift upon extent of halogenation in the fluoromethanes and chlorofluoromethanes.

character may be important. However, most of the trends in δ_H for the halomethanes in Fig. 1 can be interpreted qualitatively as changes in the ionic character of the C–H bond, though admittedly the situation is more complex.

Remembering that increased ionic character increases δ_H, the general increase in δ_H upon successive halogenation reflects the increasing inductive effect of the halogen atoms in removing electrons from about the less electronegative protons. Or stated another way, the electron distribution in the halides incorporates larger fractions of ionic forms, as shown below, than does that in methane

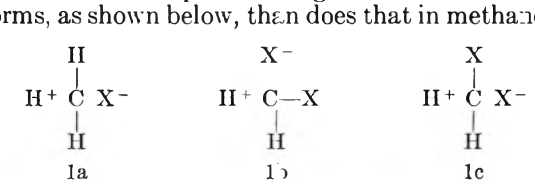

Following this argument, one would expect δ_H for a given type of molecule to follow the electronegativity order, *i.e.*, F > Cl > Br > I. In reality, just the opposite is observed, except for methylene iodide and iodoform as mentioned above.

The substituent effects of the halides in benzene

have a similar reversal from predictions based on electronegativities alone.[5] The mechanism invoked there is suggested by double bonded structures of the type

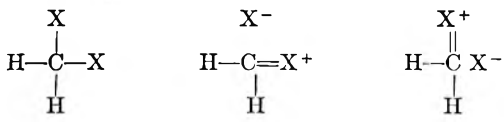

2a 2b 2c

This "electromeric" or resonance effect opposes the inductive effect, making the carbon more eletropositive and reducing δ_H; moreover, the order of importance is F > Cl > Br > I, as the larger atoms form multiple bonds less readily.[5] With the inductive and "electromeric" effects in opposition but with magnitudes depending upon the halogens in the same order, the actual sequence of resultant effect is constructed readily.

The carry-over of this relatively simple interpretation from one class of compounds to a rather different class is encouraging. However, the anomalous results for the iodomethanes emphasize the complexity of the problem. The fact that methyl iodide follows the trends of the other halomethanes while the methylene iodide and iodoform have low δ_H-values suggest the difference may lie in the comparatively large size of the iodine atom. Some internal consistency prevails inasmuch as the δ_H-value for HI is low compared to the other hydrogen halides.

The inductive and double-bond structures introduced in discussion of the δ_H-values should apply also to the δ_F-values shown in Fig. 2 for the fluoromethanes and chlorofluoromethanes. The δ_F-value is small for the fluoride ion and increases quite linearly with increasing covalent character.[13] Formulas 1 and 2 suggest that successive fluorination of methane would introduce competition between the fluorines for the electrons from a decreasing number of hydrogens. This would reduce the ionic character of the C–F bonds and increase the δ_F-values, as is indeed observed.

The double-bond mechanism is essential in explaining the continued increase of δ_F on proceeding from CF_4 to $CFCl_3$ by successive substitution of chlorine for fluorine. If only inductive effects were important then, since Cl is more electronegative than H but less than F, δ_F for $CFCl_3$ should be between CFH_3 and CFF_3, whereas it is found to be the largest of both series. Introducing the double-bond structures below, form 3a is more important than 3b, for chlorine forms a double bond less readily than does fluorine.[5]

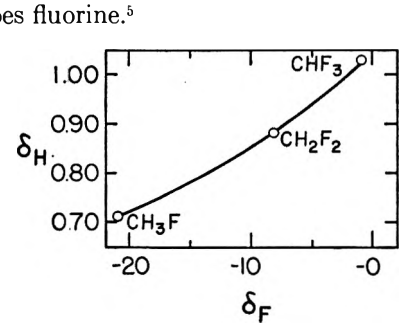

Fig. 3.—The interdependence of the proton and fluorine magnetic resonance shifts in the fluoromethanes.

3a 3b

In the simple halomethanes, the inductive effect was more important than the double-bonding; however, the electronegativity of chlorine is considerably larger than that of hydrogen, so the double-bond effect could be greater than the inductive in the chlorofluoromethanes. The net result would then be the C–F bonds becoming less ionic in the sequence CH_3F ... CF_4 ... $CFCl_3$, as shown by the observed increase in the corresponding δ_F-values.

The interdependence of the C–H and C–F bond characters in the fluoromethanes is shown graphically in Fig. 3, where the δ_F-values are plotted against the δ_H-values for the same compound. Both δ_H and δ_F increase in the sequence CH_3F, CH_2F_2 and CHF_3 indicating the ionic character of the C–H bond increases as that of the C–F bond decreases. This is to be expected, for an inductive change in one part of the molecule would require balancing by an opposite effect in another part of the molecule.

Multiplet Lines in the Fluoromethanes.—Table III gives the structure and splittings of the multiplet proton and fluorine resonance lines in the fluoromethanes. In Fig. 4 are oscilloscope photographs of the typical proton and fluorine triplets in CH_2F_2. These multiplets arise from an indirect coupling of the fluorine and proton nuclear spins by the valence electrons; the results agree in detail with the analysis of similar multiplets in a number of inorganic phosphorus and fluorine compounds.[6] The coupled H and F nuclei are not directly bonded, so the magnitudes of the splittings are determined by the nature of both the C–H and C–F bonds. The spin coupling depends primarily upon the p-character of the bonds; the ionic struc-

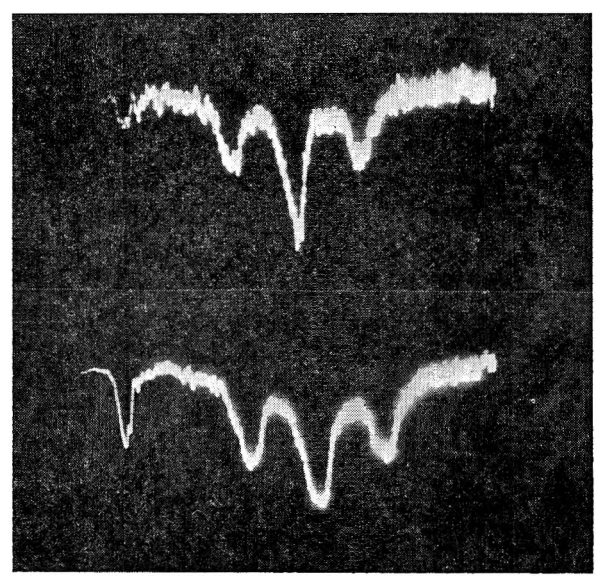

Fig. 4.—Oscilloscope photographs of the triplet proton (top) and fluorine (bottom) magnetic resonance lines in liquid CH_2F_2. The splitting of the proton line is 11.3 milligauss and that of the fluorine 13.2. The sweep amplitude is 75 milligauss for both lines.

tures and s-electrons are unimportant in this case. But since the net effect observed comes from both bonds, no conclusions can be drawn regarding either one, in spite of the systematic increase in the splitting upon successive substitution of fluorine. The results do suggest, however, that the preparation of C^{13}-concentrated halomethanes and the observation of the C^{13}–H and C^{13}–F coupling would be profitable.

TABLE III

MULTIPLET RESONANCES IN THE FLUOROMETHANES

Compound	Proton resonance: Structure[a]	Proton resonance: Splitting, mgauss	Fluorine resonance: Structure[a]	Fluorine resonance: Splitting, mgauss	H^1 Splitting[b]/F^{19} Splitting
CH_3F	(1–1)	9.5	(1–3–3–1)	11.0	0.865
CH_2F_2	(1–2–1)	11.4	(1–2–1)	13.2	0.865
CHF_3	(1–3–3–1)	18.4	(1–1)	20.2	0.910

[a] The numbers are the relative intensities of the components in each resonance. [b] Theoretically, this ratio should be the inverse ratio of the nuclear gyromagnetic ratios, 0.885.

Comparisons of δ_H and δ_F with the Chlorine Quadrupole Coupling.—In Fig. 5, δ_H and δ_F are plotted against $|eqQ|_{Av}$ at 20°K. for Cl^{35} in the chloromethanes and chlorofluoromethanes, respectively. An increase in the p-orbital character used by the chlorine in bond formation increases the chlorine quadrupole coupling constant, while increased ionic character and double-bond character decrease the coupling.[12] In the chloromethanes, both δ_H and the chlorine coupling increase upon successive chlorine substitution. This indicates the ionic character of the C–H bond increases as that of the C–Cl bond decreases, primarily an inductive effect analogous to that found in the fluoromethanes discussed above.

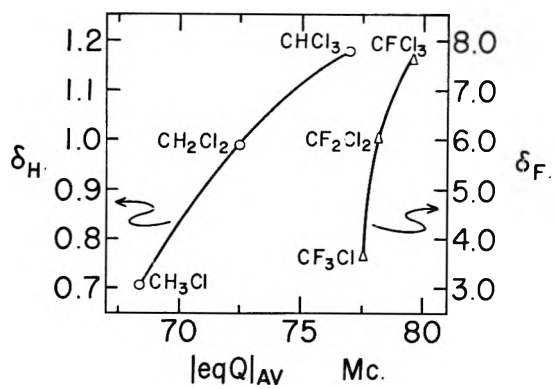

Fig. 5.—The interdependence of the magnetic resonance shifts and the chlorine quadrupole couplings in the chloromethanes and chlorofluoromethanes.

In the chlorofluoromethanes, both δ_F and the chlorine coupling increase upon successive chlorination, suggesting in this case decreasing ionic character of *both* the C–F and C–Cl bonds. The double-bond structures such as 3a and 3b proposed above in explanation of the decreasing C–F ionic character also account for the decreasing C–Cl ionic character, if the same assumption is made that the double-bond effects exceed the inductive. In CF_3Cl, all three C–F bonds try to form structures $Cl^-C{=}F^+$, so the single C–Cl bond has a high ionic character while the three C–F bonds have low double-bond character. In $CFCl_3$, on the other hand, there is only one C–F bond feeding electrons into three chlorines, so the C–F bond has an increased double-bond character, while the C–Cl bonds have decreased ionic character, agreeing with experiment.

δ_H, δ_F and the C–H and C–F Bond Distances.—In Fig. 6 δ_H is plotted against the corresponding C–H bond distances, and in Fig. 7, δ_F against the C–F distances. For both nuclei, increasing δ's are associated with decreasing bond distances. The increase in δ_H indicates that increasing ionic character occurs with decreasing C–H bond length. This agrees with the suggestion of Schomaker and Stevenson[15] that ionic character reduces bond lengths. The proton data are of further interest in that the points for the CH_3X, CH_2X_2 and CHX_3 molecular types fall along different curves, with the halogens in the same sequence for each type.[16] In the discussion, Dailey pointed out that the accuracies of the microwave analyses are limited by zero-point vibrational effects[16]; however, the differences between the different molecular types are large enough to be real, suggesting changes in bond

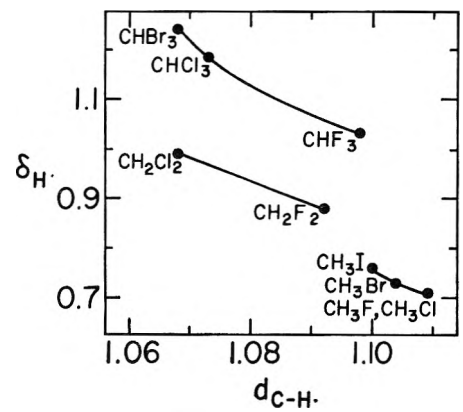

Fig. 6.—The interdependence of the proton magnetic resonance shifts and the C–H bond distances in the halomethanes.

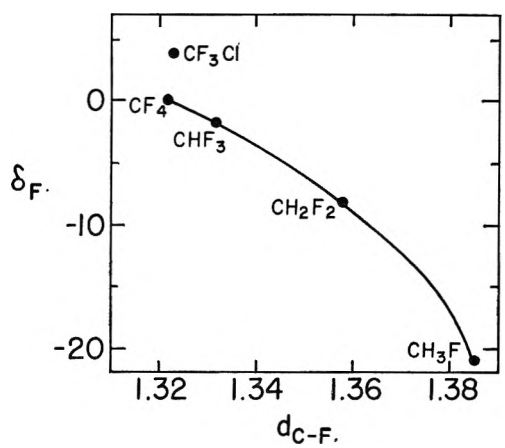

Fig. 7.—The interdependence of the fluorine magnetic resonance shifts and the C–F bond distances in the halomethanes.

(15) V. Schomaker and D. P. Stevenson, *J. Am. Chem. Soc.*, **63**, 37 (1941).

(16) The trend shown for the methyl halides is not borne out by the recent detailed analysis of the microwave data, by S. L. Miller, L. C. Aamodt, G. Dousmanis, C. H. Townes and J. Kraitchman, *J. Chem. Phys.*, **20**, 1112 (1952).

hybridization as well as in ionic character. On the basis of the δ_H-values and the trends in Fig. 6, the C–H bond distances in CH_2Br_2 and CH_2I_2 should be both about 1.065 Å., while that in CHI_3 might be as large as 1.12 Å.

The δ_F-values show *decreasing* ionic character with decreasing C–F bond length. This agrees however with the double-bond shortening proposed by Pauling[17] provided the double-bond structures are more important than the ionic in determining the C–F bond length. The point for CF_3Cl in Fig. 7 confirms the greater importance of the double-bond structures in the chlorofluoromethanes compared to the fluoromethanes, as suggested in an earlier section.

C. General Comments.—In conclusion, the most striking feature of these results is probably their internal consistency. A wide range of molecular parameters are at least qualitatively fitted by a few quite simple concepts. Some features, for instance the chemical shift data on the iodides, are not clear. But, with continued research on the various halomethanes, with observations such as the bromine and iodine quadrupole coupling constants, with additional good bond distances as well as the determination of force constants from vibrational spectra, it should prove possible to make more critical tests of our notions about molecular structure. And, of course, it is to be hoped that quantitative as well as qualitative agreement will be reached.

(17) L. Pauling, "The Nature of the Chemical Bond," 2nd Ed., Cornell University Press, Ithaca, N. Y., 1945, p. 236.

Acknowledgment.—We wish to thank Mr. Apollo Saika for his assistance with the measurements, and the Jackson Laboratory, E. I. du Pont de Nemours and Company, for generously donating many of the samples. A Grant-in-Aid from the Research Corporation provided most of the equipment.

DISCUSSION

B. P. DAILEY (Columbia University).—In attempting correlations between microwave bond-lengths and the chemical shifts, one must recognize that the bond lengths are really averaged over the vibrational state.

B. BOLGER (Pennsylvania State College).—When one regards chemical shifts, one has also to take into account a second order paramagnetism, which can appear when there exist several low lying states of the molecule near the ground state. As this effect is often greater than the diamagnetic shift (for several Co salts nearly 1%), has this effect been taken into account in these experiments?

H. S. GUTOWSKY.—The separation of the chemical shifts, by Ramsey, into a diamagnetic term and a second-order paramagnetic term is rather artificial, and was done mainly for computational purposes. The analysis given here is qualitative, and is based largely on the empirical result that the chemical shifts in the binary fluorides and hydrides can be related simply to the ionic characters of the bonds, and this is independent of what may be the actual magnitudes of the opposing diamagnetic and second order paramagnetic terms in the theoretical treatment.

MAGNETIC RESONANCE SPECTRUM OF A LINEAR THREE-SPIN SYSTEM: THE CONFIGURATION OF THE BIFLUORIDE ION[1]

BY JOHN S. WAUGH, FLOYD B. HUMPHREY AND DON M. YOST

Gates and Crellin Laboratories of Chemistry, California Institute of Technology, Pasadena 4, California

Received January 14, 1953

The nuclear magnetic resonance spectrum is calculated for a system of three nuclei of spin 1/2, two of which have identical g factors. The results are applied to a study of the bifluoride ion in KHF_2, and comparisons with experiment are made for both proton and fluorine resonances. The data obtained, together with a study of the second moment of the fluorine resonance, confirm a symmetrical structure for the ion, the proton being found to lie within ±0.06 Å. of the ion center. Second moment data on the fluorine resonance in $NaHF_2$ permit a partial determination of the HF_2^- structure in that substance.

The bifluoride ion HF_2^- embodies the simplest known example of hydrogen bonding, and an anomalous one in that its total length, 2.26 Å.[2] is considerably shorter than "normal" distances of this type. It is therefore of interest to determine whether or not the hydrogen atom is bound to an asymmetrical position on the FF axis, as it must be if this ion conforms to the example set by all other known hydrogen bonds.

Analysis of infrared spectroscopic data by Glockler and Evans[3] and by Ketelaar[4] led to the adoption of asymmetrical $C_{\infty v}$ models, the equivalent potential minima for the proton being separated by 0.52 and 0.75 Å., respectively. Doubt has since been cast on these conclusions by the dielectric constant measurements of Polder[5] and a convincing thermodynamic study by Westrum and Pitzer,[6] both of which are in accord with a situation of symmetry $D_{\infty h}$[. The polarized infrared spectra obtained by Newman and Badger[7] also appear to support the symmetrical model. The use of nuclear magnetic resonance spectra for structure determination, first employed by Pake,[8] appeared suitable for a study of the problem, and an investigation was accordingly undertaken by means of this entirely independent experimental method. Since the inception of this research, Ketelaar and Ved-

(1) Summary of part of a Ph.D. thesis submitted by J. S. Waugh, 1952.

(2) R. M. Bozorth, *J. Am. Chem. Soc.*, **45**, 2128 (1923).

(3) G. Glockler and G. E. Evans, *J. Chem. Phys.*, **10**, 607 (1942).

(4) J. A. A. Ketelaar, *Rec. trav. chim.*, **60**, 523 (1941); *J. Chem. Phys.*, **9**, 775 (1941).

(5) D. Polder, *Nature*, **160**, 870 (1947).

(6) E. F. Westrum, Jr., and K. S. Pitzer, *J. Am. Chem. Soc.*, **71**, 1940 (1949).

(7) R. Newman and R. M. Badger, *J. Chem. Phys.*, **19**, 1207 (1951).

(8) G. E. Pake, *ibid.*, **16**, 327 (1948).

TABLE I

State	m representation	Energy
(1)	$(+++)$	$E_0^H - 2E_0^F + a + c - 2b$
(2)	$(R^2+1)^{-1/2}[(++-) + R(+-+)]$	$E_0^H - 2b + S$
(3)	$(R^2+1)^{-1/2}[R(++-) - (+-+)]$	$E_0^H - 2b - S$
(4)	$(-++)$	$-E_0^H + 2E_0^F - a - c - 2b$
(5)	$(---)$	$-E_0^H - 2E_0^F + a + c - 2b$
(6)	$(R^2+1)^{-1/2}[(-+-) - R(--+)]$	$-E_0^H + 2b - S$
(7)	$(R^2+1)^{-1/2}[R(-+-) + (--+)]$	$-E_0^H + 2b + S$
(8)	$(+--)$	$E_0^H - 2E_0^F - a - c - 2b$

der[9] have reinterpreted the infrared spectra, and Peterson and Levy[10] have published the results of a neutron diffraction study of KHF_2. Both of these investigations lend strong support to the single minimum hypothesis.

Energy Levels of a Linear Three-Spin System.—In the nuclear magnetic resonance determination, we shall be primarily interested in the fine structure of the H^1 and F^{19} absorptions produced by dipole–dipole interactions within isolated bifluoride ions. While we shall find that only the results for a symmetrical system are needed, it is of interest to calculate the spectrum of a slightly more general rigid, linear system of three spin $^1/_2$ particles, any two of which are alike. For clarity in application to the bifluoride case, we shall call the particles H, F_1 and F_2.

The Hamiltonian operator for the dipole–dipole coupling in the present case may be written

$$\mathcal{H} = a\sigma_z(H)\sigma_z(F_1) + c\sigma_z(H)\sigma_z(F_2) + b[\sigma_x(F_1)\sigma_x(F_2) + \sigma_y(F_1)\sigma_y(F_2) - 2\sigma_z(F_1)\sigma_z(F_2)] \quad (1)$$

where

$$a = (g_H g_F \beta^2/4r_{HF_1^3})P_2(\cos\theta);$$
$$c = -(g_H g_F \beta^2/4r_{HF_2^3})P_2(\cos\theta)$$
$$b = (g_F^2\beta^2/8r_{F_1F_2^3})P_2(\cos\theta)$$

Here the σ's are Pauli spin matrices, g_H and g_F are the nuclear g factors, β is the nuclear magneton and θ is the angle between the system axis and the direction of an externally applied Zeeman field $\mathbf{H}_0$. The r's are the separations between the various pairs of nuclei indicated by the subscripts.

Assuming that the Zeeman splittings are large in comparison to the perturbations represented by (1), we label the states of the system by the individual magnetic quantum numbers of the various spins, and obtain the matrix elements directly.

$\mathcal{H}$ =

$(m_H\ m_{F_1}\ m_{F_2})$	(+++)	(++−)	(+−+)	(−++)	....
(+++)	$a + c - 2b$	0	0	0	....
(++−)	0	$a - c + 2b$	$2b$	0	....
(+−+)	0	$2b$	$-a + c + 2b$	0	....
(−++)	0	0	0	$-a - c - 2b$	....
.	.	.	.	.	
.	.	.	.	.	
.	.	.	.	.	

(2)

The lower right hand corner of the matrix is identical. The perturbation energies are obtained by diagonalization, and the unitary transformation which performs this function also gives the "correct zeroth order wave functions" for the interacting spin system. The eigenfunctions and their characteristic energies are given in Table I. The latter include the contributions of the Zeeman terms, which are diagonal in either representation

$$E_0^H = {}^1/_2 g_H \beta \mathbf{H}_0; \qquad E_0^F = {}^1/_2 g_F \beta \mathbf{H}_0$$

Also, in this table and the next, the following abbreviations are employed: $S = \sqrt{4b^2 + (a-c)^2}$; $R = (S - a + c)/2b$.

The selection rules and intensities for absorptive magnetic dipole transitions between these states are obtained by calculating the corresponding matrix elements of the properly-rotating components of magnetic moment of the system.

$$\beta^{-1}M_+ = g_H[\sigma_x(H) + i\sigma_y(H)] + g_F[\sigma_x(F_1) + i\sigma_y(F_1) + \sigma_x(F_2) + i\sigma_y(F_2)] \quad (3)$$

The positions and intensities of the fine structure components thus obtained are given in Table II. The well-known results[8] for pairs of like and unlike spins are implicit in the above analysis for the cases $b >> a, c$ and $a >> b, c$, respectively.

Application to the Bifluoride Ion.—Direct applications of the above results may be made only to an isolated, rigid system—conditions not satisfied in any real case. In particular, for HF_2^- we must consider the effects of vibrations and possible tunnelling between double minima, both of which are executed with effective frequencies much greater than the Larmor frequencies of the nuclear precessions in the external field $\mathbf{H}_0$. When such rapid motions occur, the interaction parameters a, b and c of the previous section must be replaced by their expectation values over the corresponding vibrational eigenfunctions. Using approximate spectroscopic data from a number of sources, the necessary corrections to the values of a, b and c may be estimated by carrying out the averages over classical orbits which approximate the true motion. In this way it is found that the bending and symmetric stretching vibrations and the torsional oscillation of HF_2^- in the lattice potential may be entirely neglected. The asymmetric stretching vibration introduces a positive correction to a and c of about 3% in the case of a roughly parabolic single minimum potential function.

Since tunnelling between two separated potential minima of any reasonable form, if they exist, must

(9) J. A. A. Ketelaar and W. Vedder, *J. Chem. Phys.*, **19**, 654 (1951).

(10) S. W. Peterson and H. Levy, *ibid.*, **20**, 704 (1952).

occur with an average frequency much larger than the frequency width of the absorption, the probability density of the proton must effectively be symmetric about the ion center. Thus the constants a and c must be treated as equal, although their values still depend on the degree of extension of the motion over which they are averaged. The averages are most simply approximated by treating the tunnelling as an exchange of the proton between two point wells, and correcting the results slightly when necessary by reestimating the effects of vibrations centered at each of these wells.

With the above restrictions, the spectrum produced by an isolated bifluoride ion is given by Table II. In any real situation, such as a crystal of potassium bifluoride, the ions are of course *not* isolated: the presence of heretofore neglected dipolar groups gives rise to a further splitting of the resonance lines into a large number of components. Since the over-all crystal structure of KHF_2 is known,[2] this effect can be treated in the usual way by substituting for each fine structure component a Gaussian whose width is characteristic of the intermolecular interactions, calculated by the second moment formula of Van Vleck.[11] Further, for the study of powder samples, one must weigh these results by an isotropic angular distribution function to take account of the random orientations of the F–F axes in space. This is made relatively easy in the present case by the simple dependence of all terms on $1 - 3\cos^2\theta$.

TABLE II

Transition	Position	Relative intensity
$\|4\rangle \rightarrow \|1\rangle$	$2E_0^H + 2a + 2c$	1
$\|7\rangle \rightarrow \|2\rangle$	$2E_0^H$	$2R(1 + R^2)^{-2}$
$\|7\rangle \rightarrow \|3\rangle$	$2E_0^H - 2S$	$(1 - R^2)(1 + R^2)^{-2}$
$\|6\rangle \rightarrow \|2\rangle$	$2E_0^H + 2S$	$(1 - R^2)(1 + R^2)^{-2}$
$\|6\rangle \rightarrow \|3\rangle$	$2E_0^H$	$2R(1 + R^2)^{-2}$
$\|5\rangle \rightarrow \|8\rangle$	$2E_0^H - 2a - 2c$	1
$\|2\rangle \rightarrow \|1\rangle$	$2E_0^F + a + c - 4b - S$	$(R + 1)^2(1 + R^2)^{-1}$
$\|3\rangle \rightarrow \|1\rangle$	$2E_0^F + a + c - 4b + S$	$(R - 1)^2(1 + R^2)^{-1}$
$\|8\rangle \rightarrow \|2\rangle$	$2E_0^F + a + c + 4b + S$	$(R + 1)^2(1 + R^2)^{-1}$
$\|8\rangle \rightarrow \|3\rangle$	$2E_0^F + a + c + 4b - S$	$(R - 1)^2(1 + R^2)^{-1}$
$\|7\rangle \rightarrow \|4\rangle$	$2E_0^F - a - c - 4b - S$	$(R + 1)^2(1 + R^2)^{-1}$
$\|6\rangle \rightarrow \|4\rangle$	$2E_0^F - a - c - 4b + S$	$(R - 1)^2(1 + R^2)^{-1}$
$\|5\rangle \rightarrow \|7\rangle$	$2E_0^F - a - c + 4b + S$	$(R + 1)^2(1 + R^2)^{-1}$
$\|5\rangle \rightarrow \|6\rangle$	$2E_0^F - a - c + 4b - S$	$(R - 1)^2(1 + R^2)^{-1}$

Experimental Details

Two commercial samples of KHF_2 (potassium acid fluoride, Merck and Co., Inc., (pure) and Kalium bifluoratum, Kahlbaum, No. 01958) were used after recrystallization from aqueous solution in polyethylene and paraffin containers. A sample of J. T. Baker sodium bifluoride (tech.) was employed after a similar but more extended procedure. Weighed portions of each sample were titrated with 0.1 N NaOH to a phenolphthalein end-point, and all titers agreed with the predicted acid content within 2%. All crystals exhibited their characteristic habits when grown from aqueous solution. The Merck KHF_2 was taken from the same bottle as that used by Newman and Badger in their infrared investigation.[7] These facts were taken as indicating adequate purity of the samples.

After extended drying over anhydrous magnesium perchlorate, powders of both substances were squeezed in an arbor press into cylinders 0.32″ in diameter and *ca.* 1″ long, to fit snugly into the sample receptacle of the radiofrequency spectrometer. Attempts were made to prepare a single crystal of KHF_2 which would be suitable for confirming the expected angular dependence of the spectrum, but none of sufficient size and perfection could be made. It is likely that this aim could be accomplished by more elaborate means than we have employed.

Spectra were obtained using a bridge-type apparatus similar to that described by Bloembergen, Purcell and Pound.[12] The electromagnet has rectangular pole pieces of Armco iron, 6 in. by 14 in. in cross-section, and separated by a gap of 1.455 in. The field near the center is homogeneous within ±0.002% over regions of about 1 cm³. Current is supplied by a bank of large lead storage cells, and is at present unregulated. Operating at a fixed frequency in the neighborhood of 20 Mc./sec. supplied by a General Radio 1001-A signal generator, the magnetic field is swept slowly through the resonance region by means of an auxiliary magnet winding excited by a linearly regulated power supply.[13] The sweeping rate has been calibrated by a number of methods, including measurement with a nuclear magnetic resonance fluxmeter. Field modulation at a variable low frequency is accomplished by an audiofrequency signal generator. The resonance signal is amplified by a cascade tuned preamplifier whose noise figure is 4 db. and by a National communications receiver. Final detection is made by means of a balanced mixer of minimum band width 0.1 c.p.s., whose output is presented on a Brown recording potentiometer. Permanent records of the line shape derivatives are thus conveniently obtained. Signals may also be visually displayed on the screen of a cathode ray oscilloscope connected to the receiver output. Absolute frequency measurements can be made by means of a BC 221-N frequency meter coupled loosely to the signal generator.

Comparison of Experimental and Theoretical Line Shapes.—One wing of the line shape derivative for the proton resonance in KHF_2 calculated in the manner described above for a symmetrical equilibrium configuration and a 2.26 Å. F–F distance, is shown in Fig. 1. Points of relative maximum absorption (zero slope) are also indicated for similar curves computed for double minimum separations of 0.2, 0.52 and 0.75 Å., respectively. The experimental derivative, which is the composite of a number of recording meter tracings, is shown on the same plot. These data were

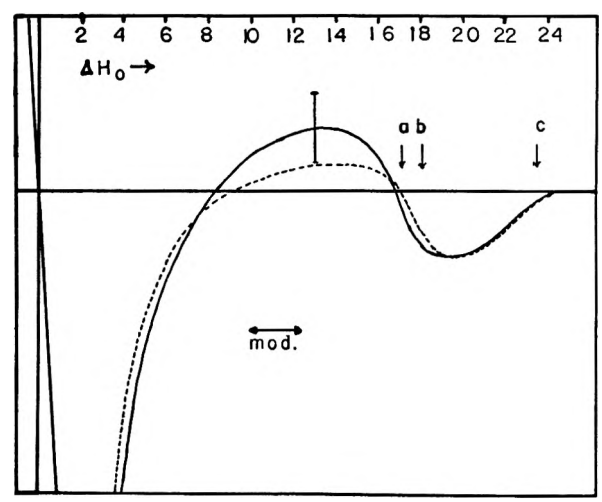

Fig. 1.—Proton resonance derivative. The solid line represents the experimental data and the dashed one is the result of calculation for a symmetrical model. a, b and c indicate points of theoretical relative maximum absorption for models in which symmetrically disposed double minima are placed, respectively, at 0.00, 0.10 and 0.26 Å. from the ion center. The corresponding point for 0.38 Å. displacement lies off the figure at 34.4 gauss.

(11) J. H. Van Vleck, *Phys Rev.*, **74**, 1168 (1948).

(12) N. Bloembergen, E. M. Purcell and R. V. Pound, *ibid.*, **73**, 679 (1948).

(13) J. S. Waugh, J. N. Shoolery and D. M. Yost, *Rev. Sci. Instruments*, **23**, 441 (1952).

obtained with 0.03 v. of r.f. input to each arm of the bridge, a modulation amplitude of about 1.2 gauss, and a sweeping rate of 5 gauss/min. Tests at higher sweep rates and r.f. power levels showed that there is no distortion of the absorption curve due either to saturation of the spin system or to low-pass filter action in the balanced mixer.

F^{19} resonance curves have been obtained at 0.03 v. r.f. input and 1.8 gauss modulation width, with a necessarily narrower audio bandpass owing to the great width and consequent low intensity of the absorption. A slow sweeping rate was thus required to obviate distortion of the signals. Under these conditions small, random fluctuations in the unregulated magnet current produced a spurious broadening of all resonance lines, for which empirical corrections had to be made. In effect, the recorded intensity at a given field strength has become a nearly complete average over a normal distribution of random fluctuations about that point. Theoretical line profiles have been calculated for several sets of structural parameters, and broadened with Gaussian functions which include the contributions of both the calculated intermolecular second moment and the random field variations. Figure 2 shows the results for a symmetrical ion and for the model in which each of the potential minima is displaced by 0.26 Å. from the center of the ion. Both are computed for an F–F distance of 2.26 Å. Points from the integrated experimental derivatives are also shown for comparison.

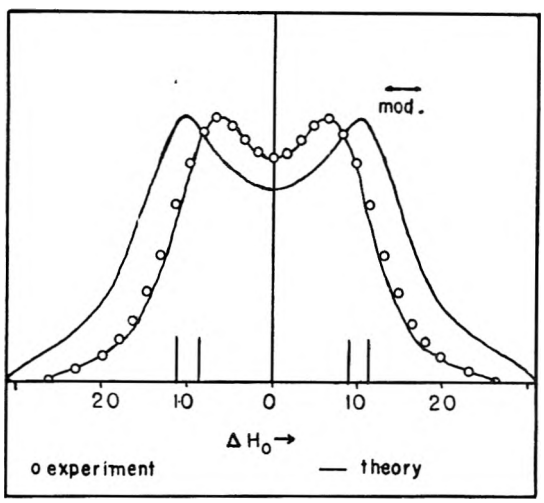

Fig. 2.—Fluorine resonance curves: the narrower theoretical profile is calculated for a symmetrical structure. The other solid line represents a calculation for double minima placed 0.26 Å. from the center of the F–F axis. Vertical bars indicate the theoretical unbroadened fine structure for the symmetrical case.

Further information is available from comparisons between the total theoretical second moments obtained by the formula of Van Vleck, and the experimental values obtained by double integration of the experimental data. In the proton resonance, the outer wings contribute very strongly to this mean square width, and consequently no very reliable measurements have been possible. For that reason, no arguments have been made on this basis in the present case. The F^{19} resonance presents a somewhat more favorable picture, however, and reasonably accurate measurements of the second moment have been possible. The experimental value is found to be 93 ± 4 gauss^2. The theoretical value for a symmetrical, 2.26 Å. model in the lattice described by Bozorth is 84.5 gauss^2, if we assume a +6% contribution from the asymmetric stretching vibration. Addition of 7.1 ± 0.5 gauss^2 for the spurious broadening due to magnetic field fluctuations, we obtain a semi-theoretical result of 91.6 gauss^2. The closeness of agreement between this and the experimental value is to be regarded as somewhat fortuitous, in view of the approximate nature of some of the assumptions involved. However, an idea as to its significance may be derived from the fact that approximate theoretical second moments for the Glockler and Evans and Ketelaar models are respectively, 200 and 460 gauss^2. For a model in which each minimum of the potential function lies 0.1 Å. from the ion center, the calculated second moment, including the same features as above, is 106 gauss^2.

Sodium Bifluoride.—Preliminary examination of proton and fluoride resonances in $NaHF_2$ has failed to resolve the weak fine structure of the former, and has not permitted any meaningful analysis of the line profile in the latter. Both appear to have the same basic structure as in KHF_2, but are somewhat more broadened. In particular, a combination of true intermolecular broadening and spurious broadening due to the apparatus has created a situation in which the F^{19} doublet is not even completely resolved. It is possible, however, to make certain incomplete statements about the ion structure from measurements of the second moment of the fluorine resonance. The experimental value of this quantity, obtained by averaging the results of four determinations, is 87 ± 6 gauss^2. Comparison with the many trials made in fitting the KHF_2 data to the theory indicates that this value is higher than that for the unbroadened fine structure by a quantity in the neighborhood of 15 gauss^2 so that we may assign a "true" intramolecular mean square width of something like 72 ± 10 gauss^2.

Neither the general structure of the $NaHF_2$ crystal nor the F–F distance therein is known reliably, so that no unique assignment of configuration, even approximate, may be made. However, one can at least assign a region of permissible values for one H–F distance as a function of the other, as shown in Fig. 3.

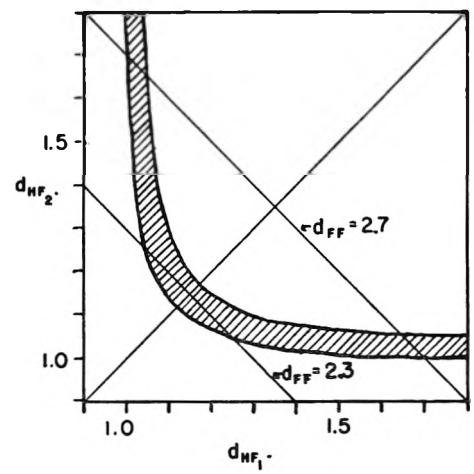

Fig. 3.—Allowed bifluoride ion configurations in $NaHF_2$. The cross-hatched region is that in which the theoretical second moment agrees with the experimental value of 72 ± 10 gauss.[2] The two labeled diagonal lines include the region permitted by an approximate X-ray structure determination.[14]

Conclusions

The KHF_2 data are clearly consistent with a symmetrical equilibrium configuration for the anion, and not with any structure so asymmetrical as was at one time postulated on the basis of infrared measurements. A consideration of the various possible sources of random and systematic errors inherent in the experiment and in the calculations leads to the conclusion that the equilibrium position for the proton lies within ±0.06 Å. of the center of the ion axis. It therefore appears extremely probable that the potential indeed has a single minimum. Even if two minima do exist, assuming that the potential function does not vary in space much more rapidly than is usual in molecular systems, the lowest vibrational state very likely lies above the central maximum, so that no tunnelling occurs in any real sense.

(14) F. Rinne, H. Hentschel and J. Leonhardt, *Z. Krist.*, 58, 629 (1923).

No complete assignment can be made for the HF_2^- configuration in $NaHF_2$ at the present time, a reliable value of the F–F distance being necessary to specify the proton position. In any case, this phase of the problem is certainly worthy of further study, in order to determine whether or not the hydrogen bond in the bifluoride ion always occurs in the "anomalous" form found in the potassium salt.

Acknowledgment.—In conclusion, the authors wish to express their gratitude to the Research Corporation, whose grant-in-aid made possible the construction of most of the apparatus. In addition, the first-named author would like to thank the United States Rubber Company for a predoctoral fellowship, and the E. I. du Pont de Nemours Company for a summer research grant.

DISCUSSION

R. A. OGG (Stanford University).—Couldn't additional or more precise information be obtained about the structure of the bifluoride ion, $(F–H–F)^-$, if deuterium or tritium were substituted for the proton?

J. S. WAUGH.—Presumably so, if the apparatus could be improved sufficiently. The more closely the potential approximates a square well, the slighter the difference would be. The deuteron, since its moment is considerably smaller than that of the proton, would yield a poorer signal-to-noise ratio for the H resonance and a smaller broadening of the F^{19} resonance under the same experimental conditions. In addition, I would expect the deuteron resonance to be strongly broadened by quadrupole interactions in the non-cubic crystal. As for the tritium, I suspect that it would be impossible at present to collect a large enough sample for a good experiment.

R. A. OGG.—"Isn't that purely a matter of politics?"

H. S. GUTOWSKY.—That'll probably depend on who wins the election this fall.

THE CHEMICAL SIGNIFICANCE OF QUADRUPOLE SPECTRA[1]

BY B. P. DAILEY

Department of Chemistry, Columbia University, New York, N. Y.

Received January 14, 1953

The deviation of certain nuclei, such as Cl, Br, I and N from a spherical shape gives rise to an energy of orientation of the nucleus with respect to the molecular or crystalline electric field in which the nucleus is located. This gives rise to a characteristic pattern of energy levels, dependent on nuclear and molecular parameters, which is described. The electrostatic interaction between the nucleus and the molecule exerts a torque on the molecule which modifies its pattern of rotational energy levels, giving rise to a hyperfine structure. The resulting modification of the rotational spectra is discussed. The quantity eqQ may be experimentally determined either from direct quadrupole spectra in the region of 10–1000 mc. or from the quadrupole hyperfine structure in microwave rotational spectra. The experimental techniques used are briefly outlined. The values of eqQ may be interpreted to cast light on the number and kind of valence bonds formed by the nucleus in question. The principles and assumptions in the theory of Townes and Dailey are reviewed. The conclusions which can be drawn from the data such as a new relation between ionicity and electronegativity, the presence of intermolecular covalent bonding in crystalline iodine, the completely ionic nature of the gaseous alkali halides, etc., are discussed.

Introduction

One of the important tasks of theoretical chemistry is to develop methods of describing the chemical properties of a substance in terms of the distribution of electric charge in its molecules. Using quantum theory, if the wave function of the electrons in the molecule can be specified in sufficient detail, it should be possible to calculate many of the interesting molecular properties. Unfortunately, with the exception of the hydrogen molecule, these wave functions cannot be obtained by purely theoretical methods.

An alternative approach to the problem is to set up a wave function containing various parameters and to try to evaluate these parameters by empirical measurement of certain molecular properties. The location of the centers of positive charge, the nuclei, is possible through such techniques as electron diffraction and the study of rotational spectra. The determination of the distribution of the negative charge is a more difficult matter, since most molecular properties, such as the dipole moment, are properties of the entire molecule.

Classically, a macroscopic charge distribution may be studied by inserting a charged probe at different points within the distribution and determining the forces exerted upon it or its potential energy. No suitable probes for insertion within a single molecule seem to exist. Fortunately, however, certain molecules are found to be equipped with "built-in" probes. These are nuclei which have potential energies of orientation within the molecule.

Transitions between these orientational energy levels give rise to what in this paper are termed Quadrupole spectra. The process by which chemically significant conclusions may be drawn from a study of these spectra is outlined in the following sections.

Energy of Nuclear Orientation.[2-4] In order to calculate the allowed orientational energies of a nucleus in an inhomogeneous molecular electric field the energy operator must be obtained. This is derived as follows.

If the center of mass of the nucleus is chosen as the origin of the coördinate system, the electro-

(1) Work supported in part by the Signal Corps.

(2) J. Bardeen and C. H. Townes, *Phys. Rev.*, **73**, 97 (1948).

(3) H. B. G. Casimir, "On the Interaction between Atomic Nuclei and Electrons," Teyler's Tweede Genootschap. E. F. Bohn, Haarlem, 1936.

(4) (a) J. K. Bragg, *Phys. Rev.*, **74**, 533 (1948); (b) R. Bersohn, *J. Chem. Phys.*, **20**, 1505 (1952).

static energy of a charge element $\rho d\tau$ may be written

$$E = \int \rho V d\tau + \frac{\partial V}{\partial x}\int \rho x d\tau + \frac{\partial V}{\partial y}\int \rho y d\tau + \frac{\partial V}{\partial z}\int \rho z d\tau + \frac{1}{2}\frac{\partial^2 V}{\partial x^2}\int \rho x^2 d\tau + \frac{1}{2}\frac{\partial^2 V}{\partial y^2}\int \rho y^2 d\tau + \frac{1}{2}\frac{\partial^2 V}{\partial z^2}\int \rho z^2 d\tau + \frac{\partial^2 V}{\partial x \partial y}\int \rho xy d\tau + \frac{\partial^2 V}{\partial y \partial z}\int \rho yz d\tau + \frac{\partial^2 V}{\partial z \partial x}\int \rho zx d\tau \quad (1)$$

where ρ is the density of charge in the nucleus and V is the electrostatic potential produced at the origin by all of the molecular charges external to the nucleus. V has been expanded in a Taylor's series and all terms higher than the quadratic ones have been neglected. The integration is over the entire nuclear volume.

The first term in eq. (1) is simply ZeV (Z is the atomic no.) which is not dependent on the nuclear orientation. The next three terms are zero because they involve the non-existent nuclear dipole moment. The classical energy of orientation of the nucleus is

$$E_Q = E - ZeV - \frac{\Delta^2 V}{6}\int \rho r^2 d\tau \quad (2)$$

The energy term $\frac{\Delta^2 V}{6}\int \rho r^2 dr$ arises from the electronic charge which penetrates the nucleus and is independent of nuclear orientation.

Equation (2) may be written

$$E_Q = \frac{1}{6}\left[\frac{\partial^2 v}{\partial x^2}\int \rho(3x^2 - r^2)d\tau + \frac{\partial^2 v}{\partial y^2}\int \rho(3y^2 - r^2)d\tau + \frac{\partial^2 v}{\partial z^2}\int \rho(3z^2 - r^2)d\tau + 6\frac{\partial^2 v}{\partial x \partial y}\int \rho xy d\tau + 6\frac{\partial^2 v}{\partial y \partial z}\int \rho yz d\tau + 6\frac{\partial^2 v}{\partial z \partial v}\int \rho zx d\tau\right] \quad (3)$$

The Hamiltonian operator, in tensor notation, then becomes

$$H_Q = -\frac{1}{6}\vec{\vec{Q}} : \vec{\Delta}\vec{E} \quad (4)$$

which is the product of the nuclear quadrupole moment tensor

$$Q = \int(3\vec{r}\vec{r} - r^2 1)\rho d\tau$$

and the gradient of the molecular electric field. If the electric field gradient is assumed constant and the nuclear charge distribution axially symmetric then the nuclear quadrupole moment tensor's off-diagonal elements and its trace are equal to zero and the entire quadrupole moment tensor may be expressed in terms of

$$Q = \frac{1}{e}\int(3z^2 - r^2)\rho d\tau \quad (5)$$

where Q is called the nuclear quadrupole moment.

As seen in Fig. 1, the quadrupole moment is a measure of the lack of spherical symmetry of the nucleus since for a sphere $3z^2$ equals the average value of r^2. If the nucleus is stretched out along the axis of spin (cigar shaped) Q is positive. If the nucleus is flattened along the axis of spin (pin cushion shaped) Q is negative.

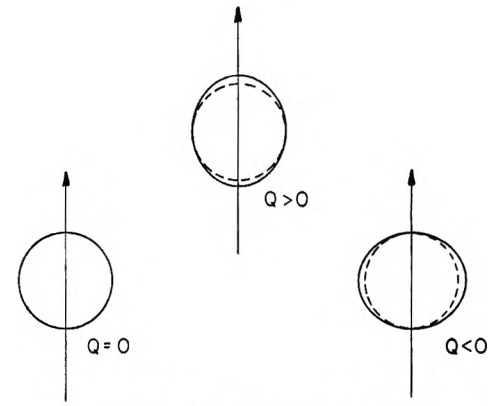

Fig. 1.—The shape of nuclei.

There are two cases of interest in determining nuclear quadrupole energy levels. In direct quadrupole spectroscopy the nucleus is located in a non-rotating molecule or ion and interacts with the crystal field. Here the Hamiltonian operator has the form

$$H_Q = \frac{eQ}{2I(2I-1)}\left(\frac{3}{2}I^2_z - \frac{1}{2}I^2\right)\frac{\partial^2 v}{\partial z^2} \quad (6)$$

if the coördinate system is lined up along the principal axes of the field gradient and the field is symmetric about Z, chosen as the axis along which the second derivative of the potential has its greatest value.

The corresponding allowed energy values are

$$E_Q = \frac{eQ_{zz}}{4I(2I-1)}[3M^2_I - I(I+1)] \quad (7)$$

If the field gradient is not symmetric about Z a more complicated set of energy levels may be derived, involving an asymmetry parameter η. These levels are given in Table I for several values of I.

TABLE I

SOLID STATE ENERGY LEVELS

$I = 1$

$E_{M_I} = 0 = -(1/2)eqQ_{zz}$

$E_{M_I} = \pm 1 = ((1/4) \pm (\eta/4))eqQ_{zz}$

$I = 3/2$

$E_{M_I} = \pm 1/2 = -(1/4)(1 + (\eta^2/3))^{1/2}eqQ_{zz}$

$E_{M_I} = \pm 3/2 = (1/4)(1 + (\eta^2/3))^{1/2}eqQ_{zz}$

$\eta = |(\partial^2 V/\partial x^2) - (\partial^2 V/\partial y^2)|/\partial^2 V/\partial z^2|$ $\quad q_{zz} = \partial^2 V/\partial z^2$

$I = 5/2$

$E_{M_I} \cong \pm 1/2 = -(1/5)(1 + (4\eta^2/9))eqQ_{zz}$

$E_{M_I} \cong \pm 3/2 = -(1/20)(1 - (3\eta^2/2))eqQ_{zz}$

$E_{M_I} \cong \pm (5/2) = (1/4)(1 + \eta^2/18)eqQ_{zz}$

The second case is the one of interest in the study of microwave spectra. The nucleus is located in a rotating molecule. The appropriate Hamilton operator is

$$H_q = \frac{eQ}{2I(2I-1)J(2J-1)}[3(I.J)^2 + \frac{3}{2}(I.J) - I^2J^2]\left(\frac{\partial^2 v}{\partial z^2}\right)_{ave} \quad (8)$$

The corresponding allowed energy values are given by

$$E_Q = \frac{eQ}{2I(2I-1)J(2J-1)}\left[\frac{3}{4}C(C+1) - IJ(I+1)(J+1)\right]\left(\frac{\partial^2 v}{\partial z^2}\right)_{ave}$$

$$C = F(F+1) - I(I+1) - J(J+1) \qquad (9)$$
$$F = I + J$$

For each type of rotating molecules $\partial^2 v/\partial z^2$ must be averaged over the rotational wave functions. Values of $(\partial^2 v/\partial z^2)$ for diatomic and linear, symmetric rotor and asymmetric rotor molecules are given in Table II.

TABLE II

VALUE OF $(q_{zz})_{av}$ FOR VARIOUS MOLECULAR CASES

Linear molecules

$-(Jq/2J+3)$

Symmetric rotor molecules

$Jq/(2J+3)(3K^2/(J(J+1)) - 1)$

Asymmetric rotor molecules

$(\alpha^2_{zx})_{av}(\partial^2 V/\partial x^2) + (\alpha^2_{zy})av(\partial^2 V/\partial y^2) + (\alpha^2_{zz})av(\partial^2 V/\partial z^2)$

Detection of Direct Quadrupole Spectra.—When a solid sample containing appropriate nuclei is placed in an alternating magnetic field with a component perpendicular to the z axis, magnetic dipole transitions occur between the quadrupole energy levels described in eq. (7) when the frequency of the field is equal to a transition frequency. The selection rule for these transitions is $\Delta M_I = \pm 1$. For chlorine nuclei the resulting transition frequencies are $\nu = eqQ/2$.

The absorption transitions cause the higher energy term to become more populous. The absorbed energy is transferred to the lattice through the coupling of the spin system to the lattice vibrations. The physical situation is similar to that existing in the nuclear magnetic resonance experiment.

The spectrometer whose block diagram is given in Fig. 2 is the one first used by Dehmelt and Krüger[5] who were the pioneers in this field. Quadrupole spectrometers with a number of improved features are discussed in some of the succeeding articles.

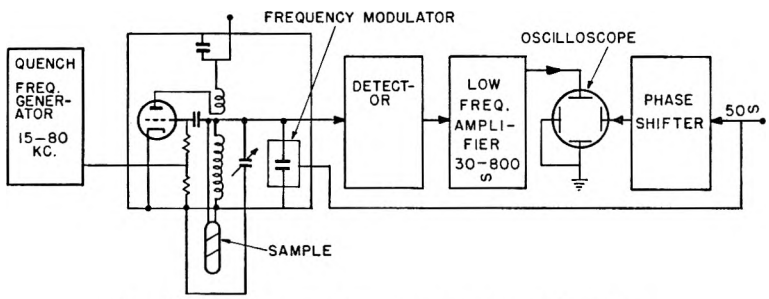

Fig. 2.—A nuclear quadrupole resonance spetrometer.

In the Dehmelt and Krüger apparatus the sample (10 to 100 g.) is located in a coil which forms part of the tank circuit of a super-regenerative oscillator. The external quench frequency generator is operated at approximately 1% of the main oscillator frequency. The super-regenerative oscillator is frequency modulated by a vibrating condenser. When its frequency is swept over the resonant frequency of a direct quadrupole transition for the solid sample a change in the output amplitude of the oscillator results. The oscillator output is fed through a detector and a low frequency amplifier and is displayed on an oscilloscope screen. The oscilloscope sweep is synchronized with the frequency of modulation of the vibrating condenser so that the oscilloscope presents a plot of oscillator output amplitude *versus* frequency. Frequencies of direct quadrupole absorption are measured accurately by mixing energy from a frequency meter with the oscillator energy and superimposing the resultant pipe on the absorption patterns.

(5) H. G. Dehmelt and H. Krüger, *Z. Physik*, **129**, 401 (1951).

The absorption intensity in this experiment is proportional to the imaginary part of the magnetic susceptibility. At the maximum of the resonance curve and in the absence of saturation effects

$$\chi'' = \frac{2N_0\mu^2_I[I(I+1) - M_I(M_I \pm 1)]}{3KTI^2(2I+1)}\frac{\nu}{\Delta\nu_H} \qquad (10)$$

where N_0 is the number of quadrupole nuclei in one cc., μ_I is the nuclear magnetic moment, ν is the resonant frequency and $\Delta\nu_H$ is the half width of the resonance curve. The absorptions observed for chlorine compounds are of the order of magnitude of 10^{-10} cm.$^{-1}$. These intensities can be considerably modified by saturation and relaxation time effects.

Determination of Nuclear Quadrupole Coupling Constants from Microwave Spectra.—Microwave absorption spectra in the presence of quadrupole hyperfine structure involve transitions between energy levels which are the sums of the rotational energies and the quadrupole orientation energies. These energy levels are specified by the quantum number F. The selection rule for these spectra is $\Delta F = 0, \pm 1$.

To observe the microwave spectrum of a molecule it is necessary that the molecule possess a permanent electric dipole moment and that it have a vapor pressure of at least 0.1 mm. at some convenient working temperature. If the intensities are to be sufficient for spectral analysis the molecule must not be too large or complex. If the quadrupole coupling constant is to be measured there should be in general no more than two quadrupole nuclei in the molecule.

A number of experimental and theoretical aspects of microwave spectroscopy are reviewed in a recent monograph.[6]

In order to obtain values of the nuclear quadrupole coupling constants a relatively complicated spectral pattern must be analyzed and small frequency differences must be accurately determined. As a result it is quite difficult to obtain quadrupole coupling constants by microwave techniques to the same degree of accuracy possible in direct quadrupole spectroscopy. However, their interpretation is free from the complication of effects due to crystal structure.

Interpretation of Quadrupole Coupling Constants in Molecules.—The accumulation of a large number of values of eqQ for various molecules should cast some light on the nature of the charge distribution and therefore on the pattern of chemical bonding in those molecules, if eQ is known or remains the same for a series of molecules. The contribution of each of the molecular electrons to q is given by the relation

$$\partial^2(e/r)/\partial z^2 = e(3\cos^2\theta - 1)/r^3 \qquad (11)$$

$$\partial^2 v/\partial z^2 = e\int\psi^*[(3\cos^2\theta - 1)/r^3]\psi d\tau \qquad (12)$$

If the contribution of each electron must be considered separately the problem appears quite formidable. Townes and Dailey[7] have shown, however, that if certain approximations are valid, the problem can be greatly simplified.

In their discussion the charges which influence q at a particular nucleus in a molecule are divided into the inner core electrons, the valence electrons, and the electrons and nuclei external to the atom under consideration. The contribution to q of the valence electrons which have a high probability of being found near the nucleus is shown to be larger by an order of magnitude than the contributions due to the other charges.

If an atom (part of a molecule) is considered which has a single valence electron outside of a

(6) "Microwave Spectroscopy," *Ann. N. Y. Acad. Sci.*, **55**, 743–966 (1952).

(7) C. H. Townes and B. P. Dailey, *J. Chem. Phys.*, **17**, 782 (1949).

TABLE III

CALCULATED QUADRUPOLE COUPLING CONSTANTS FOR MOLECULES CONTAINING Cl^{35}

Molecule	Resonant structures	% s hybridization	Unbalanced p electrons	% importance	eqQ, Mc. Calcd.	Obsd.
Cl (atomic)			−1	100	−109.6	−109.6
BrCl	BrCl	0	−1.00	95	−104.1	−103.6
	+ −					
	BrCl		0.0	5		
ICl	ICl	18	−0.82	91	− 82.2	− 82.5
	+ −					
	ICl		0.0	9		
FCl	FCl	0	−1.00	78	−146.3	−146
	+ −					
	FCl		−2.50	22		
TlCl	TlCl	18	−0.82	18	− 16.2	− 15.795
	+ −		0.0	82		
	TlCl					
KCl	KCl	18	−0.82	0	0.0	< 0.07
	+ −					
	KCl		0.0	100		
CH_3Cl	CH_3-Cl	18	−0.82	80	− 73.0	− 75.13
	+ −					
	CH_3 Cl		0.0	20		
Cl–CN	Cl—C⁻≡N	18	−0.82	83	− 82.2	− 83.2
	+ −					
	Cl=C=N		−0.40	17		

closed shell, then the wave function for this electron may be written

$$\psi = \Sigma_{nlm} a_{nlm} \psi_{nlm} \qquad (15)$$

In this series a rather large number of different ψ_{nlm} will be present, since it is necessary that the electron have some probability of being found in an orbit of the atom to which it is chemically bound. The coefficients a_{nlm} should be largest for the lowest energy atomic orbits outside the closed shells. If the wave function of eq. (13) is substituted into eq. (12) the following expression for q is obtained

$$\frac{\partial^2 v}{\partial z^2} = \Sigma_{nlm} |a_{nlm}|^2 q_{nlm,nlm} + \Sigma_{nlm,n'l'm'} a_{nlm} a^*_{n'l'm'} q_{nlm,n'l'm'} \qquad (14)$$

$$q_{nlm,n'l'm'} = \int \psi_{nlm} \left(\frac{3\cos^2\theta - 1}{r^3} \right) \psi_{n'l'm'} \, d\tau$$

The quantities of $q_{nlm,nlm}$ are simply the values of q for each of the atomic states and are multiplied by the fractional importance of the respective atomic states in the molecular wave function, $|a_{nlm}|^2$.

Townes and Dailey indicate that to a first approximation the cross-product terms of eq. (14) may be neglected. In addition, since $q_{nlm,nlm}$ is shown to be a rapidly decreasing function of n and l the dominating terms in eq. (14) will be the state of lowest allowed n because for it both a_{nlm} and q_{nlm} are large. For an s orbit, q_{nlm} is equal to zero. As a result of all of these considerations the electrons occupying the lowest energy atomic p orbitals ordinarily may be considered as the only significant contributors to q.

The usual molecular wave function is not in the form of eq. (13) but instead involves atomic functions of both bonded atoms as well as parameters to allow for effects such as ionic character and s–p hybridization. In ref. (7) such a wave function is written for a diatomic halide and the following equation for eqQ is derived.

$$eqQ \backsimeq (-1 - S^2 + c^2 + b) eqQ_{310} \qquad (15)$$

$$i = C^2 + \sqrt{2}\, CS$$

where S is the overlap integral, i, the ionicity, $= C^2 + \sqrt{2}\, cs$, and b is the amount of s character in the bond orbital.

In the actual analysis of data the simpler, approximate relation

$$eqQ \backsimeq (-1 + i + b) eqQ_{310} \qquad (16)$$

is used. The effect of the withdrawal of charge from the inner region of the atom due to overlap may be partially compensated by the additional charge due to the bonding electron from the adjacent atom.

Chlorine Compounds.—The use of this equation in the analysis of quadrupole data is shown in applying it to chlorine compounds in Table III. For atomic chlorine the valence shell contains two 3s electrons and five 3p electrons. Since the addition of a 3p electron would form a spherically symmetric closed shell the chlorine atom is said to have −1 "unbalanced" p electrons. The chloride ion, after gaining its electron, has zero unbalanced p electrons.

For chlorine compounds which are neither completely ionic nor completely covalent the possible presence of s–p hybridization must be considered. The amount of s–p hybridization assumed in a given case is necessarily somewhat arbitrary but as shown in reference (8) the following principles lead to the best general agreement with the entire body of experimentally observed quadrupole coupling data.

Bonds between atoms of only slightly differing electronegativities are assumed to involve electrons occupying pure p orbitals. For bonds with considerable ionic character in which chlorine is negatively ionic the chlorine bonding orbital is as-

(8) C. H. Townes and B. P. Dailey, *J. Chem. Phys.*, to appear.

sumed to a hybrid with 18% s character. Because of the large promotional energy required bonds in which the chlorine ion has a positive charge are assumed to involve only pure p orbitals.

These assumptions seem reasonable and as may be seen in Table III the quadrupole coupling constants calculated with this use are in good agreement with the observed data. Since the diatomic chlorides in Table III cover the entire range of electronegativity differences they may be used to derive a relation between ionic character and electronegativity difference. This relation is compared with an older one, derived by Pauling[9] from the dipole moments of the hydrogen halides, in Fig. 3. The two curves differ mainly in the region of large ionic character. The quadrupole data show unambiguously, without any question as to hybridization, that the alkali halides are completely ionic.

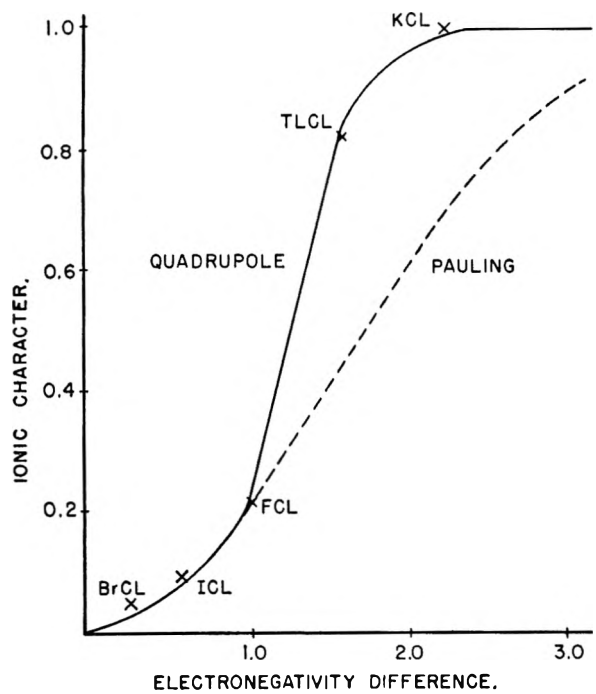

Fig. 3.—Ionic character *versus* electronegativity differences.

In these simple diatomic molecules there is no evidence of double-bond character. However, in vinyl chloride the quadrupole data have been used to determine the amount of double-bond character in the C–Cl bond. The calculation as presented by Bragg and Goldstein[10] is outlined in Table IV. It may be seen that the C–Cl bond in this molecule has 20% ionic character and 5% double-bond character, as revealed by the lack of cylindrical symmetry of the quadrupole tensor.

Quadrupole and other structural data have been used by Mays and Dailey[11] to obtain a picture of the bonding in XH_3–Cl molecules.

This analysis is presented in Table V. It is evident from a consideration of these data that the double bond structure seems to play an important role in SiH_3Cl, a lesser role in GeH_3Cl and to be completely absent in methyl chloride. These results agree with Pauling's[9] ideas on the role of partial double bond character for the halogen compounds of elements which are not found in the first row of the Periodic Table. Germanium, a third row element, would be expected to form double bonds less readily than silicon which is found in the second row of the Periodic Table. Carbon has no d orbitals in its valence shell suitable for double bond formation. Similar results have been found for the XH_3–Br compounds and by Sheridan and Gordy[12] in their study of the trifluorosilane derivatives.

(9) L. Pauling, "Nature of the Chemical Bond," Cornell University Press, Ithaca, N. Y., 1945.

(10) J. H. Goldstein and J. K. Bragg, *Phys. Rev.*, **75**, 1943 (1949).

(11) J. M. Mays and B. P. Dailey, *J. Chem. Phys.*, **20**, 1695 (1952).

TABLE IV

CALCULATED QUADRUPOLE COUPLING CONSTANTS FOR VINYL CHLORIDE

Resonant structures	% s hybridization	Unbalanced p electrons	% importance	*eqQ*, Mc. Calcd.	Obsd.
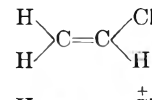	18($p\sigma$)	p_z −0.82	75	69.6	67
		p_x +0.41		39.9	
		p_y +0.41		29.6	
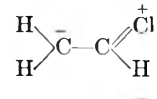		p_z −0.40	5		
		p_x +1.14			
		p_y −0.74			
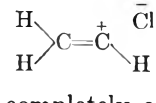		0.0	20		

TABLE V

BOND CHARACTER OF H_3X–Cl MOLECULES

Structure	CH_3Cl[33], %	SiH_3Cl[35], %	GeH_3Cl[35], %
H_3X–Cl	80	34	44
$H_3X^+Cl^-$	20	37	43
$H_3X^-=Cl^+$		29	15
eqQ calcd., Mc.	−73	−40	−46
eqQ obsd., Mc.	−75.13	−40.0	−46
Dipole moment	1.88	1.30	2.12
Electronegativity difference	0.5	1.2	1.3

Compounds of Nitrogen and Arsenic.—The analysis of some of the quadrupole data available for compounds of nitrogen and arsenic is shown in Table VI. It is of interest to note that nitrogen in structures where it forms four bonds gives rise to a very small quadrupole coupling constant as would be expected from such a highly symmetrical arrangement. This is shown in CH_3NC and even more strikingly in N_2O where the center N is symmetrically bonded and the end N is not. It is also of interest to note the apparently large s–p hybridization and ionicity in NH_3 and NF_3.

The AsF_3 case is an important one because it reveals the presence of s–p hybridization in a rather straightforward and unambiguous fashion. This may be seen from the following discussion.

If the bonding orbitals used by As in AsF_3 are pure p orbitals they will be equally filled, producing a spherical charge distribution and a very small quadrupole coupling constant. Since a rather large coupling is observed, some sort of hybridization must be taking place. If the hybrid bonds are thought of as constructed from a set of p orbitals

(12) J. Sheridan and W. Gordy, *Phys. Rev.*, **77**, 719 (1950).

TABLE VI

CALCULATED QUADRUPOLE COUPLING CONSTANTS FOR MOLECULES CONTAINING N^{14} OR As^{75}

Molecule	Resonant structures	% s hybridization	Unbalanced p electrons	% importance	eqQ, Mc. Calcd.	eqQ, Mc. Obsd.
NH_3	NH_2H	25	−0.40	100	−4.0	−4.1
NH_3	NF_2F	25	−0.63	100	−6.3	−7.07
ClCN	Cl—C≡N	45(pσ)	−0.45	83	−3.7	−3.63
	Cl=C=N		0.0	17		
HCN	H—C≡N	45(pσ)	−0.45	90	−4.1	−4.7
	H—C=N		0.0	10		
CH_3NC	H_3C—N=C	45(pσ)	+0.60	5	+0.3	+0.5
	H_3C—N≡C		0.0	95		
N_2O	N=N=O	45(pσ)	−0.05	55	−1.7	−1.03
(end N)	N≡N—O		0.45	45		
N_2O	N=N=O	45(pσ)	0.0	55	0.0	−0.27
(central N)	N≡N—O		0.0	45		
AsF_3	AsF_2F	15	0.38	100	228.0	235

directed so that p_z is along the molecular symmetry axis and are appropriate to the observed bond angle, then a defect of electrons along the molecular axis might be expected since the p_z orbital directed along this axis would not be filled as much as the p_x and p_y orbits perpendicular to the axis. If, however, the hybrid bond orbitals are constructed using the s orbital of the valence shell the two non-bonding electrons of the valence shell must be promoted to a hybrid orbital containing a p_z component. This would not be true if any other type of orbital (d, f, etc.) were used in the hybridization. Since the non-bonding orbital contains two electrons while the bonding orbital on the average contains only one an excess of p electrons along the molecular symmetry axis results. Such an excess is proved by the sign of the quadrupole coupling in AsF_3.

Interpretation of Solid Quadrupole Data.—The quadrupole coupling data so far considered in this paper have been derived from measurements on gases. The techniques of direct quadrupole spectroscopy are now being used to accumulate a large body of data for solids. Since the electrostatic fields in solids are more complicated than those in gases the quadrupole coupling constants measured in the two states may be expected to differ. This expectation is borne out by a comparison of the quadrupole coupling constants listed for a number of compounds in both the solid and gaseous state in Table VII. While there is good rough agreement between the values of the quadrupole coupling constants measured in the solid and in the vapor, in a number of cases there are appreciable intermolecular effects in the solid state. Most of the molecules in Table VII involve bonds with partial ionic character and the data indicate that for the most part the molecules in the solid form bonds which are more ionic than those in the gas. This is shown by the decrease in eqQ for solid CH_3Cl, CH_2Cl, CH_3I, CH_3Br and CF_3Cl and the increase in eqQ for ICl (since I^+ is involved there).

TABLE VII

COMPARISON OF QUADRUPOLE COUPLING CONSTANTS FOR SOLIDS AND GASES

Molecule	Nucleus	eqQ, Mc. Solid	eqQ, Mc. Gas
CH_3Cl	Cl^{35}	68.4	75.13
CH_2Cl_2	Cl^{35}	72.47	78.0
CF_3Cl	Cl^{35}	77.58	78.05
CH_3Br	Br^{79}	528.9	577.0
CH_3I	I^{127}	1753	1931.5
ICN	I^{127}	2549	2420
ICl	I^{127}	3037	2944
I_2	I^{127}	2140	(2500)
Cl_2	Cl^{35}	108.95	(109.5)

I_2 and ICN are cases where intermolecular effects are important.[13] The decrease in eqQ for I_2 and the large value of the asymmetry parameter η may be explained by assuming the existence of weak covalent intermolecular bonds as shown in Fig. 4. If these bonds were not present no such a comparatively large value of η could be explained.

For solid ICN lattice effects cause a decrease in ionic character for the solid. An additional factor tending to increase eqQ is the polymerization of ICN molecules into long chain structures such as $-I^+-C^-\equiv N-I^+-C^-\equiv N-$. The observed eqQ for

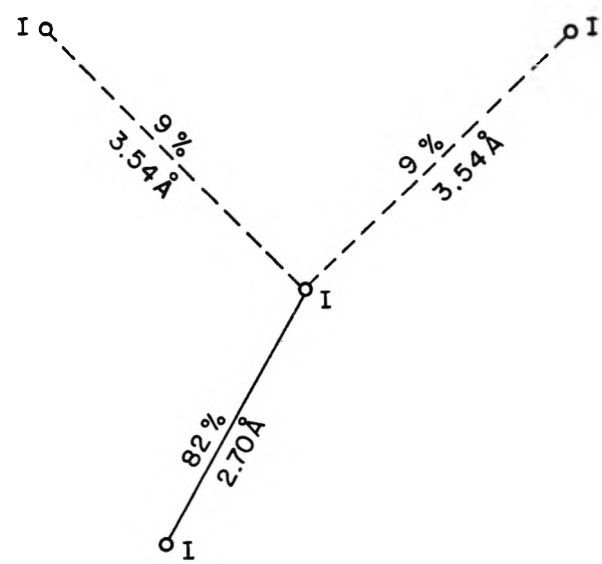

Fig. 4.—Structure of crystalline iodine.

(13) C. H. Townes and B. P. Dailey, *J. Chem. Phys.*, **20**, 35 (1952).

solid ICN can be accounted for by assigning 10% importance to this structure, 2% to $I^+ C{\equiv}N^-$ and 88% to $I{-}C{\equiv}N$.

ICN is one of the few molecules which has been studied both as a solid and a vapor and for which the crystal structure of the solid is known. Unfortunately in the majority of interesting cases some of the important information is missing.

Solid quadrupole data can in many cases be accumulated with less effort and interpreted with greater ease to give values of eqQ than hyperfine structures in microwave spectroscopy. In the microwave case a successful analysis of the rotational energy levels must be made before eqQ can be obtained. Furthermore, values of eqQ obtained from the direct quadrupole spectra of solids are generally more precise than microwave values.

All of this makes the difficulties in the chemical interpretation of values of eqQ obtained for solids rather frustrating. The solid state eqQ's are influenced not only by the pattern of chemical bonds in the isolated molecule but by crystal structure effects as well. Unravelling the two influences in the absence of crystal structure data may lead to considerable ambiguity.

However, as is shown in the following papers, many of the chemical effects are so striking that they are revealed merely by a qualitative comparison of eqQ for a series of similar chemical compounds. The assumption is made in these studies that crystal structure effects are small and that they do not vary greatly in comparing two closely similar molecules.

DISCUSSION

R. A. OGG (Stanford University).—Have any deuterium pure quadrupole spectra been observed?

B. P. DAILEY.—Allen is reporting his results on DCl.

R. A. OGG.—What is the effect of deuterium substitution on the chlorine coupling constants in a hydrogen containing compound?

B. P. DAILEY.—The effects are not large and seem related to zero-point vibrational effects. The change in eqQ for a covalently bonded chlorine is of the order of 0.5 Mc. or a little less than 1%.

PURE QUADRUPOLE SPECTRA OF SOLID CHLORINE COMPOUNDS[1]

BY RALPH LIVINGSTON

Oak Ridge National Laboratory, Oak Ridge, Tennessee

Received January 14, 1953

Quadrupole couplings have been determined for a number of covalently bonded chlorine compounds that form molecular crystals. Multiple resonances due to non-equivalent Cl lattice positions, resonances for the two stable Cl isotopes and the variation of resonance frequency with temperatures down to 4°K. are briefly discussed. A comparison of quadrupole couplings gives a measure of the variation from one molecule to another of the electric field gradient experienced by the chlorine nuclei. Such comparisons are given for the chloromethanes, "Freons," chloroethanes and related compounds. A number of quadrupole coupling values determined in the solid are compared with microwave values found for the gas.

Introduction

A nucleus possessing an electric quadrupole moment, Q, will interact with an electric field gradient, $-q$, giving rise to a set of energy levels that correspond to different orientations of the quadrupolar nucleus in the field gradient system. If such nuclei are present in appropriate solid substances there will be field gradients present at the nuclear positions that arise from properties of the substance itself, and transitions between the resulting energy levels can be observed in the radio frequency region of the spectrum. This paper will be concerned with observations on a number of solid chlorine compounds that are appropriate for viewing the phenomena.

The energy levels are given by

$$E_m = eqQ[3m^2 - I(I+1)]/4I(2I-1)$$

where I is the nuclear spin, 3/2 for both Cl isotopes, e the proton charge and m the magnetic quantum number. The levels for Cl are $E_{\pm 1/2} = -eqQ/4$ and $E_{\pm 3/2} = +eqQ/4$ and with the selection rule $\Delta m = 1$ give a transition $h\nu = |eqQ/2|$. The quantity eqQ, the quadrupole coupling, is usually expressed in frequency units and for Cl is equal to twice the observed transition frequency. In the above formulation the field gradient has axial symmetry. The consequence of departure from axial symmetry will be briefly discussed later. The sign of eqQ is not determined by this method so only its magnitude and the magnitude of q are considered.

All measurements, unless otherwise noted, were made with a frequency modulated, regenerative oscillator type spectrometer which has been described elsewhere.[2]

Resonance Lines for Cl^{35} and Cl^{37}.—Separate transitions for each of the Cl isotopes can be observed since they have different quadrupole moments, and it follows from the above equation that if each experiences the same field gradient the ratio of the resonance frequencies should be the quadrupole moment ratio of the two nuclei. Table I summarizes measurements of this type.

The constancy of the ratio has already been pointed out[3] but is presented here to demonstrate that to very high precision the same field gradients are experienced by each Cl isotope in a given compound. Hence it is only necessary to measure the transition frequencies for one isotope to study the manner in which the field gradient at the nucleus varies from one substance to another. Recently more accurate frequency measurements on the above ratio in several Cl compounds have been re-

(1) This work was performed for the AEC.

(2) R. Livingston, *Ann. N. Y. Acad. Sci.*, **55**, 800 (1952).

(3) R. Livingston, *Phys. Rev.*, **82**, 289 (1951).

TABLE I

MEASURED FREQUENCIES AND RATIOS FOR SOLID Cl COMPOUNDS AT 77°K.

Compound	$\nu(Cl^{35})$, Mc.	$\nu(Cl^{37})$, Mc.	$\nu(Cl^{35})/\nu(Cl^{37})$
$SOCl_2$	32.0908	25.2935	1.26874
	31.8874	25.1331	1.26874
$POCl_3$	28.9835	22.8432	1.26880
	28.9378	22.8067	1.26883
CH_2Cl_2	35.9912	28.3673	1.26876
$CHCl_3$	38.3081	30.1921	1.26881
	38.2537	30.1500	1.26878
C_6H_5Cl	34.6216	27.2872	1.26879
Cl_2	54.2475	42.7544	1.26882
ClF_3[a]	75.1295	59.2147	1.26876

[a] 20°K. This measurement was made in collaboration with D. F. Smith.

ported,[4] and a small significant variation was found and interpreted. The variation was too small to be of concern in the following discussion.

Only frequencies of the stronger resonance lines due to the more abundant Cl^{35} isotope will be reported. In most cases the Cl^{37} lines were also observed to remove any ambiguity in interpreting which isotope transition was being measured.

Multiple Resonance Lines.—More than one resonance is frequently found for each Cl isotope. A similar effect was first seen and explained by Dehmelt[5] for the iodine resonance in SnI_4. The number of lines corresponds to the number of non-equivalent halogen positions in the crystal lattice. Each set of halogen nuclei thus experiences its own characteristic electric field gradient.

Table II summarizes additional measurements for Cl^{35} and it is noted that multiple lines are frequently seen. Unfortunately the crystal structures for most of these materials are unknown; however, some comment is in order. CCl_4 is particularly interesting in that it shows an unusually large number of non-equivalent lattice positions. Fourteen lines were originally seen and these were measured at 20°K. Later, with a more sensitive recording spectrometer, one of the lines at 77°K. was resolved into a doublet which now gives a total of 15 lines. The crystal structure at low temperatures may be like that of CBr_4[6] which is reported to be monoclinic and of large cell dimensions, apparently with 32 molecules per unit cell. It is likely that there is a sixteenth resonance line in CCl_4 that has not yet been observed.

There is a striking similarity in the four-line spectra of $SnCl_4$, $GeCl_4$ and $SiCl_4$ which suggests

TABLE II

OBSERVED FREQUENCIES AND QUADRUPOLE COUPLINGS FOR Cl^{35}

Compound	77°K.	20°K.	$\lvert eqQ\rvert_{av}$, 20°K., Mc.
$SnCl_4$	24.294		
	24.226		
	24.140		
	23.719		
$SiCl_4$	20.464	20.552	40.97
	20.415	20.521	
	20.408	20.501	
	20.273	20.370	
$GeCl_4$	25.746		
	25.736		
	25.714		
	25.451		
$SiHCl_3$[a]		19.30	38.6
PCl_3	26.202		
	26.107		
BCl_3	21.585		
	21.580		
$SbCl_3$	20.912		
	19.304		
HCl		26.695	53.39
ClF[b]		70.700	141.40
$COCl_2$	36.225		
	35.081		
$POCl_2F$		29.272	57.99
		28.715	
$C_6H_5CH_2Cl$	33.627		
cis-CHClCHCl		35.029	70.00
		34.968	
trans-CHClCHCl[c]		35.584	71.17
$ClCH_2OCH_2Cl$	32.381		
	32.587		
CCl_4	40.465	40.732	81.85
	40.521	40.794	
	40.540	40.800	
	40.549	40.826	
	40.576	40.831	
	40.587	40.888	
	40.607	40.895	
	40.639	40.918	
	40.643	40.965	
	40.655	40.972	
	40.696	41.022	
	40.721	41.045	
	40.782	41.109	
	40.797	41.139	
	40.817		
CF_2BrCl	38.342	38.675	77.35
CF_2Cl_2	38.450	39.078	78.16
CF_3Cl	38.089	38.790	77.58
$(CH_3)_2CCl_2$	34.883	35.046	70.09
CCl_3CCl_3	40.761	40.885	81.58
	40.714	40.823	
	40.685	40.798	
	40.551	40.652	
$CHCl_2CCl_3$	39.862	39.988	79.91
	39.836	39.954	
	39.758	39.923	
	38.759	38.888	77.74
	38.711	38.852	
CH_2ClCH_2Cl	34.361	34.442	68.88
CH_2FCl		33.799	67.60

[a] 4°K. [b] Measured in collaboration with D. F. Smith. [c] Measured by Dehmelt and Krüger, *Naturwissenschaften*, **37**, 111 (1950), at a higher temperature. The values are consistent.

(4) T. C. Wang, C. H. Townes, A. L. Schawlow and A. N. Holden, *Phys. Rev.*, **86**, 809 (1952).

(5) H. G. Dehmelt, *Naturwissenschaften*, **37**, 398 (1950).

(6) R. W. G. Wyckoff, "Crystal Structures," Interscience Publishers, Inc., New York, N. Y., 1951.

that these substances may be isomorphous. The spectra appear to consist of three lines grouped together with a fourth line at noticeably lower frequency.

It has already been shown[7] that the type of bonding experienced by Cl in the molecules discussed here is a sufficient condition for a large electric field gradient at the Cl nuclear positions. In addition there is an effect from other charge distributions in the crystal lattice. This effect appears to be secondary in importance as evidenced, in part, by the small spacing of the multiple resonance lines frequently seen. It must be pointed out that these substances generally have low melting points and presumably form molecular crystals where the intermolecular forces are principally of the weak van der Waals type.

The quadrupole coupling values of Table II are obtained by taking twice the average of the frequencies measured when multiple resonances are observed. This is a convenience in giving a single coupling value for discussing properties of the halogen bond for these substances in the solid state.

The Temperature Effect.—Dehmelt and Krüger[8] found that pure quadrupole resonance frequencies increased with decreasing temperature and explained the effect as arising from lattice vibrations. The electric field gradient at the nucleus is time-averaged over thermal lattice motions of high frequency.

Table III gives the results of measurements down to liquid helium temperature. There is a moderate frequency increase in cooling from 77 to 20°K. and a very small additional increase on further cooling to 4°K. In our apparatus the resonance line intensities increase on cooling from 77 to 20°K., probably as a result of the improved Boltzmann factor, while further cooling to 4°K. gives a marked decrease in intensity, possibly due to power saturation resulting from a large increase in the thermal relaxation time. Most of the measurements to be discussed were made at 20°K. in order to minimize the effects of lattice vibrations.

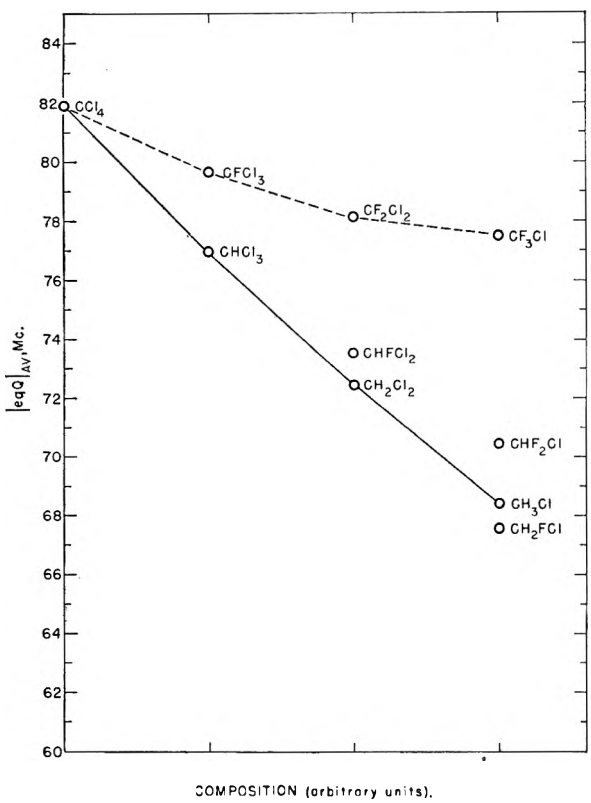

Fig. 1.—Cl^{35} quadrupole couplings in the substituted methanes at 20°K.

(7) C. H. Townes and B. P. Dailey, *J. Chem. Phys.*, **17**, 783 (1949).
(8) H. G. Dehmelt and H. Krüger, *Z. Physik*, **129**, 401 (1951).

TABLE III

MEASURED FREQUENCIES FOR Cl^{35}

Compound	Observed frequency, Mc. 77°K.	20°K.	4°K.
CH_3Cl	34.029	34.199	34.206
CH_2Cl_2	35.991	36.233	36.243
$CHCl_3$	38.254	38.486	38.506[a]
	38.308	38.490	
$AsCl_3$	24.960	25.048	25.054
	25.058	25.158	25.167
	25.406	25.520	25.528

[a] A doublet with a few Kc. spacing.

The Substituted Methanes.—Figure 1 is a plot of the quadrupole couplings at 20°K. for Cl^{35} in various substituted methanes. Those transition frequencies not found in Tables II and III have appeared in an earlier preliminary report.[9] The coupling trend, a measure of the manner in which the electric field gradient at the Cl nuclei vary, may be explained by using the molecular structure concepts of Pauling[10] as applied to the problem by Townes and Dailey.[7] Using this approach, the coupling value reflects the amount of p-orbital character used by Cl in forming the bond. Briefly this follows from the concept that using a p-orbital to form the covalent bond produces an asymmetry in the Cl electron distribution, and since the p-orbital is a penetrating orbital the asymmetry will give a large electric field gradient at the nucleus. Increasing amounts of s-character, through hybridization, cause a decrease in the field gradient at the nucleus because of the spherical symmetry property of s-states. Similarly increasing ionic character causes a decrease in the field gradient at the nucleus. An extreme case would be Cl^- where the electron distribution is spherically symmetric and there should be no field gradient at the nucleus. Increasing amounts of double bond character, through the use of π-orbitals, also causes a decrease in the field gradient. This follows from tensor properties of the electric field gradient and the spatial distribution of the bonding orbitals.

The increasing couplings in the sequence CH_3Cl, CH_2Cl_2, $CHCl_3$ to CCl_4 may reflect a decrease in ionic character in the C–Cl bond. This is consistent with the view that replacing H by much more electronegative Cl in progressing through the sequence from CH_3Cl to CCl_4 gives a progressively greater competition for the carbon electrons and hence a decreased ionic character in the C–Cl bonds. When H is replaced by F a still larger coupling change would be expected since F is much

(9) R. Livingston, *J. Chem. Phys.*, **19**, 1434 (1951).
(10) L. Pauling, "The Nature of the Chemical Bond," second Ed., Cornell University Press, Ithaca, N. Y., 1944.

more electronegative than Cl. As seen from Fig. 1 this is not the case in progressing from the chloromethane to the corresponding "Freons." It has been proposed,[10] in order to explain the shortening of the C–Cl bond, that in such a sequence there is an increase in double bond character due to contributions of resonant structures of the type F–C=Cl^+. Since double bond character is in the direction of decreasing the coupling this effect would be in the opposite direction to the ionic character effect discussed above and could explain the smaller coupling increase when H is replaced by F as compared to Cl. Furthermore, replacing the H in $CHCl_3$ by F gives a moderate coupling increase while in CH_2Cl_2 replacing the first H gives a smaller increase and finally in CH_3Cl replacing the first H gives a small decrease in coupling. This situation suggests the argument presented for the chloroethylenes[10] where there is possible competition among the number of Cl atoms present for the double bond. It would be of interest to obtain couplings in chlorobromomethanes, Br being a little less electronegative than Cl, but unfortunately resonances were not seen in any of the six compounds tried. The resonance in CF_2BrCl was observed, however, and a comparison of its value (Table II) with that of CF_2Cl_2 and CF_3Cl indicates that the substitution of Br for Cl is consistent with the above ionic character concept.

The Chloroethanes and Related Compounds.—Figure 2 shows a correlation of quadrupole couplings at 20°K. for Cl^{35} in various chloroethanes and related compounds that may be regarded as "methyl substituted chloromethanes." Those transition frequencies not found in Table II have appeared in an earlier preliminary report.[11] In every case replacing one or more of the H atoms in a chloromethane by a CH_3 group gives a systematic decrease in coupling. This effect is consistent with the view that the ionic character in the C–Cl bond increases as a result of the CH_3 group acting in an electropositive manner. Hence the ionic character in the C–Cl bond of $(CH_3)_3CCl$ is greatest with a systematic decrease in going to other compounds. Observations have been attempted on compounds that form an homologous series, but resonances have only been seen in a few of the ones tried. The coupling in $CH_3CH_2CH_2Cl$ is 0.6% higher than in CH_3CH_2Cl while the value in $C_2H_5(CH_3)_2CCl$ is 0.8% lower than in $(CH_3)_3CCl$. These small differences are of the same order as the separation of lines seen in crystals with non-equivalent Cl lattice positions and hence the coupling changes could be largely due to the effects of the environment of the molecule in the crystal lattice.

The remaining chloroethanes may be correlated in a similar manner. CCl_3CCl_3 may be regarded as $CHCl_3$ with the H replaced by a CCl_3 group. In this case the CCl_3 group acts as if it were very electronegative, giving a coupling increase, 4.60 Mc., very much like a Cl substitution which gives a 4.87 Mc. increase. In $CHCl_2CCl_3$ there are chemically two kinds of chlorine, and five resonance lines are observed that group together in two sets with couplings of 77.74 and 79.91 Mc. The two line set,

(11) R. Livingston, *J. Chem. Phys.*, **20**, 1170 (1952).

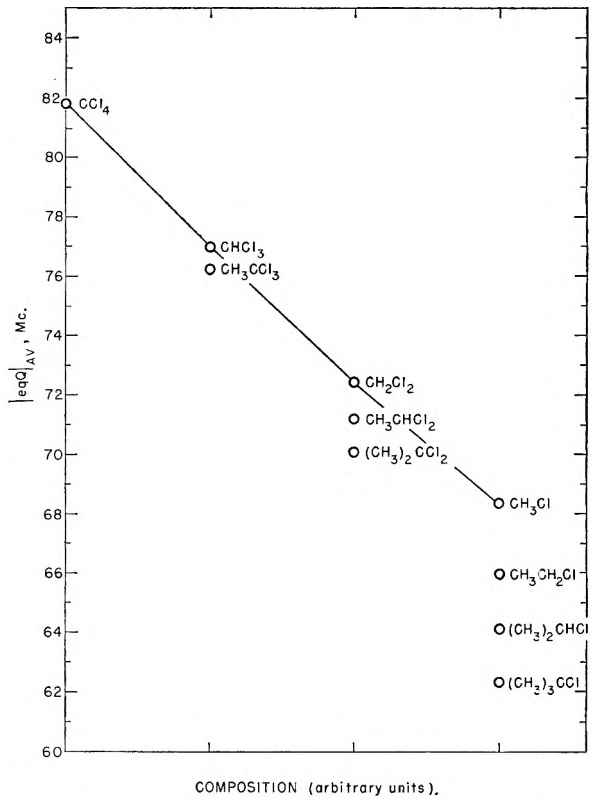

Fig. 2.—Cl^{35} quadrupole couplings in alkyl chlorides at 20°K.

77.74 Mc., appears to belong to the $CHCl_2$ part of the molecule for it can be considered to be like CH_2Cl_2 where one H is replaced by a CCl_3 giving a 5.27 Mc. coupling increase much like replacing the H by a Cl which gives a 4.51 Mc. increase. On the other hand the three line set, 79.91 Mc. appears to belong to the CCl_3 half of the molecule which can be derived from $CHCl_3$ where the H is replaced by a $CHCl_2$ group giving a smaller coupling increase of 2.93 Mc.

In CH_2ClCH_2Cl the coupling is very much like that in CH_3Cl indicating that replacing an H by a CH_2Cl group gives very little coupling change. The effectiveness of the various groups would be ranked as CCl_3 acting very much like electronegative Cl, $CHCl_2$ less, CH_2Cl still less and very much like H and finally CH_3 acting more electropositive than H.

The above comparisons of couplings have a parallelism in chemical observations. Such observations include the increased halogen reactivity in progressing from primary to secondary to tertiary alkyl chlorides, the CH_3 group often regarded as acting in an electropositive manner, and the ease of precipitating AgCl with $AgNO_3$ decreasing in the sequence CH_3Cl to CCl_4.

Relation of Coupling to Electronegativity Difference.—Figure 3 is a plot of the couplings for solids as a function of electronegativity difference.[10] The general trend of decreasing coupling with increasing electronegativity difference reflects the increase in ionic character in the halogen bond. The scattering of points may represent such complications as varying amounts of double bond character, s-hybridization, etc. For example, the

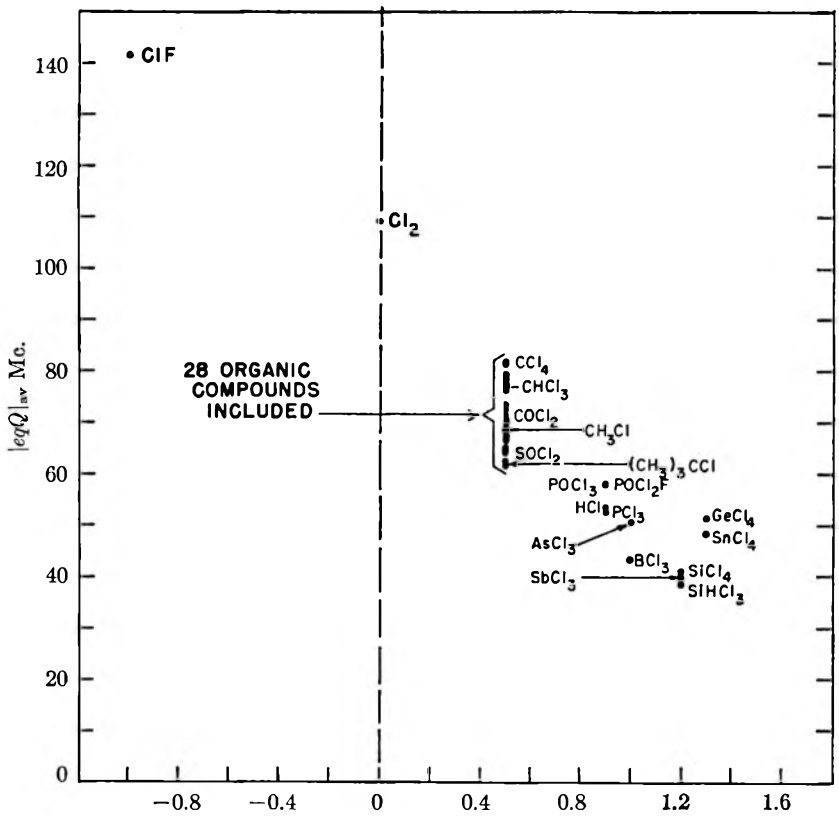

Fig. 3.—The ionic character trend in quadrupole couplings.

organic compounds are listed with an electronegativity difference of 0.5, implying the same ionic character for all of them. This is not the case since the previous discussion has indicated that there is a variation in ionic character among many of the compounds. An effective electronegativity difference somewhat different than 0.5 might have been used for many in order to take account of the formal charge[10] on the atoms in the appropriate resonating structures that one might write.

Comparison of Couplings in Solids with Gases.—Quadrupole couplings from microwave studies of gaseous substances are known for Cl^{35} in a few of the substituted methanes. The coupling in solid CF_3Cl is 0.6% lower than the microwave value of 78.05 Mc.[12] On the other hand the value for CH_3Cl is 9.0% lower than the microwave value of 75.13 Mc.[13] much like Dehmelt and Krüger's[14] values for Br in solid CH_3Br which is 8.3% lower than the microwave value and I in CH_3I which is 9.3% low.[5] The value for CH_2Cl_2 is about 7.6% lower than the microwave value of 78.4 Mc.[15]

The reasons for the departure of the solid from gas values is not understood. One approach has been to assume that in the substituted methanes the difference between the solid and gas values varies in a systematic way with composition, say with the number of hydrogen atoms in the molecule. This would follow from the above comparisons and from the argument that a uniform coupling trend has been found in the solids and a similarly uniform trend would be found if all the gas values were known. A possible mechanism might be a type of hydrogen bonding, but this could not be substantiated from the crystal structure determination made by Burbank[16] on solid CH_3Cl. Although the hydrogen positions were not found the use of reasonable parameters did not give a close approach of H to the nearest intermolecular neighbor, a Cl.

The couplings for Cl^{35} in $SiCl_4$ and $SiHCl_3$ (Table II) appear to be the start of a sequence like the chloromethanes. The extrapolated value for SiH_3Cl, roughly 34 Mc., is 15% lower than the microwave gas value of 40 Mc.[17]

Although caution must be exercised in comparing solid with gas values other cases of particular interest are Cl_2, CH_2-CHCl and ClF_3. The coupling for Cl^{35} in Cl_2 at 20°K. is 108.95 Mc.,[9] 0.7% lower than the value for Cl determined by the atomic beam method.[18] The closeness of these values suggests that a pure p-orbital is used in the Cl_2 bond. The value in solid vinyl chloride at 20°K. is 67.23 Mc.[19] in agreement with the gas value of 67 Mc.[20] computed along the bond direction. It has been pointed out[19] that the agreement indicates that the assumption that the bond direction is a principal axis of the field gradient tensor is a good one. This case is also of interest since it is found from the gas measurement that the field gradient departs from axial symmetry. The energy levels[19] for a quadrupolar nucleus in an asymmetric field gradient indicate that for moderate asymmetries the coupling is changed very little from the value found by taking twice the transition frequency. For vinyl chloride, ignoring the asymmetry in computing the coupling gives a negligible error. ClF_3 is probably an extreme case of field gradient asymmetry. Microwave measurements[21] have shown the molecule to have a planar, slightly distorted T structure with the in-plane principal components of the quadrupole coupling to be −65 and −81 Mc. giving +146 Mc. for the major component located normal to the plane. Using the above asymmetry and the frequency found in the solid (Table I) the computed coupling is 149.96 Mc. as compared to 150.26 Mc. found by taking twice the transition

(12) D. K. Coles and R. H. Hughes, *Phys. Rev.*, **76**, 858 (1949).
(13) W. Gordy, J. W. Simmons and A. G. Smith, *ibid.*, **74**, 243 (1948).
(14) H. G. Dehmelt and H. Krüger, *Z. Physik*, **129**, 401 (1951).
(15) R. J. Myers and W. D. Gwinn, *J. Chem. Phys.*, **20**, 1420 (1952).
(16) R. D. Burbank, *J. Am. Chem. Soc.*, **75**, 1211 (1953).
(17) A. H. Sharbaugh, *Phys. Rev.*, **74**, 1870 (1948).
(18) V. Jacarino and J. G. King, *ibid.*, **83**, 471 (1951).
(19) J. H. Goldstein and R. Livingston, *J. Chem. Phys.*, **19**, 1613 (1951).
(20) J. H. Goldstein and J. K. Bragg, *Phys. Rev.*, **75**, 1453 (1949).
(21) D. F. Smith, *J. Chem. Phys.*, in press.

frequency. Comparisons with gas values indicate that all couplings reported here have negative signs except the value for ClF_3.

Acknowledgments.—I have benefited greatly from many helpful discussions with H. A. Levy. The $(CH_3)_2CCl_2$ was synthesized by B. Benjamin, the sample of $POFCl_2$ loaned by H. Gutowsky, the $SiHCl_3$ furnished by the General Electric Company and the CF_2BrCl furnished by the Dow Chemical Company.

PURE QUADRUPOLE SPECTRA OF MOLECULAR CRYSTALS[1]

By Harry C. Allen, Jr.[2]

Mallinckrodt Chemical Laboratories, Harvard University, Cambridge, Massachusetts

Received January 14, 1953

Two radio frequency spectrometers suitable for investigation of pure quadrupole spectra are described. The first of these is a frequency modulated super-regenerative spectrometer which has a workable range of 20–40 Mc. The second spectrometer is a simple regenerative Zeeman modulation spectrometer with a workable range of 1–40 Mc. Information which can be obtained from pure quadrupole spectra of solids, such as intermolecular hydrogen bonding, phase transition detection, electron withdrawal ability of substituent groups and the correlation of Hammett's σ with the quadrupole coupling frequencies are discussed. Preliminary reports are made of the effect of substituting deuterium for hydrogen on the chlorine quadrupole coupling frequencies in two compounds.

Introduction

In two of the previous papers some experimental results have been presented and methods have been described by which these data may be used to obtain information concerning chemical bonding. In this paper apparatus will be described which is suitable these spectra, more data will be presented, and additional information which can be inferred from pure quadrupole spectra will be pointed out.

Apparatus.—In this Laboratory two radio frequency spectrometers are in use. Both of these spectrometers have been described in detail by the workers who designed them,[3] but it is felt that a brief description of the equipment is appropriate here.

A block diagram of the first of these spectrometers is shown in Fig. 1. It consists of a frequency modulated, externally quenched super-regenerative oscillator, the frequency modulation being at 30 c.p.s. The signal is detected, amplified and applied to the vertical plates of a cathode ray oscilloscope. The horizontal plates of the display oscilloscope are fed from a second output of the 30 c.p.s. generator which provides the modulation frequency. The quench voltage is obtained by squaring the output of a Hewlett–Packard audio oscillator. The quench frequencies giving the best results are in the range of 30–100 Kc. This spectrometer has a workable range of from 20–40 Mc., which is the range in which the spectra of most compounds containing covalently bonded chlorine are found.

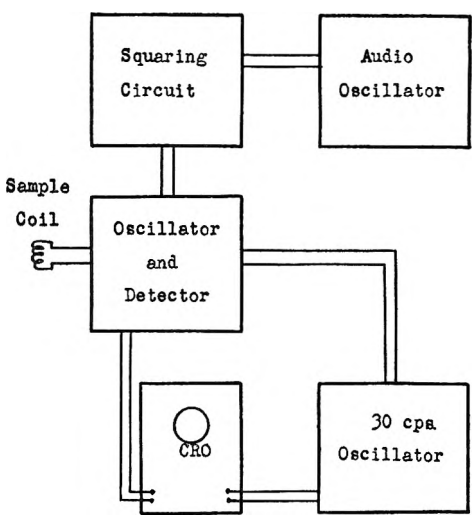

Fig. 1.—Block diagram of frequency modulated super-regenerative spectrometer.

The samples are sealed in two dram vials which are inserted directly in the coil of the oscillator tank circuit. The coils consist of a number of turns of bare No. 8 copper wire. When making temperature runs the sample and coil are immersed directly in a non-polar cooling bath, and temperatures are measured by means of a thermocouple or pentane thermometer. Figure 2 shows the absorption line in *p*-dichlorobenzene at room temperature. Considerable difficulty has been experienced with false signals at liquid nitrogen temperature. The source of these spurious signals seems to be in the low temperature dielectric properties of the amphenol connector used to connect the tank coil into the oscillator. This difficulty was largely overcome by heating the connector or keeping the connector sufficiently remote from the cooling bath. A true signal is easily distinguished from the false ones since a false signal is unaffected by a magnetic field.

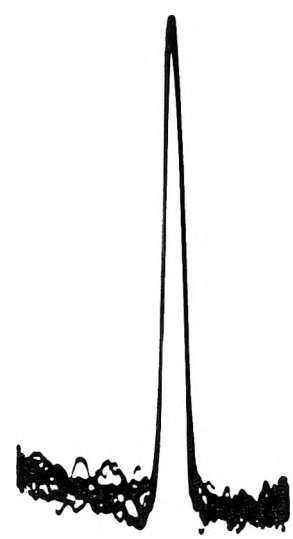

Fig. 2.—*p*-Dichlorobenzene resonance line at room temperature.

The second spectrometer is shown in the block diagram of Fig. 3. The main component is a simple regenerativ

(1) The research reported in this paper was supported in part by the Office of Naval Research under Contract N5ori-76, Task Order V.

(2) Atomic Energy Commission Postdoctoral Fellow.

(3) (a) C. Dean, Thesis, Harvard University, 1952; (b) G. D. Watkins, Thesis, Harvard University, 1952.

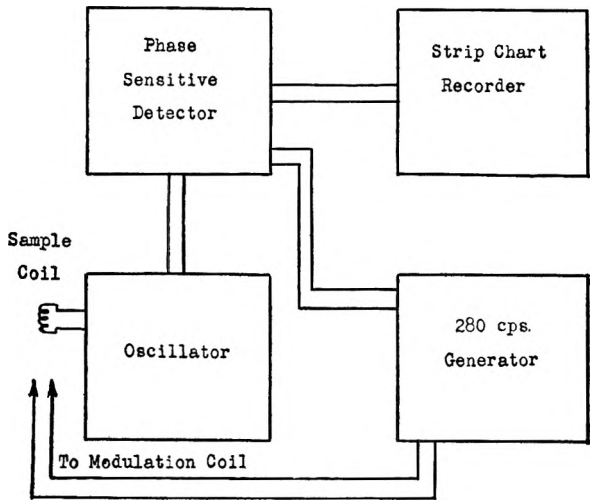

Fig. 3.—Block diagram of a Zeeman modulation spectrometer.

oscillator. In this spectrometer modulation is obtained by applying an on–off magnetic field to the sample, thus splitting the line into its Zeeman components while the field is applied and leaving the line undisplaced when the field is off. The signal is sent through a phase sensitive detector and displayed on a strip chart recorder. The modulation field is 280 c.p.s. square wave supplied by an oscillator which also supplies the reference voltage of the phase sensitive detector. The spectrometer is tuned through its range when searching by driving the tuning condenser with a one r.p.m. motor which is suitably reduced. In typical operation a reduction of 8000 is used which allows the use of an electrical filter on the output with a time constant of 10–20 seconds. This particular sweeping speed corresponds to about 300 c.p.m. The oscillator tank coil is about 30 turns of No. 32 Formax coated wire. The modulation coil is wound around a form large enough to hold a half-liter dewar flask, and is made of some 200 turns of No. 30 cotton covered wire. This spectrometer operates in the range of 1–40 Mc., hence it is suitable for work with chlorine-containing compounds and also for nitrogen-containing compounds, since the latter absorb in the region of 1–4 Mc. Figure 4 shows a trace of the nitrogen line in hexamethylenetetramine taken while sweeping at $^1/_{100}$ r.p.m. (about 6 Kc. per minute) with an electrical time constant of two seconds. The sensitivity of the super-regenerative spectrometer can be increased by a factor of from 5 to 10 by using magnetic modulation and strip chart recording. Frequencies are measured with a war surplus frequency meter set SCR 221 AC.

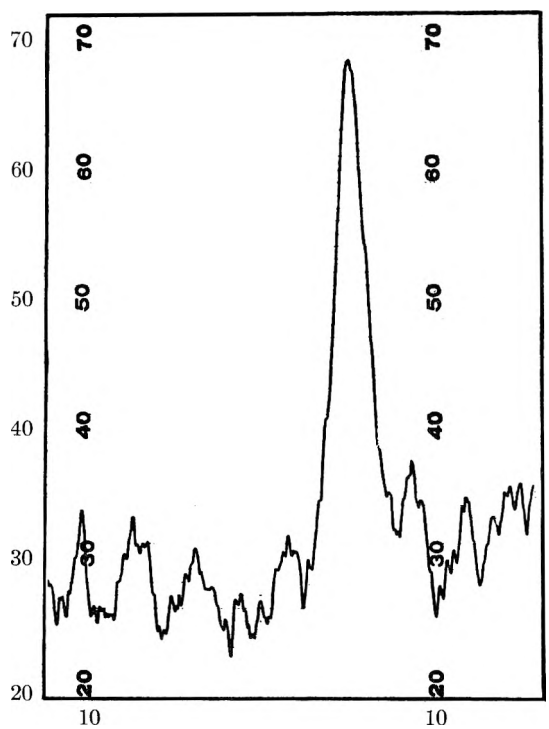

Fig. 4.—Nitrogen resonance in hexamethylenetetramine.

The chief advantage of the super-regenerative oscillator is that it furnishes a high level of r.f. power; hence it should be used to search compounds which are not easily saturated. Most compounds containing covalently bonded chlorine fall in this class. The disadvantages are that such oscillators are inherently noisy and unstable. In contrast the simple regenerative oscillators can be made to be very stable and relatively free from noise; however, they furnish a low r.f. level. This second spectrometer can be used to advantage for nitrogen resonances since these compounds can be saturated by this apparatus; thus there is nothing to be gained by going to a higher r.f. level. Searching with the super-regenerative is rather rapid, whereas it takes considerably longer to scan a comparable region with the simple regenerative apparatus.

Experimental Results

Table I shows the experimental results obtained for the chloroacetic acids and several related compounds.[4] The temperature dependence of the frequencies has been determined for these resonances and extrapolated to 0°K. in order to minimize the effect of lattice vibrations. From the extrapolated frequencies the quadrupole coupling constants have been calculated assuming cylindrical symmetry of the electric field gradient. Where multiple lines

TABLE I

OBSERVED FREQUENCIES, MC.

Compound	295°K.	196°K.	77°K.	eqQ_{av} Mc. extrapolated
$CH_2ClCOOH$	34.919	35.602	36.131	73.15
	35.461	35.981	36.429	
$CH_2ClCOOC_2H_5$		35.058	35.962	72.50
$CH_2ClCOCH_2Cl$	34.902	35.441	35.943	72.46
$(CH_2ClCHO)_3$	34.464	34.934	35.363	
	34.783	35.231	35.691	71.55
$CH_2ClCOCH_3$		34.452	35.075	
		34.461	35.484	70.98
$CH_2ClCONH_2$	34.227	34.599	34.882	70.06
$CH_2ClCOONa$	33.943	34.417	34.794	70.00
$CCl_3CH(OH)_2$	37.513	37.869	38.190	76.68
	38.699	39.086	39.429	
	38.784	39.167	39.515	79.25
CCl_3CONH_2		39.106	38.850	
		39.229	39.478	
		39.598	39.599	79.11[a]
			39.665	
			39.817	
			40.007	
CCl_3COOH			39.967	
			40.165	80.25[a]
			40.240	
CCl_3COCl			33.721	67.44[a]
			40.132	
			40.473	
			40.613	80.81[a]
$CHCl_2COOH$		37.436	37.979	
		38.163	38.807	

[a] 77°K.

(4) H. C. Allen, Jr., *J. Am. Chem. Soc.*, **74**, 6074 (1952).

were observed, and the splitting is small, an average of the observed lines was used to calculate eqQ. Small splittings are attributed to crystallographically non-equivalent atoms.[5] Splittings of greater than 0.5 Mc. must be attributed to a different type of chemical bonding to the chlorine atoms. The most extreme example is CCl_3COCl in which there are four lines, three near 40 Mc., due to the CCl_3 group, and the fourth at 33.7 Mc. due to the more ionic chlorine bonded to the carbonyl group.

A less drastic splitting occurs in chloral hydrate. In this compound three lines are observed. Two of these lines are separated by about 80 Kc. while the third is almost 1.25 Mc. lower than the other pair. This suggests that two of the bonds are about the same while the third is somewhat different. The crystal structure of chloral hydrate has been investigated by Kondo and Nitta,[6] their results showing three different C–Cl distances, 1.79, 1.78 and 1.72 Å. The two chlorines at the longer distances are presumably hydrogen bonded through the hydroxyl groups of adjacent molecules. Such an interpretation is consistent with the quadrupole resonance spectrum if the lowest frequency line is attributed to the non-hydrogen bonded chlorine while the two higher frequency and slightly split lines are attributed to the chlorines involved in hydrogen bonds. However, theoretical considerations indicate that the hydrogen bonded chlorines should have a lower frequency. In dichloroacetic acid two lines are observed which are separated by about 0.8 Mc. This is again too large to be caused by crystallographic differences, but in this case the decision as to the cause must await a crystal structure determination.

In several of the compounds investigated sharp discontinuities have been observed in the spectra as the temperature dependence has been measured. Although CCl_3COOH is a solid at room temperature no absorption was observed above $-158°$ and no lines were observed in CCl_3CONH_2 above $-43°$. Below this temperature CCl_3CONH_2 has three absorption lines down to $-158°$, but at $-196°$ six lines were observed. In *p*-dichlorobenzene[7] a sharp discontinuity was observed at about 35° which corresponds to a known phase transition. Presumably these other discontinuities correspond to phase transitions also, although no reference to them has been found in the literature.

If the frequencies of the monochloro compounds are considered, some information can be obtained concerning the electron withdrawal ability of the substituent groups. Since as the frequency of absorption increases, it is presumed that the ionic character of the bond decreases, then from a consideration of the observed frequencies it would be predicted that the electron withdrawal ability of the substituent groups increases in the order COO^-, $CONH_2$, $COCH_3$, $COCH_2Cl$, $COOC_2H_5$, $COOH$. This series is in agreement with that obtained on the basis of purely chemical evidence. Further evidence for this order comes from the shifts of the carbonyl frequencies in the infrared spectra of these compounds. The carbonyl frequency is presumably related to the charge on the carbon atom of this group in some manner. The same residual charge determines the electron withdrawal effect from the CH_2Cl group; hence one might expect a correlation between these two frequencies. Unfortunately these frequencies are not available for all these monochlorinated compounds but if the analogous non-chlorinated compounds[8] are considered, it is found that the C=O infrared frequencies increase in the same order as the coupling constants.

Another correlation that can be made is between the quadrupole coupling constant of substituted benzenes and Hammett's substituent constant σ.[9]

In a plot of eqQ *vs.* σ most of the points fall very close to a straight line. The points which are not on the line are for compounds in which there is resonance stabilization of the ring and in general this causes the correlation to fall down, although there are not very reliable values of σ in most of these cases.

In making these correlations one must be careful, because the quadrupole coupling constant determined from the pure quadrupole spectra of solids may differ by as much as 10% from that determined from the hyperfine structure of rotational spectra in the microwave region. Some comparisons between gaseous and solid state values are given in Table II. In the series pointed out here, the solid state effect is either practically a constant for all the compounds in these two series or it is very small, although it is entirely possible that some of the bad points on the eqQ *vs.* σ plot are due to solid state effects.

TABLE II

COMPARISON OF eqQ IN GAS AND SOLID

Compound	Gas, Mc.	Solid, Mc.
CH_3Cl	75.13	68.40
CH_2Cl_2	78.3	72.47
CF_3Cl	78.05	77.58
CH_2FCl	70.48	67.60
$CH_2{=}CHCl$	67.2	67.2

Recently, with the help of Mr. Harlan Meal, the pure quadrupole spectra of HCl and DCl have been measured. A single line was found for each chlorine isotope in each compound. The frequency of the Cl^{35} line in HCl is 26.469 mc. at $-196°$. Assuming cylindrical symmetry of the field gradient this gives a quadrupole coupling constant of 52.938 Mc.

The frequency in DCl, 27.309 Mc. at $-196°$, is somewhat higher. This might have been predicted for it is well known that by freezing out lattice vibrations one increases the absorption frequency. The lower zero-point energy of DCl may have the same effect as a freezing out of the lattice vibrations, and hence one would predict, on this basis, a higher frequency.

Robinson[10] has discussed the dipole moment of HCl and concluded that dipole moment data do not

(5) H. G. Dehmelt, *Z. Physik*, **130**, 356 (1951).

(6) S. Kondo and I. Nitta, *X Sen*, **6**, 53 (1950).

(7) C. Dean and R. V. Pound, *J. Chem. Phys.*, **20**, 195 (1952).

(8) Randall, Fowler, Fuson and Dangl, "Infrared Determination of Organic Structures," D. Van Nostrand Co., Inc., New York, N. Y., 1949.

(9) H. C. Meal, *J. Am. Chem. Soc.*, **74**, 6121 (1952).

(10) D. Z. Robinson, *J. Chem. Phys.*, **17**, 1022 (1949).

provide a good method of determining ionic character. It has been shown[11] that in some cases ionic character can be determined from quadrupole coupling constants. The two main contributing structures for HCl are H^+Cl^- and H–Cl. If the nature of the purely covalent part of the bond is established, then the ionic character of the bond can be calculated from *eqQ*. Assuming that the chlorine bonding orbital is pure p, one calculates a value of 52% for the ionic character, which seems unreasonably high. After considering the chlorine bond in several compounds, Townes and Dailey have concluded that the chlorine bonding orbital is 18% s and 82% p. On this assumption, and ignoring solid state effects, this leads to an ionic character of 40%. It is unlikely that the solid state effects are greater than 10%, and in all known instances are in a direction which would decrease the solid state frequency. If a 10% decrease is assumed in the case of HCl, one finds an ionic character of 36%, still considerably higher than any previously suggested value.

The pure quadrupole spectrum of $CH_2ClCOOD$ also has been measured. As in $CH_2ClCOOH$, two lines were found and the separation of the two lines is the same in both compounds, indicating the same crystal structure. However, the lines in the deuterated compound were shifted 20 kc. higher at −196°. This shift is undoubtedly caused by the difference between the O...H–O and O.... D–O bonds in the acid dimer which presumably exists in the solid state.

Acknowledgments.—The author wishes to thank Professor E. Bright Wilson, Jr., for many helpful discussions during the course of this work. He is also indebted to Mr. Harlan Meal for making certain unpublished data available.

(11) C. H. Townes and B. P. Dailey, *J. Chem. Phys.*, **17**, 782(1949).

PARAMAGNETIC RESONANCE ABSORPTION OF FREE RADICALS[1]

BY T. L. CHU, G. E. PAKE, D. E. PAUL, J. TOWNSEND AND S. I. WEISSMAN

Departments of Physics and Chemistry, Washington University, St. Louis, Mo.

Received January 19, 1953

The paramagnetic resonance behavior of a set of polyatomic free radicals is discussed. The effects of exchange, dipolar interactions and relaxation mechanism on line shapes are sketched. The appearance of hyperfine splittings in dilute solution of certain free radicals and the inferences which can be drawn from the splittings are presented.

This report will be limited in the main to a description of the paramagnetic resonance behavior of polyatomic free radicals. The range of splitting factors and crystalline anisotropies thus far observed among the polyatomic free radicals is much narrower than among the paramagnetic salts of the transition elements and rare earths. The splitting factors of a large number of free radicals cluster within a few tenths of 1% around the free electron value of 2.0023, while among the transition elements and rare earths, values ranging from one to six have been observed.

One reason for this difference probably lies in the complete removal of orbital degeneracy in the polyatomic free radicals, and the smallness of the spin orbit couplings existing in them. The absence of orbital degeneracy is necessitated in almost all organic free radicals by their low molecular symmetry. In the few cases where the symmetry permits orbital degeneracy the unpaired electron seems to occupy a non-degenerate orbital.[2,3]

A striking feature of the paramagnetic resonance spectra of many free radicals is their sharpness. In the crystalline state at room temperature line widths of only a few oersteds are common. In dilute solutions at room temperature individual lines as narrow as 0.5 oersted[4] are observed. The rare earth and transition element compounds both in the crystalline form and in liquid solution frequently exhibit bands hundreds or even thousands of oersteds wide at room temperature. For many of these substances only at liquid hydrogen or liquid helium temperature do the lines become as narrow as those of the polyatomic free radicals at room temperatures.[5]

A discussion of the reasons for the relative breadth of the lines in the two classes of substances requires some elaboration of the mechanism of line broadening. Limiting the sharpness of any line are the lifetimes of the quantum states involved in the transition which produces it. The breadth of the line in frequency units, cannot be less than the reciprocal lifetime of either of the states with which it is associated.[6] Any mechanism which shortens the lifetime of either of these states broadens the line. In the case of paramagnetic resonance interchange between magnetic energy of the oriented magnetic dipoles and thermal energy of the environment is one of the most prominent of the lifetime determining mechanisms. The characteristic time associated with this mechanism is usually called the thermal relaxation time. Ex-

(1) Assisted by the joint program of O.N.R. and A.E.C.

(2) In the later paper by Bleaney (p. 508) the manner in which residual orbital degeneracy and spin orbit couplings effect a large range in splitting factors has been described.

(3) Should the unpaired electron occupy a degenerate orbital, distortion of the molecule through the Jahn-Teller effect would remove the degeneracy.

(4) Solutions of metals in liquid ammonia possess even narrower lines; C. A. Hutchison and R. Pastor, *Phys. Rev.*, **81**, 282 (1951).

(5) Many examples are given by Lancaster and Gordy, *J. Chem. Phys.*, **19**, 1181 (1951).

(6) Discussions of these effects are included in most books on quantum theory. See for instance W. Heitler, "The Quantum Theory of Radiation," Oxford University Press, 1944, p. 110 f.

amples of line broadening through thermal relaxation are numerous. Many dilute solid solutions of paramagnetic ions in diamagnetic crystals have very broad lines at room temperature and fairly narrow lines at low temperatures. The line breadth at the higher temperatures is almost unquestionably determined by thermal relaxation effects.

Interchange of energy between magnetic and thermal varieties apparently may proceed by way of coupling through the orbital motion of the electrons. Vibrational motion of atomic nuclei and orbital motions are coupled through electrostatic interaction; electronic spins and orbital motion are coupled through spin orbit interaction.[7] It has been demonstrated that spin orbit interactions in many aromatic molecules are extraordinarily small.[8] The matrix elements of spin orbit interaction energy in these molecules appear to be smaller by several orders of magnitude than the corresponding matrix elements in atomic carbon. In all likelihood, the fact that many of the polyatomic free radicals possess thermal relaxation times sufficiently long, even at room temperature, to permit the occurrence of sharp lines is associated with these extraordinarily small spin orbit energies.

While the thermal relaxation mechanism determines a minimum line breadth, magnetic dipolar and exchange effects may intervene to yield considerable departures from the line shape which the relaxation mechanism alone would yield. The former influences the line shape through modification of the magnetic field at the site of each free radical molecule by the magnetic moments of its neighbors. The local magnetic fields at the positions of the various free radical molecules in solutions or crystals will thus be distributed over a range of values. A broadening of the observed line ensues.

The second effect, exchange, comes about through electrostatic interactions between free radical molecules. The electronic spins become involved in this interaction because of the exclusion principle.[9] A spin dependent coupling, although it may be so small as to make a negligible contribution toward chemical binding, may be large enough to yield observable modifications of the paramagnetic resonance spectrum. It has been demonstrated by Van Vleck[10] that the exchange effect between like molecules leads to bands which are narrower than those which are expected when dipolar broadening alone is considered.

A further modification of the spectrum is the hyperfine splitting which appears in consequence of the presence in the molecule of atomic nuclei which possess magnetic moments. This effect has been described in the preceding paper. A theoretical account may be found in the work of Abragam and Pryce.[11]

(7) The spin orbit coupling may be important in the absence of orbital magnetic moments. The effect may be described as a coupling between the electric dipole moment, which accompanies motion of the spin magnetic moment of the electron, and the electric field.

(8) (a) D. S. McClure, *J. Chem. Phys.*, **20**, 682 (1952); (b) M. Mizushima and S. Koide, *ibid.*, **20**, 765 (1952).

(9) See for instance J. H. Van Vleck, "Electric and Magnetic Susceptibilities," Oxford University Press, 1932, p. 316.

(10) J. H. Van Vleck, *Phys. Rev.*, **74**, 1168 (1948).

(11) A. Abragam and M. H. L. Pryce, *Proc. Roy. Soc. (London)* **205**, 135 (1951).

Most of the results to be presented here were obtained at 9000 megacycles per second. High sensitivity was achieved through modulation of the magnetic field and phase sensitive detection. This technique presents the first derivative of absorption with respect to field as a function of field.

A large number of polycrystalline free radicals have been examined. These are listed in Table I. Anomalous behavior among the substances in this list is exhibited by Wurster's blue perchlorate. The intensity of the absorption is very small at liquid nitrogen temperature, rises rapidly to a maximum at about 190°K. and decreases normally with increasing temperature above 190°K.

TABLE I

SOME FREE RADICALS WHICH EXHIBIT PARAMAGNETIC RESONANCE ABSORPTION

Free radical	g value	Line width, oersteds[a]
I. Polycrystalline free radicals		
Diphenylpicrylhydrazyl	2.0037[b]	1.9
Tris-*p*-nitrophenylmethyl	2.0037	0.7
Tri-*p*-xenylmethyl	2.0031	5.7
Di-*p*-xenylphenylmethyl	2.00	Several oersteds
Wurster blue perchlorate	2.003	2.7
Tetramethylbenzidine formate	2.00	3.4
Tetraphenylstibonium-peroxylamine disulfonate	2.00	100
Porphyrindine	2.001	10.7
Kenyon and Banfield's radical	2.000	8.9
Dianisyl nitric oxide	2.00	Several oersteds
Triphenylamine perchlorate	2.003	2
Biphenylenetriphenylethyl	2.00	5
II. Dilute solutions		
Naphthalene negative ion	2.00	10 (hyperfine splitting)
Anthracene negative ion	2.00	10
Napthacene negative ion	2.00	10
Difluorenyl nitrogen	2.00	11 (hyperfine splitting)
Nitrobenzene + Na	2.00	25 (10 peaks)
m-Dinitrobenzene + Na	2.00	25 (8 peaks)
1,3,5-Trinitrobenzene + Na	2.00	25 (8 peaks)
2,4,7-Trinitrofluorenone + Na	2.00	25
Tris-*o*-anisylmethyl	2.00	...
Chlorine dioxide	2.00	50
Tetraphenylhydrazine perchlorate	2.00	Several oersteds
Tetramethylbenzidine perchlorate	2.00	Several oersteds
Benzophenone anil-sodium	2.00	Several oersteds
Di-(dimethylamino)-diphenylnitrogen	2.00	Several oersteds

[a] Line widths are given as width between points of extreme slope. [b] Hutchison's value.

In all the cases listed, with the exception of the salts of peroxylamine disulfonate, the line breadths are considerably smaller than those anticipated from dipolar broadening. No exact estimates of the dipolar broadening can be made in the cases cited because crystal structures of the substances are not known. Nevertheless, very conservative assumptions would lead to line breadths of at least one hundred oersteds. We may conclude

that in the cases cited, the exchange effects are important.[12]

Although the dipolar and exchange effects are of great intrinsic interest, their operation in crystals or concentrated solutions tends to obscure the features of the spectra which are characteristic of the individual free radical molecules. In very dilute solution (liquid or solid) both obscuring effects become small, and characteristics of individual molecules become observable. A good example is provided by the peroxylamine disulfonate ion. A polycrystalline mass of tetraphenylstibonium peroxylamine disulfonate yields broad bands about one hundred oersteds wide. A solution of the same substance in chloroform at a concentration of 0.001 M yields a spectrum of three lines of equal intensity and equal spacing. The interval between adjacent peaks is 13 oersteds; the individual peaks are less than 0.5 oersted wide. A reproduction of the spectrum is given in Fig. 1. With increasing concentration, the lines broaden, finally merging into a single broad line.

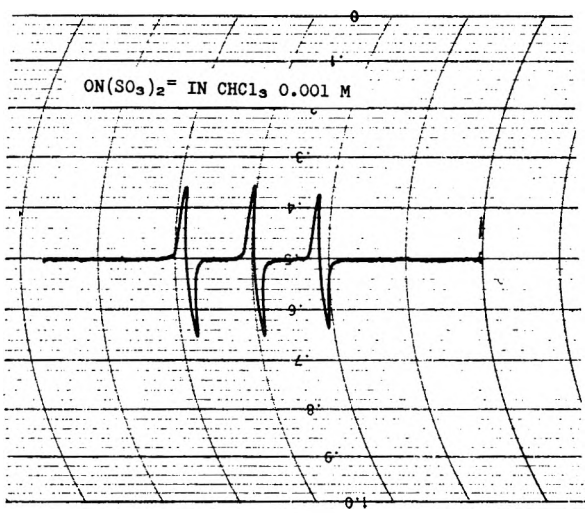

Fig. 1.—Spectrum of peroxylamine disulfonate ion.

The appearance of three lines in the spectrum of peroxylamine disulfonate ion is unquestionably a result of interaction magnetic moment of the nitrogen nucleus with the magnetic moment of the electron. N^{14}, a nucleus of spin one, is the only abundant isotopic species in the molecule possessing a nuclear magnet moment. The magnetic interaction of a nucleus of spin one with the electronic spin leads, at high magnetic fields,[13] to a spectrum of three equally spaced equal intensity lines. At lower fields, a change in the nature of the spectrum occurs. The positions of the energy levels and absorption lines at various field systems of two interacting magnetic moments have been calculated.[14] Only one parameter, the coupling constant for the interaction between nuclear and electronic spins, is required for prediction of the entire field dependence of the levels and the spectrum. This parameter may be easily evaluated from a single measurement at the spectrum at a high field. In Fig. 2 are given the measurements at fields ranging upward from a small fraction of an oersted. The curves are those computed from the Breit–Rabi treatment. The agreement between the measured frequencies and the predicted values is good and leaves little question concerning the validity of the interpretation.

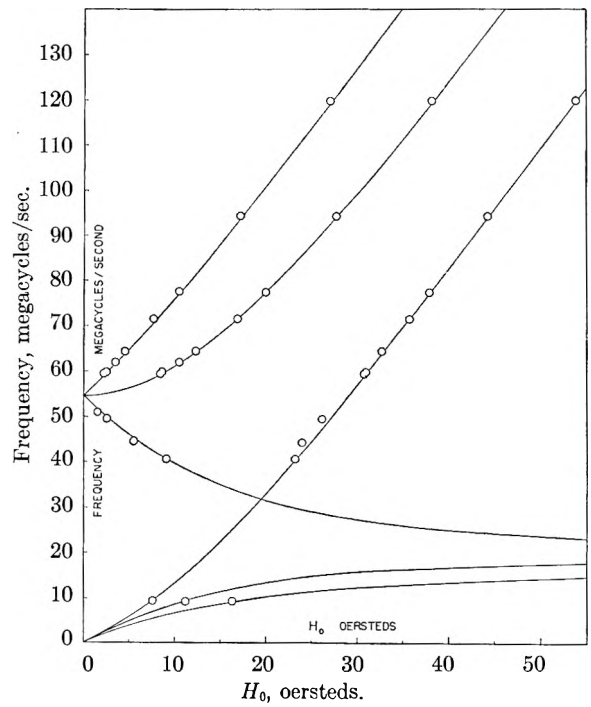

Fig. 2.—Field dependence of spectrum of peroxylamine disulfonate ion.

The magnitude of the coupling constant between electronic magnetic moment and the magnetic moment of a nucleus in a free radical molecule is dependent on the behavior of the electron in the vicinity of the nucleus. Any "s" component in the electronic wave function about a particular nucleus leads to an isotropic interaction, dependent on the magnitude of the electronic wave function at the nucleus. This part of the nuclear interaction is independent of orientation of the molecule in the external magnetic field. It is certainly observable in a randomly oriented set of molecules such as are encountered in solution.

Components of the electronic wave function other than "s" lead to a hyperfine splitting whose magnitude may depend on the orientation of the molecule in the external field. This part of the interaction is observable in single crystals. An understanding of its behavior in solutions requires further experimental and theoretical work.

Despite the aforementioned uncertainty in the interpretation of hyperfine splittings, conclusions of chemical significance may be drawn from the observed splittings in dilute solution. When hyperfine splittings appear, the unpaired orbit must come close to the appropriate nuclei, and certain deductions concerning the closeness of approach to these nuclei may be made. When hyperfine splittings are absent it may not be clear

(12) Exchange interactions of the order of one wave number are capable of producing the effects described.

(13) A high field is one which is substantially greater than the magnetic field produced by the nuclear moment at the electron. The latter field in our case is of the order of 10 oersteds.

(14) G. Breit and I. Rabi, *Phys. Rev.*, **38**, 2082 (1931).

whether their absence is to be ascribed to the electron's avoidance of the appropriate nuclei or to cancellations of the non "s" part of the interaction. From the spectra of single crystals, dilute in the magnetic constituent, it should be possible to extract more information than from the spectra of liquid solutions.

The number of cases thus far reported of hyperfine splittings in dilute solutions is rather small. In addition to the peroxylamine disulfonate ion and diphenylpicryl hydrazil,[15] we may describe a few others. The free radicals produced when nitrobenzene, *m*-dinitrobenzene, and 1,3,5-trinitrobenzene are treated with alkali metals in 1,2-dimethoxyethane as solvent have complex spectra. Thus a spectrum of at least ten peaks, covering about 25 oersteds is observed from the nitrobenzene free radical. Eight peaks are observed from the *m*-dinitrobenzene radical (Fig. 3). The trinitrobenzene radical also has a spectrum with eight peaks, but of different spacing and intensity distribution from the dinitrobenzene radical spectrum. No detailed analysis of these spectra has as yet been made. but it seems certain that interaction with both nitrogen and hydrogen nuclei must be taken into account.

The free radical negative ion of naphthalene at concentrations lower than 10^{-4} *M* also reveals a complex spectrum. An incompletely resolved spectrum, about 10 oersteds wide, contains at least eight peaks.[16] These peaks must arise from interactions between the electronic moments and the proton moments. The interactions are very small, corresponding to average separations between electrons and protons in the neighborhood of two ångströms. If the splittings are produced by a small non-vanishing component of the electronic wave function at the hydrogen nuclei, only a very small admixture of hydrogen "s" function is required.[17]

Another instance of the same kind is seen in difluorenyl nitrogen. The absorption band in dilute solution is about 11 oersteds wide, and although but poorly resolved, reveals at least twelve peaks. Part, if not all, of this splitting must come from interaction with protons. The interaction with the nitrogen nucleus, if it is present at all, must be much smaller than in peroxylamine disulfonate or diphenylpicrylhydrazyl.

(15) C. A. Hutchison, Jr., R. C. Pastor and A. G. Kowalsky, *J. Chem. Phys.*, **20**, 532 (1952).

(16) D. Lipkin, D. E. Paul, J. Townsend and S. I. Weissman, *Science*, in press.

(17) The splitting from a pure hydrogen "1s" function is over five hundred oersteds.

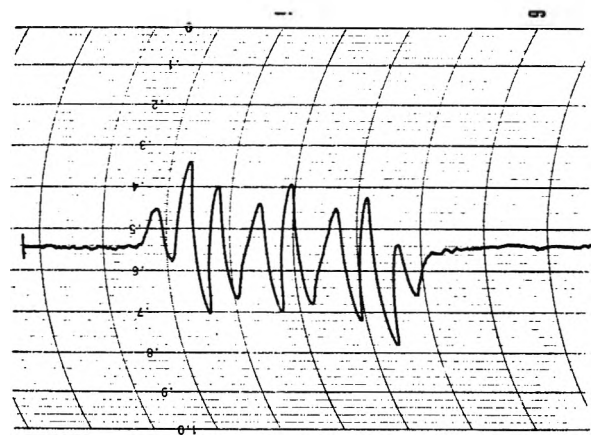

Fig. 3.—Spectrum of free radical derived from *m*-dinitrobenzene.

DISCUSSION

R. A. OGG (Stanford University).—Has electronic paramagnetic resonance been observed in liquid oxygen or in solutions containing O_2?

S. I. WEISSMAN.—Paramagnetic resonance has been observed in gaseous oxygen. I don't know about liquids or olutions.

B. BLEANEY (Clarendon Laboratory).—The absorption bands appear to be smeared out past detection in the liquid state. Resonance from oxygen in liquid air cannot be detected, nor can it in solution.

R. A. OGG (Stanford University).—Has electronic paramagnetic resonance been observed in the alkali metal superoxides such as NaO_2 and KO_2?

S. I. WEISSMAN.—We looked for paramagnetic resonance in the superoxides and found none. Apparently the resonance is too broad for detection in our apparatus. One should look at dilute solid solutions of the superoxides in peroxides.

G. K. FRAENKEL (Columbia University).—What was the concentration of the free radical solutions in which hyperfine structure attributable to protons was observed?

S. I. WEISSMAN.—Lower than 10^{-4} molar.

J. R. SCHAEFGEN (Experimental Station, du Pont and Co.).—Can electronic paramagnetic resonance be observed in gases?

S. I. WEISSMAN.—Yes. It has been observed by Beringer in nitric oxide, oxygen and atomic hydrogen.

J. R. SCHAEFGEN.—Has electronic paramagnetic resonance been found in the unstable free radical intermediates postulated for many chemical reactions; *i.e.*, would it be possible to measure the steady state concentration of free radicals in reactions such as addition polymerizations?

S. I. WEISSMAN.—Yes, Lipkin has found paramagnetic resonance in styrene as it was undergoing polymerization, initiated by metallic sodium. However, the results have not been reproducible.

PARAMAGNETIC RESONANCE IN THE SOLID STATE

BY B. BLEANEY

Clarendon Laboratory, Oxford, England

Received March 17, 1953

In paramagnetic resonance, magnetic dipole transitions are observed between the various Zeeman components of a given atomic level. In a field of a few thousand gauss such transition lines occur at wave lengths of a few centimeters, and they may be used to investigate the magnetic properties of ions of the transition elements in the solid state. Such properties comprise the spectroscopic splitting factor g, fine structure of the Zeeman levels and hyperfine structure when the nucleus of the paramagnetic ion has a non-zero spin. Both g and the hfs are anisotropic, their magnitude depending on the direction of the external magnetic field relative to the crystal axes, and a separate spectrum is observed from each type of ion. Much more detailed information is therefore obtained than from susceptibility measurements, which are determined by the gross effect of all types of ion. The transition groups principally investigated are the 3d and 4f groups. Of special chemical interest is information on the binding of copper salts and complex salts such as cyanides of the type $K_3Fe(CN)_6$. Preliminary work on other transition groups (4d, 5d, 5f-6d) will be reported.

1. Introduction

Substances may be divided into two classes, diamagnetic and paramagnetic, according as their magnetic susceptibility is negative or positive. Broadly speaking, the latter class consists of substances containing permanent magnetic dipoles of electronic origin which are free to orient themselves in an external magnetic field. Such permanent magnetic dipoles arise only in atoms or ions containing incomplete electron shells. Most chemical compounds consist of ions or complexes with complete electron shells and are therefore diamagnetic, but exceptions arise when compounds are formed of elements belonging to the "transition groups." These groups may be conveniently designated by the quantum number of the incomplete shell, and consist of the following: 3d, 4d, 4f, 5d, 5f-6d. A few other cases of paramagnetism arise, such as the gases oxygen and nitric oxide, defective crystal lattices containing unpaired electron spins, and free radicals. This review will be confined to resonance phenomena in solid compounds of the transition groups.

If the atomic dipoles were completely free to orient themselves in an external magnetic field, the susceptibility would follow Curie's law down to the absolute zero of temperature. We should have then

$$\chi = N\mu^2/3kT = Ng^2\beta^2J(J \times 1)/3kT \qquad (1)$$

for a dipole moment μ associated with an ion of resultant angular momentum J and Landé factor g (β is the Bohr magneton $= ch/4\pi mc$). In fact Curie's law cannot hold right down to the absolute zero, since this would constitute a violation of the third law of thermodynamics (adiabatic demagnetization of a paramagnetic salt to zero field would then make it possible to reach the absolute zero). Departures from Curie's law occur at temperatures where kT is of the same order as the energy of interaction between the paramagnetic ion and its surroundings. These interactions may be divided into two classes, interaction with neighboring paramagnetic ions and interactions with neighboring diamagnetic ions. The former class contains two types of interaction, magnetic dipole–dipole interaction, varying with the inverse cube of the distance between the ions, and exchange interaction, which falls off rather more rapidly with distance. Both these types of interaction are reduced by using "dilute" paramagnetic salts which contain a large ratio of diamagnetic to paramagnetic ions, so that the distance between paramagnetic ions is increased. If this distance is greater than about 5 Å., the mutual interaction energy is generally smaller than that between an individual ion and an external magnetic field (assumed to be of the order of a few kilogauss) so that in the first approximation mutual interactions may be neglected. In more concentrated salts they give rise to ferromagnetism and anti-ferromagnetism, with which we shall not be concerned. In solids and liquids, interaction with neighboring diamagnetic ions cannot be reduced, since the distance to such ions is always of the same order as the ionic radii. The interaction is determined by the nature of the chemical binding between the ion and its neighbors, and influences the magnetic behavior of the ion profoundly. This is particularly true in cases where the valence electrons belong to the same electronic shell as those responsible for the paramagnetism. The effect of a change of valency is obviously of prime importance, since the magnetic properties of an ion are primarily determined by the number of electrons in the unfilled shell. The nature of the binding—which varies from ionic to covalent—is of equal importance, since it also affects the number of unpaired electrons. A satisfactory qualitative explanation of the magnetic properties of many covalently bound ions is provided by the valence bond theory of Pauling, and it is to be expected that the method of molecular orbitals would yield similar results, though it has not been extensively used for this purpose. A third approach to the problem of a paramagnetic ion in its surroundings is provided by the crystalline field method of Van Vleck.[1] This has mostly been used for cases of ionic binding, but it has been shown[2] that when applied to covalently bound complexes it gives results equivalent to those of the two previous methods. As it is the only method which has been applied in quantitative detail, the discussion in this paper will proceed in terms of the crystalline field theory.

2. Outline of the Crystalline Field Theory

In the theory of paramagnetism a large number of interactions must be considered. Fortunately, most of these are of different orders of magnitude, so that perturbation methods may be used. No

(1) J. H. Van Vleck, *Phys. Rev.*, **41**, 208 (1932); R. Schlapp and W. G. Penney, *ibid.*, **42**, 666 (1932).

(2) J. H. Van Vleck, *J. Chem. Phys.*, **3**, 807 (1935).

detailed account of these can be given here, but in order to follow the theory qualitatively the nature of these interactions will be outlined, and their usual magnitude indicated. In order of decreasing magnitude these are, for a free ion, as follows: (a) the coulomb interaction of the electrons with the nucleus and with each other (of order 10^5 cm.$^{-1}$); (b) magnetic interaction between the electron spins and the orbits, of which the most important is the spin-orbit coupling, of order 10^2 to 10^3 cm.$^{-1}$; (c) interaction with an external magnetic field, of order 1 cm.$^{-1}$.

If the nucleus of the paramagnetic ion does not have zero spin, the following interactions must also be considered: (d) interaction between the magnetic dipole moment of the nucleus and the magnetic field set up by the orbital and spin moments of the electrons (of order 10^{-2} cm.$^{-1}$); (e) interaction between the nuclear electric quadrupole moment and the electric field gradient at the nucleus set up by the electron cloud (of order 10^{-3} cm.$^{-1}$ or smaller); (f) interaction between the magnetic dipole moment of the nucleus and the external magnetic field (of order 10^{-4} cm.$^{-1}$).

For an ion bound in a solid, the effect of interaction with its neighbors is introduced in the form of an electrostatic potential V acting on the electrons of the paramagnetic ion through their electric charge. This potential is due to the neighbors, and can be expanded in a series of spherical harmonics, of the form

$$V = \Sigma A_n^m r^n Y_n^m(\theta, \phi)$$

Here r is a radial coördinate with origin at the nucleus of the paramagnetic ion, and A_n^m is a coefficient of the order of $a^{-(n+1)}$, where a is the distance from the nucleus of this ion to the neighboring ions. The coefficients A_n^m cannot be determined with any precision owing to lack of detailed knowledge of the charge distribution in the surroundings, though some of them may be shown to be zero by consideration of the symmetry properties of this distribution. In addition the series is not rapidly converging but fortunately only the first few terms introduce non-zero elements in the magnetic theory.

The effect of this potential is to introduce an interaction term $\Sigma - eV$, where the summation is over all the electrons of the paramagnetic ion. In treating its effect it is first necessary to decide how its order of magnitude compares with the interactions listed previously for a free ion. Three distinct cases have been considered:

(i) The effect of the crystalline field is less than the spin-orbit interaction but large compared with (c, d, e, f) above. This is the situation in the rare earth group. To a first approximation J remains a good quantum number, but the $2J + 1$ degeneracy corresponding to the spatial orientations of J is lifted. The splittings are of the order of 200 cm.$^{-1}$ or less, so that at room temperature all levels are occupied and the susceptibility is roughly the same as for a free ion.

(ii) The effect of the crystalline field is large compared with the spin orbit coupling but small compared with the electrostatic interactions (a). This is the situation in most hydrated salts of the iron group. J is no longer a good quantum number, and the $2L + 1$ degeneracy of the orbital levels is lifted, the over-all splitting being of the order of 10^{-4} cm.$^{-1}$. The spin levels are affected only indirectly through the mechanism of the spin–orbit coupling. If an orbital singlet lies lowest, and the next orbital level is well above it ($\gtrsim 10^3$ to 10^4 cm.$^{-1}$ higher), the orbital contribution to the magnetism is substantially zero, while that from the spin has its full value. The susceptibility is close to the spin-only value, and follows Curie's law from room temperadown to 1°K. or lower. If the splitting of the lowest orbital levels is comparable with the spin–orbit coupling, considerable departures from Curie's law and the spin-only value of the susceptibility result.

(iii) The interaction of the ion with its neighbors is of the same order or larger than the coulomb interaction between electrons within the ion, but smaller than the coulomb interaction between these electrons and the nucleus. In this case the binding between the ion and its neighbors is "covalent" rather than "ionic," and the crystalline field method, though adequate to a first approximation, has not been fully explored and tested. This case is typified by the iron group cyanides, and by many compounds of the 4d and 5d groups.

Understanding of these three cases may be assisted by reference to three typical cases. Figure 1 shows the energy levels of the trivalent cerium ion, which has one electron in the 4f shell. Under the influence of the spin–orbit coupling the ^2F state splits into two states with total angular momentum $J = 5/2$ and $7/2$, respectively. The latter lies higher by about 2250 cm.$^{-1}$, and so is not populated at room temperature. In a solid the crystalline field splits the levels further, the values shown in the diagram being for cerium ethyl sulfate, where the field is assumed to have C_{3h} symmetry. At room temperature all the three lowest levels are populated and the susceptibility is close to that of the free ion.

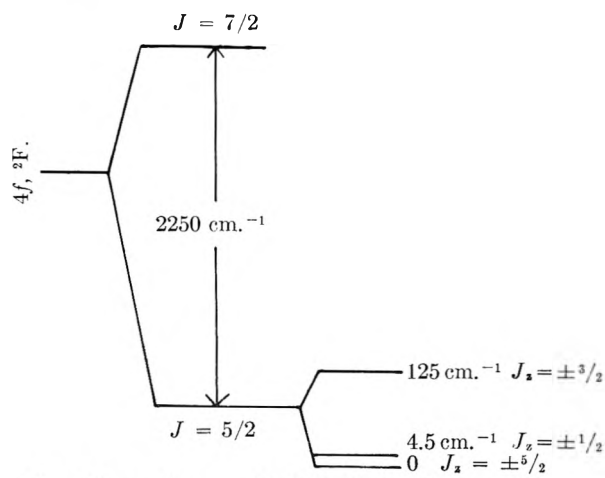

Fig. 1.—Energy levels of the Ce^{+++} ion. The values of the splittings for cerium ethyl sulfate are from ref. 32. The designations of the states as $J_z = \pm 1/2, \pm 3/2, \pm 5/2$ are correct only in a first approximation.

A typical example from the iron group is shown in Fig. 2 The Cr^{+++} ion in a hydrated compound

such as an alum is surrounded by an octahedron of water molecules, very nearly regular in shape. The crystalline field has therefore very nearly cubic symmetry, and the sevenfold orbital levels are split into a singlet ground state, and two triplets lying some 10^4 cm.$^{-1}$ higher. Under the combined effect of spin–orbit coupling and a crystalline field component of less than cubic symmetry the fourfold spin degeneracy of the orbital singlet is lifted, giving two doublets with a very small separation. The Co^{++} ion has three holes in the 3d shell and is thus also in a ^4F state, but the levels in such a cubic crystalline field are inverted, giving an orbital triplet lowest. This is split only by a few hundred cm.$^{-1}$ by the spin–orbit coupling and crystal fields of low symmetry.

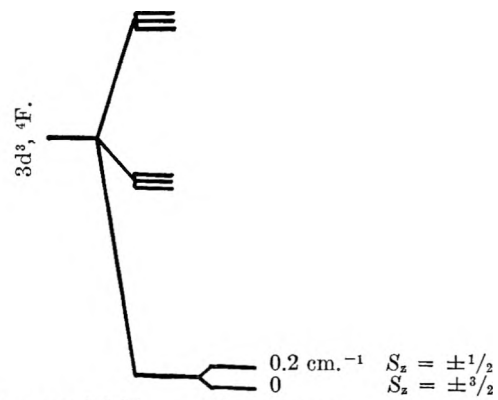

Fig. 2.—Energy levels of the Cr^{+++} ion in the solid state.

With covalent bonding, each individual electron is regarded as moving in an electrostatic field which replaces in a first approximation the interactions between the different electrons. For ions such as Fe^{+++} in $K_3Fe(CN)_6$ this field has very nearly cubic symmetry, which lifts[2] the fivefold orbital degeneracy of a d-electron to give a lower triplet state and a higher doublet state as in Fig. 3. The electrons in the complex go into these levels independently, subject to the exclusion principle. For the ferric ion, $3d^5$, one hole is left in the triplet so that the ion behaves as if it had spin $1/2$. The cobaltic ion, $3d^6$, on the other hand is diamagnetic, the six electrons just filling the triplet. The well known anisotropy of $K_3Fe(CN)_6$ is due to fields of lower than cubic symmetry, which, together with the spin–orbit coupling, split the triplet.[3] This anisotropy has recently been investigated by resonance measurements.[4]

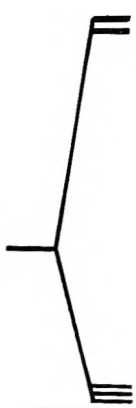

Fig. 3.—Splitting of energy levels of a d-electron in a cubic crystalline field.

The magnetic behavior of a paramagnetic ion depends on the way in which its energy levels vary when an external magnetic field is applied. In the presence of any crystalline electric field (except for the trivial case of a field of spherical symmetry), this variation in general depends on the orientation of the external field with respect to the axes of the crystalline field. If the latter has less than cubic symmetry, the susceptibility of the ion will be anisotropic, with principal axes the same as those of the crystal field. This anisotropy is not necessarily the same as observed in a crystal, since the susceptibility is the gross effect of all the ions in unit cell. Thus a cubic crystal such as $Co(BrO_3)_2 \cdot 6H_2O$ is necessarily isotropic, though the individual Co^{++} ions have a susceptibility which is 10 times as large along a trigonal axis as perpendicular to it. If the crystal field itself has cubic symmetry, the susceptibility of each ion will be isotropic, though departures from Curie's law may exist due to splittings of the energy levels. The susceptibility of a crystal gives therefore only limited information about the behavior of the paramagnetic ions, and moreover few measurements over a sufficiently wide temperature range on single crystals have been carried out. This constituted a hindrance to the advance of the theory, which was removed by the advent of resonance measurements. Each type of paramagnetic ion gives its own resonance spectrum, and precise data for each ion may be obtained, though such data are usually restricted to the ground state. A further advantage is that impurities do not affect the results, whereas they may introduce important errors in susceptibility measurements.

3. The Resonance Phenomenon

When a free ion of resultant angular momentum J is placed in a magnetic field H, the levels corresponding to the various spatial orientations of J have energies equal to $Mg\beta H$, where M is the electronic magnetic quantum number and β is the Bohr magneton. If a radiofrequency alternating magnetic field is applied at right angles to H, magnetic dipole transitions may be induced, according to the selection rule $\Delta M = \pm 1$, by quanta of frequency ν such that

$$h\nu = g\beta H \qquad (2)$$

Transitions in either direction between any pair of levels have equal *a priori* probability, but in a system in thermal equilibrium with its surroundings, the state of lower energy has the greater population, and transitions from this to the upper state occur correspondingly more often than *vice versa*. The net result is a gain of energy from the r.f. field, and a shift toward more equal population of the levels. The phenomenon can be detected by the loss of energy from the radiation field, which causes a damping of the tuned circuit in which the paramagnetic substance is placed.

This brief outline of the resonance phenomenon shows that it is exactly similar for electrons and for nuclei, but in the former case the resonance condition (2) contains the Bohr magneton rather than the nuclear magneton. Experiments are therefore carried out at correspondingly higher frequencies, of the order of 1,000 to 30,000 Mc./sec. using fields of a few kilogauss. For a free ion, as in the simple case assumed above, determination of the frequency and the field gives the Landé splitting factor g, and (2) may be rewritten in the convenient form

(3) J. B. Howard, *J. Chem. Phys.*, **3**, 813 (1935).

(4) B. Bleaney and D. J. E. Ingram, *Proc. Phys. Soc.*, **A65**, 953 (1952).

$$g = 21.4178/(H\lambda) \qquad (3)$$

where H is measured in kilogauss and λ is the wave length of the applied radiation in centimeters.

The methods of detection of paramagnetic resonance are basically the same as those used for nuclear resonance, the chief difference being the use of centimeter wave techniques. Radiation is generated by klystron oscillators (triodes have also been used for wave lengths longer than about 15 cm.), and is detected by means of silicon–tungsten crystal rectifiers (special bolometers for this purpose also have been used).[5] Radiation is fed through wave guides or co-axial lines to a loosely coupled cavity resonator. The paramagnetic sample is placed in this cavity in a region of maximum r.f. magnetic field strength. At room temperature many substances, particularly solids containing water of crystallization, show large dielectric losses, and to avoid large damping of the cavity resonance they must be kept out of the r.f. electric field as much as possible. At low temperatures such losses diminish, and are generally negligible below 90°K.

Since a cavity is very sharply resonant (the value of Q is several thousand), and microwave apparatus is generally rather frequency sensitive, it is impracticable to work at constant magnetic field and sweep the frequency of the applied radiation through resonance. Instead measurements are made at constant frequency, and the external magnetic field is varied so as to pass through the resonance point. The damping of the cavity due to the magnetic absorption may be detected either by a transmission or a reflection method. In the former a small part of the power in the cavity is fed out through a second loose coupling to the crystal detector, while in the latter the damping causes a change in the amplitude of the wave reflected from the input to the resonator. With specimens of mass 0.1 to 1 gram of ordinary paramagnetic salts, the power absorbed by the specimen at resonance is comparable with that dissipated in the resistive heating of the cavity, and substantial changes in the power reaching the detector occur. These may be plotted as the field is slowly varied through resonance. With weak lines the external field is wobbled at a low audiofrequency (*e.g.*, 50 c./sec)., and if resonance is present a corresponding modulation of the power at the detector occurs which is amplified after detection. If the amplitude of the "wobble" is large compared with the line width, the spectrum may be displayed on an oscilloscope if it is sufficiently intense. This requires an amplifier band-width of the order of 10 kc./sec. and in order to increase the sensitivity narrower band-widths may be employed. The wobble is then reduced to a fraction of the line-width in amplitude, and a lock-in amplifier used whose output may be traced on a pen-recorder as the magnetic field is slowly traversed through resonance. As silicon–tungsten crystal rectifiers have an abnormally large noise output at audiofrequencies, extra sensitivity can be obtained by using a super-heterodyne system of detection with a high intermediate frequency amplifier. It is then necessary to use a balance system to reduce the level of the microwave power reaching the detector.

(5) R. Beringer and J. G. Castle, *Phys. Rev.*, **78**, 581 (1950).

4. Fine Structure and the Spin Hamiltonian

In view of the fact that the interaction of the electron with the crystalline electric field is generally much greater than that with an external magnetic field, it might be thought that comparison with a free ion in a magnetic field is so far from reality as to be useless. It is true that the influence of the crystalline electric field is profound, but it is possible to use the comparison in a modified way which is in fact extremely useful. This possibility arises when transitions are allowed within a group of levels which lie close to one another but far from any other levels of the paramagnetic ion. An obvious example of this is the case mentioned in (ii) of §2: an ion with an orbital singlet state, well separated from other orbital levels, but retaining its $2S + 1$ degeneracy corresponding to the various spatial orientations of the electron spin. In the first approximation the spin is free, and resonance absorption can be observed through transitions between the various spin states at frequencies which satisfy the resonance condition (2) with g equal, not to the Landé factor of the free ion, but to the value 2.0023 appropriate to the spin alone without any orbital contribution. As previously noted, the behavior of the spin levels will be modified because they feel the influence of the crystalline electric field indirectly through the spin–orbit coupling mechanism. The modifications of the behavior which result are as follows.

(i) The value of g is not equal to the value for a free spin, and depends on the orientation of the external field with respect to the axes of the crystalline electric field. This anisotropy means that g must be treated as a tensor quantity, with principal values along three mutually perpendicular axes.

(ii) The degeneracy of the spin levels may be lifted in zero magnetic field, subject to the rule that for an ion with an odd number of electrons, the crystal field must always leave a double degeneracy in the levels (Kramers' theorem). This phenomenon is similar to that encountered in nuclear resonance when an electric quadrupole interaction is present.

The result of these modifications is to increase the complexity of the paramagnetic resonance spectrum, but it may be shown that it can adequately be described by the transitions between a set of energy levels characterised by a "spin Hamiltonian"

$$\kappa = \beta H \cdot g \cdot S + f(S_x, S_y, S_z) \qquad (4)$$

Here H is the external magnetic field, g the tensor of the "spectroscopic splitting factor," and S the effective spin. For the case we have been considering, that of a singlet orbital level, well separated from other orbital levels, S will equal the actual total spin quantum number of the free ion. In other cases where a few levels lie close together, and separated from other levels by an interval large compared with the splittings produced by the external magnetic field, a fictitious spin may be used, defined by setting the multiplicity of the group of levels under consideration equal to $2S + 1$.

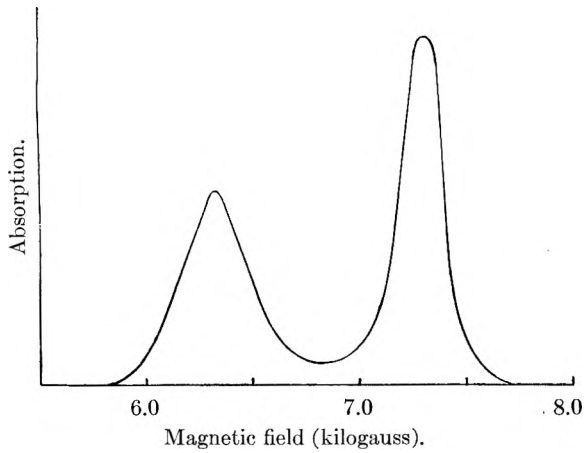

Fig. 4.—Absorption spectrum of $Cu(NH_4)_2(SO_4)_2\,6H_2O$ at 1.3 cm. wave length. The two lines are from the two ions in unit cell, which have different g-factors (the external field is parallel to the tetragonal axis of one ion, and perpendicular to that of the other).

In most cases of this type where resonance is observed, only a doublet is involved, and the fictitious $S = 1/2$. The set of levels shown for the Cr^{+++} ion in Fig. 2 illustrates well the first case, the four-fold spin levels corresponding to $S = 3/2$ both for the free ion and for the Hamiltonian (4). The second case is illustrated by cerium ethyl sulfate, where each of the doublets described approximately in Fig. 1 as $J_z = \pm 1/2, \pm 3/2, \pm 5/2$ may be treated as isolated doublets ("Kramers' doublets") with effective spin $S = 1/2$. The fact that the two lowermost doublets are rather close together in this case does not invalidate this treatment so long as the applied field is not large enough to cause levels originating in different doublets to approach one another. The g-values for these doublets are highly anisotropic and quite different from the Landé g-factor of the free ion. They are frequently much higher than 2, the maximum value for a free ion. This may be at first sight rather surprising, but the reason is quite simple, and can be appreciated from two examples. (a) If the splitting in cerium ethyl sulfate were due to a crystalline electric field of complete axial symmetry, and the approximate labelling of the doublets by values of J_z were exact, then the doublets $J_z = \pm 1/2, \pm 3/2, \pm 5/2$ would have the following anisotropic splitting factors, respectively: ($g_\parallel = g_0$, $g_\perp = 3g_0$); ($g_\parallel = 3g_0$, $g_\perp = 0$); ($g_\parallel = 5g_0$, $g_\perp = 0$), where g_0 is the Landé splitting factor of the free ion, given by the usual formula

$$g_0 = 3/2 + \{S(S+1) - L(L+1)\}/2J(J+1)$$

(b) In the cases of Cr^{+++}, the effective g is isotropic and very close to 2 if the splitting into two doublets is very small and the system is described as a quadruplet with $S = 3/2$; but if the splitting were large, the levels could again be treated as two separated doublets each with $S = 1/2$, and the g-values ($g_\parallel = 2, g_\perp = 4$); ($g_\parallel = 6, g_\perp = 0$).

The effect of an anisotropic g-factor on the resonance spectrum is to shift the center of the resonance as the external magnetic field is rotated with respect to the crystalline electric field axes. This makes it possible to distinguish between several ions in unit cell if the principal axes of their g-tensors are differently oriented in the crystal, even in cases where the principal values of the g-tensors are identical. An example of this is shown in Fig. 4. If the external field is rotated in any given plane, each line moves and reaches positions of maximum and minimum g which are mutually perpendicular. By measurements of this kind the symmetry of the g-tensor and its principal values may be found. If the tensor has axial symmetry, the g-value at angle θ with the axis of symmetry is given by the formula

$$g^2 = g_\parallel{}^2 \cos^2\theta + g_\perp{}^2 \sin^2\theta$$

The intensity of the absorption line also varies with direction, if g is anisotropic. In the case of axial symmetry, if the r.f. and steady magnetic fields are mutually perpendicular and in a plane passing through the axis of symmetry, the intensity varies as $(g_\parallel g_\perp/g)^2$. Thus if either $g_\parallel$ or $g_\perp$ is zero, no resonance line in observed, corresponding to the fact that in this case the transition probability is zero.

If $S > 1/2$, the energy levels may be split in zero magnetic field. In the Hamiltonian (4) this is represented by the term $f(S_x,S_y,S_z)$ which represents a polynomial in powers of the spin components. Only even powers occur, and if there is axial symmetry the simplest term is of the form

$$D\{S_z^2 - {}^1/_3 S(S+1)\}$$

Departures from axial symmetry can be represented by an additional term $E(S_x{}^2 - S_y{}^2)$. These terms are similar to those used to represent an electric quadrupole term in the case of nuclear resonance, though their presence arises from quite different mechanisms (influence of the crystalline electric field through the spin–orbit coupling and magnetic dipole interaction between different electrons in the same ion). Unlike the nuclear case, terms of higher power than the second are not negligible, though they affect the relative positions of the energy levels and, hence, the resonance spectrum, only when $S = 2$ or more. For example, the effect of a crystalline electric field of cubic symmetry in splitting the spin levels can be represented by the term $(S_x{}^4 + S_y{}^4 + S_z{}^4)$. For the Gd^{+++} ion, $S = 7/2$, and powers of the spin components up to the sixth are required in the Hamiltonian. The term in $S_z{}^2$ is predominant in gadolinium ethyl sulfate[6] and gadolinium magnesium nitrate,[7] however, as is shown by the fact that in strong fields the spectrum consists of a set of nearly equally spaced lines, the separation varying with $(3\cos^2\theta - 1)$ as the external magnetic field is turned to make an angle θ with the axis of the crystal field. The lines are unequal in intensity, since the transition probability for the line $M \leftrightarrow (M-1)$ is proportional to $\{S(S+1) - M(M-1)\}$.

5. Line Width

Two sources of line width in paramagnetic resonance spectra are dominant: (i) Interaction with the lattice through the spin–orbit coupling

(6) B. Bleaney, R. J. Elliott, H. E. D. Scovil and R. S. Trenam, *Phil. Mag.*, **42**, 1062 (1951).

(7) R. S. Trenam, *Proc. Phys. Soc.*, **A66**, 118 (1953).

and the crystalline electric field, by which means quanta may be exchanged between the magnetic spin system and the Debye waves of the lattice. This gives a relaxation mechanism whose characteristic time τ is extremely variable. In some cases τ is longer than 10^{-7} second at room temperature, in which case the contribution to the line width ($\Delta\bar{\nu} \backsimeq 1/2\ \pi\tau$) is negligible at all temperatures. In others τ is shorter than 10^{-12} second, when the line is so broadened as to be invisible. When the relaxation time is abnormally short, it varies with a high inverse power of the temperature (T^{-7} to T^{-9}) and hence this source of line width may be avoided by working at sufficiently low temperatures (in a few cases this requires liquid helium temperatures). Very short relaxation times are associated with small separations of the lowest orbital levels in the iron group, and of the J_z levels in the rare earths. Thus cerium salts require helium temperatures to obtain a spectrum, but in chromium salts there is no appreciable broadening at room temperature. (ii) Interactions with other magnetic ions. These may either be magnetic dipole in character, or due to exchange forces. Generally speaking, the former dominate in very dilute salts, the latter in concentrated salts. Magnetic dipole interaction gives a line width through the static magnetic fields of neighboring dipoles, which add vectorially to the external field and thus produce a spread in the actual fields acting on various ions. An additional broadening is present if the ions are identical, since they have a resonance interaction associated with the exchange of quanta.

Line width due to magnetic dipole interaction may be reduced by "diluting" the salts. That is, by replacing the paramagnetic ions by diamagnetic ions of an element which forms isomorphous salts (for example, Cr^{+++} in an alum may be replaced by Al^{+++}). In hydrated salts further dilution beyond a factor of a few hundred leaves a residual line width of the order of 12 to 15 gauss at half intensity. This is due to the protons in the water of crystallization which are located immediately around the paramagnetic ion, and may be reduced by a factor of about 3 by using salts grown from heavy water,[8] owing to the smaller magnetic moment of the deuteron.

The effects of exchange interaction are rather complex. For an assembly of identical ions with no splitting of the energy levels apart from that due to an external magnetic field, it has been shown[9] that the line is narrowed in the center, and spread out in the wings, leaving the second moment unaltered. In other cases a broadening may occur. For example, in $K_3Cr(CN)_6$ diluted with the isomorphous $K_3Co(CN)_6$ a fine structure[10] is resolved due to an initial splitting of the fourfold spin levels. In the concentrated salt the fine structure does not appear, and is replaced by a broadening of the central line in directions where the fine structure splitting should be greatest. Another interesting case is that of copper sulfate,[11] where, instead of two resolved lines being observed due to two ions in unit cell with anisotropic g-values, a single line is found at the mean position in low fields, which breaks into two at high fields where the interaction with the external field is large enough to overcome the effect of the exchange interaction.

An interesting and exceptional case of exchange interaction has been discovered in copper acetate.[12] The cupric ion normally has an effective spin $S = 1/2$, but the resonance spectrum of $Cu(CH_3COO)_2$, H_2O is similar to that for an ion of spin 1. This is attributed to isolated pairs of copper ions, coupled together by exchange forces so that the two electron spins are either parallel, forming a paramagnetic state of spin 1, or antiparallel in a diamagnetic state of spin 0. On this basis one can explain not only the abnormal fine and hyperfine structure of the resonance spectrum, but also the anomalous susceptibility. The correctness of the assumption of isolated pairs of copper ions has been verified by X-ray analysis,[13] which gives the separation as 2.6 A.

6. Hyperfine Structure

When the nucleus of a paramagnetic ion has a non-zero spin, hyperfine structure in the resonance spectrum may be expected. This is normally due to magnetic interaction between the magnetic dipole moment of the nucleus and the field of the paramagnetic electrons, though an electric quadrupole interaction may also be present if the nuclear spin is 1 or more. The former is the preponderant effect in most cases, and will be discussed first.

Most resonance measurements are made under conditions similar to those prevailing in the Back–Goudsmit region of atomic spectra. That is, the interaction between the electron and the external magnetic field is greater than that between the electron and the nucleus. This means that the magnetic field due to the nuclear magnetic dipole moment which acts on the electron is small compared with the external field, but not negligible. The frequency of precession of the electron, and hence the resonance condition, depends on the net magnetic field in which it finds itself, and the presence of a field due to the nucleus will result in a displacement of the resonance line from the position it would occupy in the absence of a nuclear interaction. When the resonance spectrum is observed at constant frequency in a variable external magnetic field, the displacement of the line is just equal to the field produced by the nucleus. Since a nucleus of spin I may set itself in any of $2I + 1$ orientations, the vector sum of the external field and the nuclear field will have $2I + 1$ possible values, and the line will be split into $2I + 1$ components. These components will be equally spaced and symmetrically disposed about the position which the unsplit line would occupy in the absence of the nuclear interaction, in the limiting case of a very large external field. This is illustrated by the

(8) B. Bleaney, K. D. Bowers and D. J. E. Ingram, *Proc. Phys. Soc.*, **A64**, 758 (1951).

(9) J. H. Van Vleck, *Phys. Rev.*, **74**, 1168 (1948).

(10) K. D. Bowers, *Proc. Phys. Soc.*, **A65**, 860 (1952).

(11) D. M. S. Bagguley and J. H. E. Griffiths, *Proc. Roy. Soc. (London)*, **A201**, 366 (1950).

(12) B. Bleaney and K. D. Bowers, *ibid.*, **A214**, 451 (1952).

(13) J. N. van Niekerk and F. R. L. Schoening, *Nature*, **171**, 36 (1953).

hyperfine structure shown in Fig. 5. In finite fields there is a small relative downwards displacement (in field) of the lines, and they are not quite equally spaced.

Fig. 5.—Hyperfine structure of ^{53}Cr ($I = 3/2$) in $K_3Cr(CN)_6$, diluted with $K_3Co(CN)_6$. The small central line is due to the even isotopes ($I = 0$) of chromium, whose abundance is a few per cent. in the sample used (enhanced in ^{53}Cr) (see ref. 10).

Since the magnetic moment of the paramagnetic electrons in a solid depends in general on the orientation of the external magnetic field with respect to the axes of the crystalline electric field acting on the ions, it would be expected that the magnetic interaction with the nucleus would also be anisotropic. This is confirmed by experiment, very large degrees of anisotropy being found in some cases such as cobalt.[14] The magnetic interaction between the electrons and the nucleus may be expressed as a term of the form SAI, where A is a tensor and S is the effective electron spin. The principal axes of this tensor are the same as those of the g-tensor, since the anisotropy in each case is due to the effect of the crystalline electric field.

The effect of a nuclear electric quadrupole moment is observable only if there is an appreciable gradient in the electric field at the nucleus, so that the energy of the quadrupole depends on its orientation with respect to this gradient. In an electronic transition the orientation of the nucleus ordinarily remains fixed and its energy is therefore independent of a quadrupole interaction, which shows up only in a transition where the nuclear orientation changes. Such transitions are generally forbidden, but may become allowed if the normal selection rules break down. Such a situation occurs if the magnetic interaction between electron and nucleus is comparable with the electric quadrupole interaction. With each of these interactions is associated an axis with respect to which the nucleus would precess in the absence of the other. If these axes are inclined to one another there is competition between them, and a breakdown of the normal selection rule. In the case of the quadrupole interaction, the axis is fixed in the crystal, being determined by the action of the crystalline electric field in producing a asymmetrical electronic charge distribution. The axis for the magnetic moment of the nucleus is not fixed, but rotates with the magnetic moment of the paramagnetic electrons, whose orientation varies with the external magnetic field. If the latter is directed along the axis of the electric quadrupole interaction, there is no competition, but for any other direction, extra transitions in the hyperfine structure may be observed, from which the size of the quadrupole interaction may be found.

The effects of an electric quadrupole interaction may be included in the spin Hamiltonian by adding a term IPI, where P is again a tensor. If P has axial symmetry this term may be written $P\{I_z^2 - 1/3I(I+1)\}$; in either case the terms are the same as those used in nuclear resonance, and arise from precisely the same phenomenon—interaction of the nuclear quadrupole moment with an electric field gradient at the nucleus. The direct effect of the external magnetic field on the nucleus may also be included in the Hamiltonian for the nuclear effects, giving altogether

$$\kappa_N = SAI + IPI - \gamma\beta_N HI \qquad (5)$$

where γ is the nuclear g-factor and β_N the nuclear magneton.

Since the hyperfine structure consists normally of just $2I + 1$ components, the nuclear spin may be determined very easily. To date, the spins of the following isotopes have been determined for the first time by paramagnetic resonance: ^{50}V, ^{53}Cr, ^{57}Co, ^{99}Ru, ^{101}Ru, ^{143}Nd, ^{145}Nd, ^{147}Sm, ^{149}Sm, ^{167}Er. One of these, ^{57}Co, was radioactive, and the total mass available was under a microgram.

7. The Iron Group

Resonance has been detected in most of the configurations $3d^n$ of the iron group, but most investigation has been carried out on the ions with Kramers' degeneracy (that is, ions for which n is odd) together with Ni^{++}, $3d^8$.

The salient characteristic of the results obtained are listed below, ion by ion.

Ti^{+++}, $3d^1$, ^2D.—Trivalent titanium forms few stable salts; among them the cesium alum, which has been studied by Bijl[15] in powder form. He found that resonance could only be observed below 8°K., and the g-values were anisotropic and departed markedly from the free spin value. Measurements on a single crystal[16] give g-values which are not quite compatible with the ordinary crystalline field theory, showing that some degree of covalent binding may exist.

Cr^{+++}, V^{++}, $3d^3$, ^4F.—The chrome alums have[17] been much studied, because of their use for adiabatic demagnetization work below 1°K. Several of them show crystallographic transitions in the region of 100°K. which are not fully understood. The g-values are isotropic and close to 2, and the spin levels are split into two doublets by the crystalline electric field, with separations of a few tenths of a wave number. Similar results are obtained with $V(NH_4)_2(SO_4)_2 \cdot 6H_2O$. The odd isotopes ^{53}Cr, ^{50}V, ^{51}V show an isotropic hyperfine structure.

Fe^{+++}, Mn^{++}, $3d^5$, ^6S.—The $3d^5$ configuration is a half filled shell, and the ion has therefore zero orbital momentum. The spin sextet is split, partly by the magnetic dipole–dipole interaction[18] between the electrons which depends on their orientation when the electron cloud does not have

(14) B. Bleaney and D. J. E. Ingram, *Proc. Roy. Soc.* (*London*), **A208**, 143 (1951).

(15) D. Bijl, *Proc. Phys. Soc.*, **A65**, 405 (1950).

(16) B. Bleaney, G. Bogle and A. H. Cooke (unpublished).

(17) D. M. S. Bagguley and J. H. E. Griffiths, *Proc. Roy. Soc.* (*London*), **A204**, 188 (1950); B. Bleaney, *ibid.*, **A204**, 203 (1950).

(18) M. H. L. Pryce, *Phys. Rev.*, **80**, 1107 (1950).

spherical symmetry, and partly by high order interactions involving the spin–orbit coupling.[19] Both are indirect effects of the crystalline electric field, but the former results in terms of the spin Hamiltonian only of the second power in S_x, S_y, S_z. The terms of higher power are more important in Fe^{+++} than in Mn^{++}, and examination of the spectra of two diluted ferric alums[20] has shown that the cubic axes of the crystalline field are slightly twisted with respect to the cubic axes of the crystal. This is in line with crystallographic determinations of the structure[21] which show such a distortion of the octahedron of water molecules round the paramagnetic ion. The Mn^{++} ion shows an isotropic hyperfine structure due to the isotope ^{55}Mn, whose magnitude is practically the same in all hydrated salts, but slightly smaller in anhydrous compounds.

Co^{++}, $3d^7$, ^4F.—It is well known that cobalt salts show a high magnetic anisotropy and that their susceptibility shows strong departures from Curie's law. This is due to the presence of low-lying orbital levels, and resonance results show that the ground state is a doublet with very anisotropic g-values; usually $g_{||}$ is between five and seven, and $g_\perp$ between two and three An exception to this rule is the blue salt Cs_3CoCl_5, where the chlorines are tetrahedrally arranged round the Co^{++} ion. This results in a cubic crystalline electric field of opposite sign so that this salt should resemble Cr^{+++} salts in its magnetic behavior. Some unpublished results[22] suggest that is the case, but with a rather smaller splitting of the orbital levels and a larger splitting ($\backsimeq 10$ cm.$^{-1}$) of the spin quartet than is found in most chromium compounds.

Ni^{++}, $3d^8$, ^3F.—The Tutton salts of nickel[23] have been investigated rather fully at room temperature. An orbital singlet is lowest, whose spin triplet is split into three components with an over-all separation of the order of two cm.$^{-1}$. The lines show broadening due to exchange forces, and this has been analyzed.[24]

Cu^{++}, $3d^9$, ^2D.—This ion has been extensively investigated. In crystalline fields of tetragonal or lower symmetry an orbital singlet lies lowest, with double degeneracy in the spin. The g-values are remarkably similar in most hydrated salts, being approximately $g_{||} = 2.4$ to 2.5, $g_\perp = 2.05$ to 2.15. Hyperfine structure due to the odd isotopes ^{63}Cu, ^{65}Cu is found to exhibit a strong electric quadrupole interaction, associated with the large asymmetry of charge distribution in the lowest orbital level. From this an estimate[25] of the nuclear quadrupole moments has been obtained.

Some general conclusions may be drawn from the measurements on the iron group. Where the g-factor departs from the free spin value, the size of the departure may be related by the crystalline field theory with the ratio of the spin–orbit coupling coefficient λ to the splitting of the orbital levels. Since λ is known fairly precisely for the free ions, accurate measurements of the g-values in the solid state would afford a quantitative check on the field theory if the splittings of the orbital levels were independently determined. Unfortunately these can at present be estimated only roughly from the absorption bands exhibited by paramagnetic salts (usually in solution) in the optical region. Even so it appears that agreement can only be obtained if the apparent value of λ is reduced in the solid state. In the case of nickel further evidence for this is obtained from a comparison of the resonance results with measurements of the anisotropy in the susceptibility. Such an apparent reduction in λ implies a similar reduction in the value of r^{-3}, where r is the distance from nucleus to electron. Furthermore, in the case of copper, it has been found that the theory of the hyperfine structure[26] can be fitted to the experimental results accurately[25] only if a reduction in the apparent value of r^{-3} is assumed also in the interaction between nucleus and electron. Such a reduction would result from a change in the radial distribution of the 3d electrons, but it seems more probable that the assumption of purely ionic binding is an over-simplification, and some admixture of covalent binding must be considered. This is supported by calculations[27] on the chromium ion, which indicate that no reduction in λ is to be expected from the presence of the crystalline field, and that the size of this field required to fit the experimental results is an order of magnitude too large.

The hyperfine structure of salts of the iron group shows a remarkable feature which has been explained by Abragam.[28] For ions where the orbital angular momentum is zero (*e.g.*, Mn^{++}, ^6S) or highly quenched in the solid state (*e.g.*, Cr^{+++}, V^{++}) there should be no hyperfine structure due to interaction with the orbit and, furthermore, the electron cloud has such high symmetry that the electron spin produces no magnetic field at the nucleus. Thus no hyperfine structure would be expected, whereas a large isotropic structure is observed. For ions where the electron orbit and spin would be expected to produce a hyperfine structure with a certain anisotropy, a quite different anisotropy is observed. Abragam suggested that owing to the electrostatic repulsion between the electrons (configurational interaction) the ground state of the ion cannot be fully described as $1s^2 2s^2 2p^6 3s^2 3p^6 3d^n$, but small admixtures of other states with the same resultant L and S must be introduced. Of these, only states with unpaired s-electrons would have an appreciable affect on the hyperfine structure. Thus a small admixture of a state $1s^2 2s^2 2p^6 3s 3p^6 3d^n 4s$ would be important because of the large hyperfine structure due to the unpaired 3s electron (the 4s electron will be anti-

(19) J. H. Van Vleck and W. G. Penney, *Phil. Mag.*, **17**, 961 (1934).

(20) B. Bleaney and R. S. Trenam, *Proc. Phys. Soc.*, **A65**, 560 (1952).

(21) H. Lipson, *Proc. Roy. Soc. (London)*, **A157**, 347 (1935); H. Lipson and C. A. Beevers, *ibid.*, **A148**, 664 (1935).

(22) J. H. E. Griffiths, J. Owen and K. W. H. Stevens (unpublished).

(23) J. H. E. Griffiths and J. Owen, *Proc. Roy. Soc. (London)*, **A213**, 459 (1952).

(24) K. W. H. Stevens, *ibid.*, **A214**, 237 (1952).

(25) B. Bleaney, K. D. Bowers and D. J. E. Ingram, *Proc. Phys. Soc.*, **A64**, 758 (1951); B. Bleaney, K. D. Bowers and R. S. Trenam, *ibid.*, **A66**, 410 (1953).

(26) A. Abragam and M. H. L. Pryce, *Proc. Roy. Soc. (London)*, **A206**, 164 (1951).

(27) W. H. Kleiner, *J. Chem. Phys.*, **20**, 1784 (1952).

(28) A. Abragam, *Physica*, **17**, 209 (1951).

parallel to the 3s, but its hyperfine structure is much smaller). This would account for the isotropic structure observed for V^{++}, Cr^{+++} and Mn^{++}, while in other cases the addition of an isotropic component to an anisotropic structure of comparable magnitude would result in a marked change in the anisotropy. Good agreement with experiment has been obtained using Abragam's suggestion, and no satisfactory alternative hypothesis has been put forward.

8. Other Transition Groups.—Of the higher transition groups, most work has been done on the rare earths. Unlike the iron group, where the normal coördination number of the ion is six, resulting in an octahedral arrangement of nearest neighbors and a crystalline field of predominantly cubic symmetry, the coördination number of the rare earths is often nine. Thus in the ethyl sulfates such as $Ce(C_2H_5SO_4)_3 \cdot 9H_2O$, on which most of the resonance work has been carried out, the nine waters of crystallization are arranged round the trivalent ion[29] in three equilateral triangles, the plane of each triangle being normal to the hexagonal axis of the crystal. One triangle is coplanar with the rare earth ion, the others are equally spaced above and below with their vertices rotated through 180° with respect to the central triangle. This gives a crystalline field of sixfold symmetry about the crystal axis. If this field has complete axial symmetry, it would split the $2J + 1$ levels of the ground state into a number of doublets if J is half-integral, and a number of doublets plus a singlet if J is integral. Each doublet would be described by the states $\pm J_z$, where J_z is the magnetic quantum number with respect to the crystal axis, while the singlet corresponds to $J_z = 0$. Since the selection rule for resonance transitions is $\Delta J_z = \pm 1$, resonance would be observed only within the $J_z = \pm 1/2$ doublet, since the crystal field separates successive doublets by an amount generally of the order of 10 cm.$^{-1}$ or more. As the crystal field has only sixfold symmetry and not complete axial symmetry, the levels are still split as above, but the states describing the doublets are mixed states containing both a given value of J_z and values differing by six. Thus a given doublet may be described by the states

$$\cos\alpha|+7/2> + \sin\alpha|-5/2>$$
$$\cos\alpha|-7/2> + \sin\alpha|+5/2>$$

and resonance is observable because the two states now contain values of J_z differing by unity.

In general, resonance is observed only in the ground doublet, since at temperatures where higher doublets are populated the spin–lattice relaxation time is so short that the lines are too broad and hence too weak for detection. Of the trivalent ions with Kramers' degeneracy (*i.e.*, J is half integral) resonance[30] has been observed in the ethyl sulfates of cerium ($4f^1$), neodymium ($4f^3$), samarium ($4f^5$) and erbium ($4f^{11}$), at 20°K. or below, and of gadolinium ($4f^9$) at all temperatures up to room temperature. Gadolinium[6] is exceptional because it contains a half-filled 4f shell, and is thus in an ^8S state, with a very small (0.245 cm.$^{-1}$ in the ethyl sulfate) over-all splitting. No resonance has been observed with dysprosium ($4f^9$) or ytterbium ($4f^{13}$) indicating that for these ions there is no allowed transition within the lowest doublet of the ethyl sulfate. For the ions without Kramers' degeneracy, no allowed transitions would be expected in the ordinary way, but resonance[31] has been observed in praseodymium ($4f^2$) and terbium ($4f^8$) with the r.f. field directed along the crystal axis. Such a resonance transition would be possible if the states corresponding to the two levels of the doublet are admixed with each other (possibly through the Jahn–Teller effect), according to the selection rule $\Delta J_z = 0$.

Well resolved hyperfine structures are observed in ions where the nuclei have a non-zero spin except for gadolinium. For this ion, as in the case of Mn^{++}, which is also in an S-state, the magnetic field at the nucleus should be zero except for admixtures of states with unpaired s-electrons which must therefore be very small in Gd^{+++}.

The theory of the paramagnetism and the hyperfine structure of the rare earth ethyl sulfates[32] has been worked out assuming a crystal field of C_{3h} symmetry, and good agreement with experiment is obtained. As in the case of gadolinium, no contribution from unpaired s-electrons is apparent in the hyperfine structure.

Of the other transition groups, a number of compounds of ions belonging to the 4d and 5d configurations have been investigated. Single crystals of such compounds are not generally easy to prepare, but the spectrum[33] of $Ru(NH_3)_6Cl_3$ diluted with $Co(NH_3)_6Cl_3$ has been analyzed. The configuration of the Ru^{+++} ion is $4d^5$, but its magnetic behavior is similar to that of $K_3Fe(CN)_6$, showing that the ions are covalently bound to give a spin of 1/2 rather than 5/2. There are three different types of ion in this salt (apart from ions which have similar g-tensors but with different orientation of the axes), with anisotropic g-values ranging both above and below the free-spin value of 2. A hyperfine structure is observed from which the spins of the two odd isotopes ^{99}Ru, ^{101}Ru have been determined.

In a salt of iridium, $(NH_4)_2IrCl_6$, diluted with the isomorphous platinum compound, a resonance has been observed with an isotropic g-value of 1.8. Here, the Ir^{4+} ion has the configuration $5d^5$, but covalent binding leaves an effective spin 1/2. A complex and unusual type of hyperfine structure is observed; this has been interpreted[34] as being due partly to the nuclear magnetic moments of the two iridium isotopes (which are almost equal) and partly to the nuclear magnetic moments of the

(29) J. A. A. Ketelaar, *Physica*, **4**, 619 (1937).

(30) G. S. Bogle, A. H. Cooke and S. Whitley, *Proc. Phys. Soc.*, **A64**, 931 (1951); B. Bleaney and H. E. D. Scovil, *ibid.*, **A63**, 1369 (1950); *ibid.*, **A64**, 204 (1951); B. Bleaney, H. E. D. Scovil and R. S. Trenam, *Phil. Mag.*, **43**, 995 (1952); G. S. Bogle and H. E. D. Scovil, *Proc. Phys. Soc.*, **A65**, 368 (1952); G. S. Bogle, R. J. Duffus and H. E. D. Scovil, *ibid.*, **A65**, 760 (1952).

(31) B. Bleaney and H. E. D. Scovil, *Phil. Mag.*, **43**, 999 (1952).

(32) R. J. Elliott and K. W. H. Stevens, *Proc. Roy. Soc.* (*London*), **A215**, 437 (1952). See also a brief review by R. J. Elliott in *Rev. Modern Phys.*, January, 1953.

(33) J. H. E. Griffiths and J. Owen, *Proc. Phys. Soc.*, **A65**, 951 (1952).

(34) J. Owen and K. W. H. Stevens, unpublished.

surrounding chlorine atoms. The electron responsible for the paramagnetism is assumed to spend part of the time in p-orbitals on the chlorine atoms, and a reduction in the orbital contribution to the g-value is associated with this.

A number of compounds of the uranium group have been examined by Baker and Bleaney at temperatures down to 20°K. without any resonance being discovered. As these compounds have not been listed elsewhere, it may be useful to give them here. They are: UO_2, $U(SO_4)_2$, UF_4 (both concentrated and diluted with ThF_4), UBr_4, UCl_3, UBr_3, PuF_3, Na (PuO_2) $(CH_3COO)_3$.

9. Conclusion

In this brief review it has not been possible to mention more than a few of the main results of the application of resonance methods to the investigation of paramagnetism in the solid state. No attempt has been made to give an exhaustive list of references, but a fuller list will be found in a forthcoming review by B. Bleaney and K. W. H. Stevens (Volume 16 of the Annual Reports on the Progress of Physics; London, Physical Society). Earlier papers of a general nature which may be found useful are listed in 35.

DISCUSSION

J. J. FRITZ (Department of Chemistry, Pennsylvania State College).—Do the two resonance peaks in $K_2Cu(SO_4)_2 \cdot 6H_2O$ show any differences other than those produced by the fact that there are two non-equivalent positions for the copper ions?

B. BLEANEY.—The two resonance peaks shown in Fig. 4 occur at different values of the field because of the anisotropy in the g-factor, and the intensities differ because they depend on the value of the anisotropic g-factor in the direction of the r. f. magnetic field. The difference in the widths is due to the presence of unresolved anisotropic hyperfine structure whose width is different for the two ions.

B. BOLGER (Department of Chemistry, Pennsylvania State College).—What is the influence of positive or negative exchange, or superior change energies on line width and signal strength?

B. BLEANEY.—Exchange forces do not in general alter the total intensity of the lines (that is, the total area under the absorption curve) but they affect the line width, and hence the intensity at the center of a line. The main effects of exchange are outlined in §5.

G. K. FRAENKEL (Department of Chemistry, Columbia University).—At what temperature were the paramagnetic resonance measurements made on the potassium ferricyanide?

B. BLEANEY.—The measurements were made at 20°K. to avoid broadening of the lines because of the very short spin-lattice relaxation time (see ref. 4).

R. N. VARIAN (Varian Associates, San Carlos, California).—There has been considerable interest recently in just how narrow electronic paramagnetic resonance lines can be. What is your view of the matter?

B. BLEANEY.—Where narrow lines are obtained in concentrated compounds exchange forces must be responsible for the narrowing. It is not easy to see what limit can be set to this process, though it is only with a set of identical spins with no anisotropy and no splittings due to fine or hyperfine structure that exchange narrowing can operate fully. In magnetically dilute compounds the residual line width is due generally to the magnetic fields of nuclear dipole moments in neighboring diamagnetic atoms. Because of the large moment of the proton anhydrous salts should give the narrowest lines. (K. D. Bowers (see ref. 10) has obtained lines of under 2 gauss full width at half intensity in $K_3Cr(CN)_6$ diluted with the diamagnetic salt $K_3Co(CN)_6$). The best salts for narrow lines would appear to be anhydrous sulfates, carbonates and silicates, where the negative radical contains no nuclear moments except those of the rare isotopes C^{13} or Si^{29}.

(35) D. M. S. Bagguley, B. Bleaney, J. H. E. Griffiths, R. P. Penrose and B. I. Plumpton, *Proc. Phys. Soc.*, **61**, 542 (1948); A. Abragam and M. H. L. Pryce, *Proc. Roy. Soc. (London)*, **A205**, 135 (1951); B. Bleaney, *Physica*, **17**, 175 (1951); B. Bleaney, *Phil. Mag.*, **42**, 441 (1951).

DYNAMIC GAS ADSORPTION METHODS OF SURFACE AREA DETERMINATION[1]

BY H. G. BLOCKER, SUSAN L. CRAIG AND CLYDE ORR, JR.

Georgia Institute of Technology, Atlanta, Georgia

Received August 8, 1952

Investigations of the phenomenon of gas adsorption, as well as investigations of gas adsorption methods for surface area determinations, have been primarily concerned with equilibrium measurements, and dynamic measurements have received little attention. Therefore, two techniques, one approximating equilibrium conditions and one requiring a measure of the rate of adsorption, have been investigated. Both are shown to give surface area results in satisfactory agreement with those of equilibrium measurements.

In recent years the measurement of the surface area of finely divided materials has become increasingly important, especially in fields employing catalytic and adsorption processes. Several methods are available for evaluating surface area, but most attention has been focused upon gas adsorption methods such as those used by Brunauer, Emmett and Teller[2] and by Harkins and Jura.[3] These and most of the other methods employed to date have dealt with some appropriate treatment of equilibrium measurements, and very little work has been done with any other method. The authors wish to report here some observations on two dynamic methods and to point out what may

(1) The work reported herein was conducted by the Georgia Tech. Engineering Experiment Station through the sponsorship of the U. S. Army Signal Corps under Contract No. DA-36-039-sc-5411.

(2) S. Brunauer, P. H. Emmett and E. Teller, *J. Am. Chem. Soc.*, **60**, 309 (1938).

(3) W. D. Harkins and G. Jura, *ibid.*, **66**, 1366 (1944).

be expected of dynamic surface area measurements.

The first method is a modification of the steady-flow adsorption techniques of Innes.[4] In this technique, equilibrium is approximated, but, because complete equilibrium is not attained, less time is required than is necessary in a conventional Brunauer–Emmett–Teller determination.

The second method is that suggested by Jura and Powell.[5] These investigators have shown that a measurement of the rate of adsorption will lead to an independent determination of the surface area of a solid, provided that there is a significant change in the rate upon completion of the first adsorbed monolayer. They found that this was the case for the adsorption of NH_3 on a silica–alumina cracking catalyst and for H_2O on anatase treated with aluminum oxide. The authors have applied this method in the study of several other solids.

In the investigation of each of these methods, nitrogen gas, at the temperature of liquid nitrogen, was used as the adsorbate.

Procedure.—The apparatus used to obtain data for each of the methods was essentially the same as that described by Emmett.[6] A Cartesian manostat, such as described by Gilmont,[7] was used to obtain the constant flow rates required in the steady-flow technique. By means of this system, constant flow rates of from one to ten ml./min. were easily attained.

Moisture was removed from the adsorbents by heating them at 110° for several hours and then cooling in a desiccator. Weighed samples were taken from this material for the adsorption studies. The removal of other adsorbed gases from the adsorbents was accomplished for each of the methods by heating the sample to between 200 and 250° while evacuating the space about the sample for at least 16 hours (usually overnight) to a pressure of approximately 5×10^{-5} mm. Since many of the determinations were made for routine surface area evaluation, and since it has been shown[8] that further evacuation after a pressure of only 10^{-3} mm. is reached increases the specific surface area value that will be obtained no more than 3%, great care was not taken to ensure more uniform pretreatment.

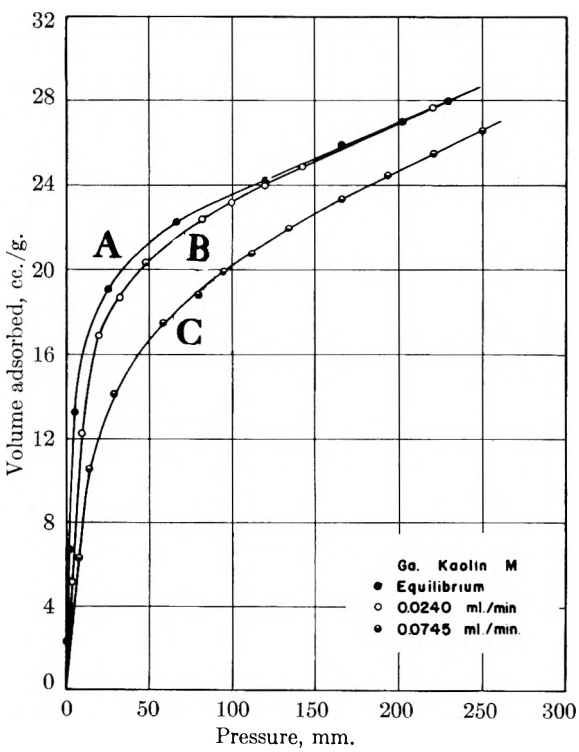

Fig. 1.—Adsorption isotherms for nitrogen on Kaolin M obtained by the steady-flow and equilibrium methods. The flow rates are on the basis of one square meter of sample surface: A, ●, equilibrium; B, ○, 0.0240 ml./min.; C, ◒, 0.0745 ml./min.

After the samples had been degassed, the volume of the adsorption space was determined with helium. Emmett[6] and others have shown that the adsorption of helium at temperatures of 77°K. or higher is quite small and can safely be neglected. Upon completion of the determination of adsorption space volume, the sample tube was filled with helium to a pressure of about 200 mm., a liquid nitrogen bath was placed around the sample tube, and the sample was left until thoroughly cooled. Cooling usually required about 30 minutes. Without helium in the sample tube to act as a heat transfer medium, a much longer time is required to cool the sample uniformly to the temperature of liquid nitrogen.

In the steady-flow technique, nitrogen gas was introduced into the adsorption system at a constant, low rate so that equilibrium was approximated at all times. The volume of gas required to form a monolayer on the surface of the adsorbent was assumed by Innes[4] to be that volume adsorbed when the system pressure was two-tenths of the vapor pressure of the liquefied adsorbate. This volume, in milliliters at standard conditions, was then multiplied by an empirical factor, 3.5, to obtain the surface area in square meters. A critical inspection of a large number of adsorption isotherms reveals that the volume of gas adsorbed at a relative pressure of 0.2 does not, in general, constitute a monolayer, although this may be a satisfactory assumption for the high specific surface materials investigated by Innes. Therefore, while the gas was introduced at a constant, low rate, the volume of gas required to form a monolayer was obtained from the isotherm by the "point B" method of Emmett[6] and with the BET equation.[2]

The volume of gas in the system at any time was determined from the flow rate and the elapsed time. The temperature was measured with an oxygen vapor pressure thermometer. From these data, adsorption isotherms could be calculated. Isotherms obtained by this method for one sample are shown in Fig. 1, as is the corresponding isotherm obtained by the conventional equilibrium method.

The same apparatus, but without the flow-controlling system, was used for the rate determinations by the method of Jura and Powell. In this method a volume of gas more than sufficient to form a monolayer on the adsorbent was admitted at one time to the sample, and the change in pressure with time was observed.

Assuming that the rate of gas adsorption is proportional to the gas pressure and that the adsorbed gas molecules are in equilibrium over the entire surface of the solid, assumptions that apply only when diffusion is not rate controlling, Jura and Powell arrived at the relationship

$$(-dP_t/dt)/(P_t - P) = F(V_t) \qquad (1)$$

where P_t is the pressure at any time, t, V_t is the volume of gas adsorbed at time t, and P is the equilibrium pressure when the amount of gas adsorbed is V_t. For ideal Langmuir adsorption the function $F(V_t)$ will be linear when plotted against V_t, becoming zero when a monolayer is completed. When multimolecular adsorption is possible, the function does not become zero when a monolayer is completed and is not always linear at low adsorption, but becomes nearly so as a monolayer nears completion. After the completion of a monolayer, the value of $F(V_t)$ has a small constant value. Figure 2 shows the type of curves obtained for three clays by this method.

Results

In the cases of the steady-flow and the equilibrium determinations the quantity of gas forming

(4) W. B. Innes, *Anal. Chem.*, **23**, 759 (1951).

(5) G. Jura and R. E. Powell, *J. Chem. Phys.*, **19**, 251 (1951).

(6) P. H. Emmett, *Symposium on New Methods for Particle Size Determination in the Subsieve Range*, ASTM, March 4, 1941, pp. 95–105.

(7) R. Gilmont, *Anal. Chem.*, **23**, 157 (1951).

(8) P. E. Bugge and R. H. Kerlogue, *J. Soc. Chem. Ind.*, **66**, 377 (1947).

TABLE I

EXPERIMENTAL CONDITIONS EMPLOYED AND SURFACE AREA VALUES OBTAINED WITH VARIOUS METHODS

Material[a]	Flow rate in steady flow measurement per square meter of sample surface[b] (ml./min.)	Specific surface area ($m.^2/g.$) by Steady-flow method Point B	Steady-flow method BET equation	Equilibrium method Point B	Equilibrium method BET equation	Rate method
Georgia umber	...	...	...	126	119	161
Kaolin M	0.0240	94.6	84.5	92.3	87.9	89.1
	.0745	95.1	85.0			
Kaolin 5DS	.0849	23.6	27.2	22.3	22.6	21.9
Kaolin 785	...	...	...	21.4	22.1	21.0
Kaolin 858	.0627	20.4	30.0	19.1	22.6	...
	.250	18.5	16.1			
Kaolin 859	.0238	42.5	49.7	47.8	41.5	...
	.891	42.7	36.9			
Kaolin 860	.0586	31.8	27.8	28.6	26.3	...
	.219	24.6	22.5			
Kaolin 884	...	...	...	34.8	34.8	29.5
Kaolin 886	...	...	...	104	105	109
Kaolin 887	...	...	...	261	260	266
Kaolin 888	.0468	16.5	24.5	16.6	22.9	...
	.165	14.6	16.3			
Kaolin 889	.0383	39.4	39.1	38.6	37.1	...
Abrasive alumina	.127	2.32	4.23	2.19	3.36	...
Adsorbent alumina	.127	200	234	195	226	...
Potassium perchlorate	.170	1.21	4.30	1.15	1.52	...
Magnesium carbonate	.0779	61.0	70.7	60.9	57.3	...
Iron powder	.0568	0.64	0.74	0.78	0.74	...
Copper powder	.151	0.22	0.76	0.24	0.30	...
	.661	0.33	0.34			

[a] Kaolin samples obtained from Georgia Kaolin Co., Dry Branch, Ga. [b] Surface calculated by BET equation from equilibrium data.

a monolayer was taken as point B, the lower extremity of the straight-line segment of the isotherm, and was also calculated by the BET equation. In the case of the rate determinations, the monolayer volume was taken as that given by the intersection of the straight line through the plotted data with the abscissa on a plot such as Fig. 2. A cross-sectional area of 15.4 square ångströms per molecule of adsorbed nitrogen, as recommended by Livingston,[9] was used for calculating the surface area of the materials from the quantity of nitrogen required to form an adsorbed monolayer. Some of the experimental conditions employed and the surface area values obtained by these dynamic methods, along with values obtained by the usual equilibrium method, are given in Table I.

Discussion

An examination of isotherms obtained by the conventional equilibrium and by the steady-flow techniques (Fig. 1) shows that, while the isotherms are similar in shape, they are not identical. However, when point B is located at the lower end of the straight-line portion of the isotherms as Emmett suggests, the quantities of gas adsorbed at point B are quite close together and are in agreement with the quantities indicated by the BET equation.

The steady-flow method is not a strictly dynamic gas adsorption technique since the flow rates employed were low enough to approximate equilibrium. Therefore, it cannot be considered an inde-

(9) H. K. Livingston, *J. Colloid Sci.*, **4**, 447 (1949).

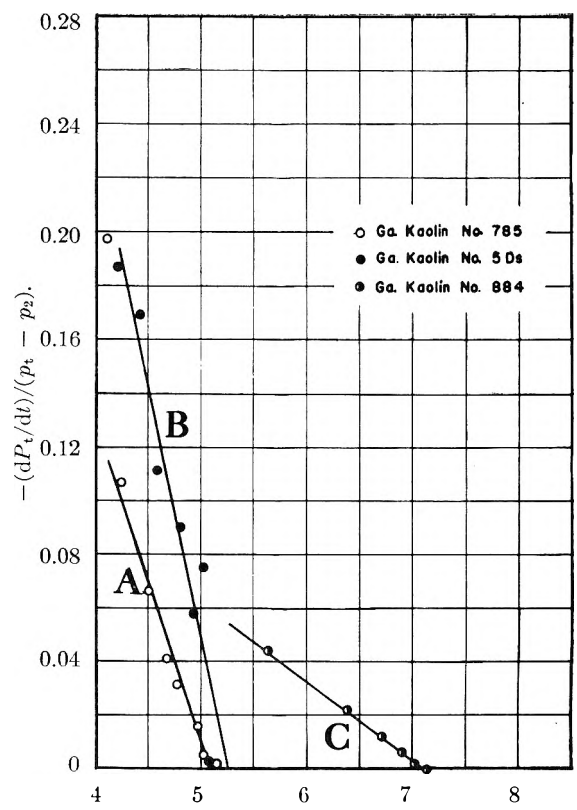

Fig. 2.—Adsorption isotherms for nitrogen plotted by the method of Jura and Powell: A, ○, Ga. Kaolin No. 785; B, ●, Ga. Kaolin No. 5 Ds; C, ◑, Ga. Kaolin No. 884.

pendent method of area determination, but rather a different technique. The only advantage of this steady-flow method is that, by using it, data for an adsorption isotherm may be determined more rapidly than by the usual method, usually in less than 20 minutes after the sample has been cooled.

The rate method depends directly upon the rate of adsorption and, therefore, affords an independent means of surface area determination. Surface area values obtained by the method, while not in as close agreement with the results of the equilibrium method as are those of the steady-flow method, are generally satisfactory. The rate method is not suited for routine determinations. The value of P in equation (1) must be determined from an equilibrium isotherm, and, while even an approximate isotherm is satisfactory, the time required for its determination renders the method impractical.

These two methods serve to show what may be expected of dynamic gas adsorption techniques of surface area determination, but many more experimental observations must be made to determine the range of applications and the dependability of the methods. There is also a need for theoretical investigations of the subject so that the mechanisms of these and other adsorption processes may be more clearly understood.

Acknowledgment.—The authors wish to acknowledge their indebtedness to Prof. J. M. DallaValle for his encouragement and many helpful suggestions and to Prof. R. L. Sessions for reading and criticizing the manuscript.

SOLID STATE PHASE CHANGES IN LONG CHAIN COMPOUNDS

BY JOHN D. HOFFMAN AND BEULAH F. DECKER

General Electric Research Laboratory, Schenectady, N. Y.

Received November 7, 1952

Three types of phase changes in n-bromides and paraffins of high chain length are discussed. Cooling curve and revised specific heat data are presented to show that the *rotational transitions* which appear just below the freezing points of some bromides and paraffins are of the first order. The phase below the transition temperature is given the general name β, and that above it is called α. It is demonstrated that the rotational transitions in purified n-paraffins are thermodynamically reversible, and that the transition temperature varies in a linear way with chain length. The entropy of transition of a number of bromides and paraffins is shown to be independent of chain length. Some X-ray data on purified paraffins are also given. The results quoted above are in accord with a recent theory of coöperative hindered rotation in long chain compounds. One conclusion reached is that torsional twisting of hydrocarbon chains in the solid state is not severe. α_1–β_2 and β_1–β_2 *transformations* are discussed next. The α- and β-phases of certain materials are unstable and spontaneously transform to a stable form on storage (the subscript 1 means unstable while 2 means stable). Such changes take place over a wide temperature range. The thermodynamic consequences of α_1–β_2 and β_1–β_2 transformations, which occur in impure C-18 and C-22-Br, are considered in some detail. The behavior of pure and impure C-18 is compared, and the concept of "monophase" premelting criticized. Finally, brief consideration is given the λ-*transitions* which occur at low temperatures in some long chain bromides and paraffins.

I. Introduction

1. General.—Several types of solid state phase changes are known to occur in n-paraffins and bromides. Among these are (a) the thermodynamically reversible *rotational transitions* between the α- and β-type phases which take place just below the freezing point; (b) the slow and irreversible α_1–β_2 and β_1–β_2 *transformations* which take place on prolonged storage at constant temperature and (c) the λ-*transitions* which occur well below the freezing or rotational transition points.

This paper will be concerned principally with the first two types of phase change mentioned above, but some experimental evidence having a bearing on the λ-transitions will be mentioned. A discussion of torsional twisting of hydrocarbon chains in the solid state will also be presented.

2. Rotational Transitions.—Rotational transitions are generally associated with the onset of hindered rotation of the rod-like paraffin chain molecules about their long axes. A number of solid n-paraffins,[1,2] alcohols,[2,3,4] esters[5,6] and bromides[7,8] exhibit discontinuous changes in a number of physical properties at a transition temperature, T_t, which have been attributed to the onset of hindered molecular rotation. In a recent paper, the rotation of long chain molecules has been treated as a typical coöperative effect.[8]

In accord with previous notation,[1] the phase above T_t is denoted α, and that below T_t is denoted by the general symbol β. Any unstable subtransitional form is denoted β_1, and stable forms are called β_2, *i.e.*, the subscript 1 means unstable and the subscript 2 means stable. Two variants of the stable (β_2) forms of pure paraffins, β_2–A and β_2–B, which are easily differentiated by X-ray methods will be mentioned in Secs. III and V. The β-forms always show less evidence of molecular rotation than α-forms.[9]

One of the principal objects of this paper is to check some of the predictions obtained from a recent theory of rotational disordering in long chain compounds,[8] especially in regard to the thermal changes at T_t in n-bromides and paraffins.

(1) A. Müller, *Proc. Roy. Soc.* (*London*), **A138**, 514 (1932).

(2) E. R. Andrew, *J. Chem. Phys.*, **18**, 670 (1950).

(3) W. O. Baker and C. P. Smyth, *J. Am. Chem. Soc.*, **60**, 1229 (1938).

(4) J. D. Hoffman and C. P. Smyth, *ibid.*, **71**, 431 (1949).

(5) R. W. Crowe and C. P. Smyth, *ibid.*, **73**, 5401 (1951).

(6) R. W. Crowe, J. D. Hoffman and C. P. Smyth, *J. Chem. Phys.*, **20**, 550 (1952).

(7) J. D. Hoffman and C. P. Smyth, *J. Am. Chem. Soc.*, **72**, 171 (1950).

(8) J. D. Hoffman, *J. Chem. Phys.*, **20**, 541 (1952).

(9) The α-form has sometimes been called the *waxy*, *rotationally melted* or *rotator* phase (ref. 4, 8). The unstable subtransitional phase (β_1) has been called *sub-alpha* and the stable (β_2) form has been called *beta* (ref. 11). The general term *rotationally frozen* or *prerotator* has sometimes been used to describe any β-phase (ref. 8).

The dielectric effects associated with rotational transitions have been discussed in an earlier publication.[8]

One of the expectations derived from the theory is that the rotational transitions at T_t should be first-order, *i.e.*, accompanied by a latent heat.

Other predictions obtained from the theory are that (a) a plot of T_t against chain length for the non-polar paraffins should be linear, (b) the observed entropy of transition should be independent of chain length, and the configurational part of this entropy should be (approximately) R ln 8 to R ln 18 and (c) a plot of ln τ against chain length for polar long chain molecules should be linear. τ is the dielectric relaxation time for a given temperature.

Items (a) and (b) were given in an earlier paper[8] and (c) will be derived here. All three items depend primarily on the approximation that the hydrocarbon chains do not undergo severe torsional twisting in the solid state; any deviation from the predictions mentioned above would be a measure of chain-twisting.

One of the assumptions employed in the theory was that the principal change at T_t involves (hindered) rotation of the molecules about their long axes rather than other types of lattice modification. This requires that the short spacing X-ray reflections show a marked change at T_t, and that the long spacing reflections show only moderate or small changes at T_t.

Cooling curves and X-ray data on highly purified hydrocarbons, and approximate specific heat data on moderately pure bromides and hydrocarbons will be presented to show that the predictions of the theory are in accord with experiment.

3. α_1–β_2 and β_1–β_2 Transformations.—Typical rotational transitions appear in long chain alcohols containing 14 to 22 carbon atoms if the measurements are made with lowering temperature.[4] On rewarming after storage below T_t, however, the transitions do not reappear. This apparent irreversibility of the rotational transitions occurs because the β-form which first appears on cooling α below T_t is unstable (β_1) and spontaneously transforms to a stable β_2-form which possesses no rotational transition. The β_2-form produced during storage melts above α.[10,11] Similarly, the α-form of the alcohols is unstable (α_1) and transforms to β_2 on storage[4,11] (where necessary, we use subscripts 1 and 2 to indicate unstable and stable α-forms). The rotational transition in the alcohols which occurs between α_1 and β_1 is not inherently irreversible as may be proved if β_1 is rewarmed quickly.[11] It should be emphasized that the α_1–β_2 and β_1–β_2 transformations in the alcohols occur over a wide temperature range. In accord with a surmise[4] based on dielectric and X-ray data, it has been shown by Kolp and Lutton that the α_1–β_2 and β_1–β_2 transformations in the alcohols are the result of the slow growth of a "tilted" β_2-phase from a "vertical" α_1- or β_1-form.

(10) In ref. 4 it was stated that the α-form of long chain alcohols sometimes melted above β_2. The reverse is true. The authors are indebted to D. G. Kolp and E. S. Lutton (ref. 11) for correcting this error.

(11) D. G. Kolp and E. S. Lutton, *J. Am. Chem. Soc.*, **73**, 5593 (1951).

The irreversible change of α_1 and β_1 to β_2 on storage must not be confused with phase transitions of the equilibrium type which take place between the α- and β-type phases at T_t. The term *transformation* will be used in this paper to denote phase changes of the irreversible kind (such as the change of β_1 to β_2 on storage) and the term *transition* is reserved for phase changes of the equilibrium kind such as take place at T_t and T_f.

As stated above, one of the manifestations of a β_1–β_2 transformation is the failure of a rotational transition which appeared on cooling to reappear on warming. Other characteristics of both α_1–β_2 and β_1–β_2 transformations which may be observed during storage of samples at constant temperature are (a) a change of opacity, density, or dielectric constant; (b) an increase of melting point and (c) the growth of a new phase as revealed by X-ray data.

Impure C-18 and C-22-Br[12] show a number of the effects mentioned above. Thermal data on these materials are presented to illustrate the thermodynamic consequences of the transformations, and the role of chain length and impurities is discussed.

4. λ-Transitions.—Small, broad maxima have been reported in the specific heat curves of C-7-Br, C-9-Br and C-11-Br,[13] and in C-18 and C-24.[14] Curiously, no such effects were reported by Parks and co-workers with C-16. The very different shape of the specific heat and dielectric constant curves, the small amount of energy involved, and the low temperatures at which the λ-transitions are encountered clearly indicate that they are to be distinguished from the rotational transitions outlined in Sec. I-2. The X-ray data obtained on purified samples of the *n*-paraffins were examined for effects traceable to λ-transitions, and a detailed thermal analysis was obtained on C-26 in an effort to locate the small thermal anomaly usually associated with the λ-transition.

II. Experimental

1. Thermal Analysis.—Samples of the *n*-paraffins C-18, C-20, C-22, C-24, C-26, C-27, C-28 and C-30 were obtained from a petroleum refining concern. These samples will be referred to as Series I samples[15] to prevent confusion with less pure samples to be discussed subsequently.

Cooling curves were obtained on Series I hydrocarbons by placing approximately 10 g. of the molten hydrocarbon in a heated glass and metal cell containing an NBS calibrated platinum resistance thermometer, inserting this cell in a large preheated brass block suspended in a Dewar flask, and allowing the whole assembly to cool. The temperature of the brass block was maintained about 0.5° below that of the cell, even during the freezing or transition process by the judicious use of an electrical resistance unit attached to the block. The average rate of cooling was about 0.2°/min., except at T_t or T_f where it was nil. Warming curves were also obtained to find out if the transition and melting

(12) The notation C-*n* will be used to designate the *n*-paraffins C_nH_{2n+2}. C-*n*-Br and C-*n*-OH will be used to denote the corresponding *n*-bromides and alcohols.

(13) R. W. Crowe and C. P. Smyth, *J. Am. Chem. Soc.*, **72**, 1098 (1950).

(14) G. S. Parks, G. F. Moore, M. L. Renquist, B. F. Naylor, L. A. McClaine, P. S. Fujii and J. A. Hatton, *ibid.*, **71**, 3386 (1949).

(15) Rough calculations based on the difference between the freezing points of the Series I hydrocarbons and the "best" values in the literature (Table I) suggest that the Series I hydrocarbons are 96 to 99+ mole per cent. pure. The consistent transition temperature data also suggest high purity.

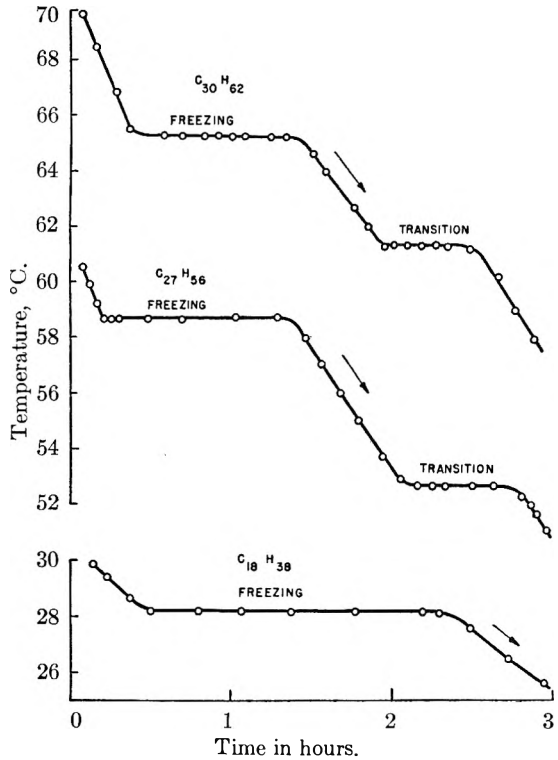

Fig. 1.—Cooling curves of: $C_{30}H_{62}$, upper curve; $C_{27}H_{56}$, middle curve; $C_{18}H_{38}$, lower curve. Series I materials.

points reappeared at the same temperature on warming, especially after storage. No significant differences were ever observed. The data are summarized in Table I. The temperature values are reliable to within 0.03°.

A thermal analysis was also carried out on a fairly impure sample of C-26-Br. Pure C-26 (Series I) was examined in a similar way between −40° and T_t in an effort to locate a λ-transition. Runs were also made on an impure commercial sample of C-18 (Series II) in order to compare its behavior with pure (Series I) C-18.

2. **Specific Heat Measurements.**—Rough specific heat measurements were carried out on samples of C-22-Br, C-30-Br and C-28, which were obtained from a commercial supply house. These samples, which were of approximately 90 mole per cent. purity, are hereafter designated as Series II materials.

The specific heat measurements were made with a differential calorimeter.[16] The data in Table II are somewhat different and more accurate than those published earlier in the form of graphs[8] because a careful recalibration of the calorimeter permitted better evaluation of the heat input.

Since the transitions in C-28 and C-30-Br were reversible, the runs on these materials were made with rising temperature. The specific heat of C-22-Br was measured on cooling, and then on rewarming after standing 48 hours at 0°. Storage permitted the transformation of β_1 to β_2 to take place.

Apart from questions of purity, the accuracy of the results is estimated to be about ±4%; the precision of the measurements is close to 1%. Comparison of our data on liquid C-28 with the careful work of Garner, Van Bibber and King[17] on compounds of comparable chain length show that our results agree with theirs within 3%. The heats of fusion and transition are given in Table III.

3. **X-Ray Data.**—Samples of the purified (Series I) *n*-paraffins obtained from the refining concern were melted on a microscope slide and cooled to room temperature. X-Ray reflections were then obtained with a General Electric recording X-ray spectrometer. All of the samples were examined when freshly prepared, but a number of them were rerun after storage. The long spacings (Table IV) are reliable to ±0.5 Å., and the short spacings (Table V) to ±0.01 Å. The spacings of C-28 and C-30 were examined from 20° up to T_t. The spacings of C-24 and C-26 were also examined at −40°.

(16) J. D. Hoffman, *J. Am. Chem. Soc.*, **74**, 1696 (1952).

(17) W. E. Garner, K. Van Bibber and A. M. King, *J. Chem. Soc.*, 1533 (1931).

III. Rotational Transitions

1. **Order of Transition; Variation of T_t with Chain Length.**—The cooling curves of the Series I hydrocarbons show that a solid state transition appears in C-22, C-24, C-26, C-27, C-28 and C-30 but not in C-18 or C-20. The cooling curves of C-27 and C-30, which are typical of those compounds possessing rotational transitions, are reproduced in Fig. 1. The appearance of a sharply defined flat in the cooling curves proves that the rotational transitions as well as the freezing points are true first-order phase changes. The cooling curve of C-18, which has no solid state transition, is also shown.

The warming curves (not shown) indicated that the transition and fusion points occurred at the same temperature on warming as on cooling, even in stored samples. Our conclusion is that the transitions are reversible, and that no transformation of the β_1–β_2 type takes place in the purified hydrocarbons. A stable α-form is in equilibrium with a stable (β_2) form at T_t.

The expected linearity of T_t with chain length (m) is apparent in Fig. 2. A more detailed analysis of the data on the even-carbon hydrocarbons shows that the equation

$$T_t(°K.) = 268.68 + 2.1917m \quad (1)$$

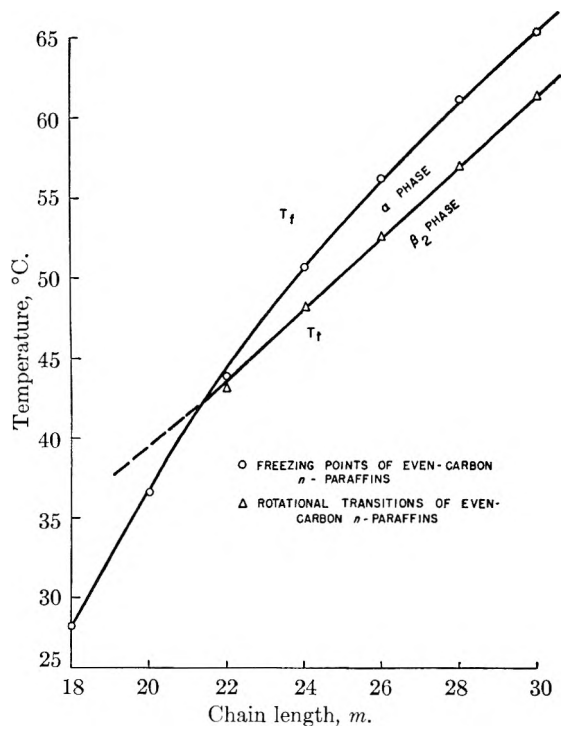

Fig. 2.—Freezing and transition temperatures as a function of chain length for the *n*-paraffins. All transitions are reversible: ○, freezing points of even-carbon *n*-paraffins; △, rotational transitions of even-carbon *n*-paraffins. Series I materials.

describes the variation of transition temperature with chain length for C-24, C-26, C-28 and C-30 to within 0.03° (see Table I). The datum for C-22 falls 0.7° low, but this compound is not as

pure as the others. The rotational transitions in pure samples of the *n*-paraffins should disappear in the vicinity of C-40 as a result of the intersection of T_f and T_t (Fig. 2).

It is interesting to note that there is no alternation of the melting points in the even–odd series C-26, C-27, C-28. Alternation of melting points occurs in the *n*-paraffins C-20 and below, and is often ascribed to differences in the mode of packing (*e.g.*, end-groups) in even and odd carbon compounds. According to the theory of rotational transitions, the molecules are "rotating" over small near-symmetrical potential energy barriers in the α-phase so that any differences in lattice packing will be minimized. On this basis, little or no alternation is to be expected in the melting point of α in C-22 and longer compounds. The rotational transition temperature, however, should show alternation because T_t depends to a large extent on the mode of packing of end-groups in the β-phase.[8] Retaining the concept that lattice forces in even and odd carbon β-type phases are different thus leads to the interesting idea that the alternation of properties which appears in the *melting* points below C-20 should appear only in the *transition* points in C-22 and longer members. The data in Table I suggest this is the case in the even–odd series C-26, C-27 and C-28. The fact that T_t for C-22 and longer compounds and T_f for C-20 and shorter compounds are both higher for even-carbon than odd-carbon paraffins is consistent with the explanation just given.

In contrast with the present results, it has been reported that both C-18 and C-20 possess first-order transitions in the solid state just below the freezing point.[18] The fusion temperatures of these materials were somewhat lower than those given in this paper, so more impurities may have been present. A similar situation regarding the presence of a transition in an impure material, and its absence in a purer sample has been encountered in the *n*-alcohols. Impure C-12-OH shows a transition, but a purer sample does not.[4] The α_1–β_2 transformation which appears in an impure sample of C-18 (Series II) will be discussed in Sec. IV-1.

The transition and melting point of both C-26-Br and C-30-Br are reversible and first-order. The freezing and transition point of C-22-Br are first-order on cooling, but a β_1–β_2 transformation in this somewhat impure substance alters the melting behavior (Sec. IV). The melting and transition data for the Series II bromides are shown in Fig. 3. While it is clear that the variation of T_t with m in bromides bears a general resemblance to that

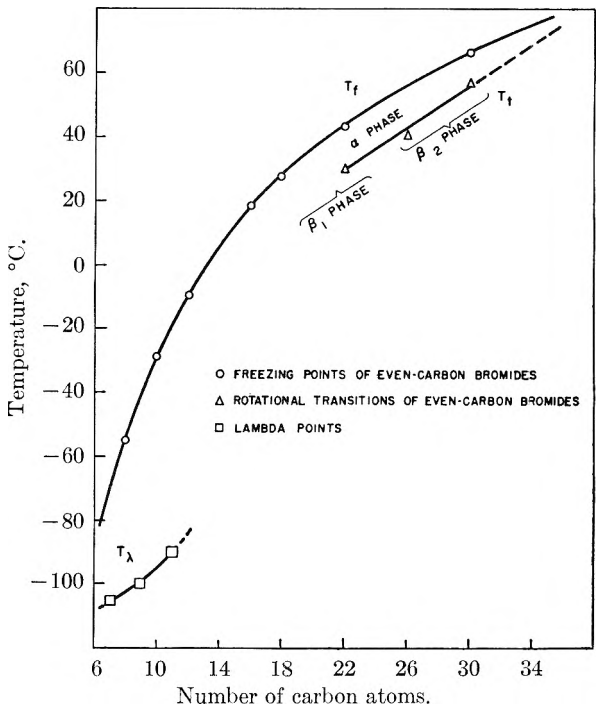

Fig. 3.—Freezing, transition and lambda points in the *n*-alkyl bromides as a function of chain length. All transitions are completely reversible except that in $C_{22}H_{45}Br$. O, freezing points of even-carbon bromides; Δ, rotational transitions of even-carbon bromides; □, lambda points of odd-carbon bromides (from Crowe and Smyth). Data on C-22-Br and longer compounds are for Series II compounds.

TABLE I

FREEZING AND TRANSITION POINTS OF SERIES I *n*-PARAFFINS C-18 TO C-30

Compound	Freezing point, T_f (°C.) This work	Lit.[a]	Transition point, T_t (°C. This work	Calcd.[b]
C-30	65.38	65.8	61.26	61.27
C-28	61.20	61.4	56.90	56.92
C-26	56.20	56.4	52.54	52.51
C-24	50.68	50.9	48.11	48.12
C-22	(43.91)	44.4	(43.05)	43.74
C-20	36.61	36.8	None	...
C-18	28.20	28.18	None	...
C-27	58.68	59.0	52.70	...

[a] Values taken from American Petroleum Institute Res. Proj. 44 Carnegie Inst. Tech. "Selected Values of Properties of Hydrocarbons," Dec. 31, 1950. [b] Calculated using T_t (°C.) = 2.1917m − 4.48 for even-carbon compounds (Sec. III-1).

(18) W. F. Seyer, R. F. Patterson and J. L. Keays, *J. Am. Chem. Soc.*, **66**, 179 (1944).

TABLE II

THE SPECIFIC HEAT OF C-28, C-22-Br AND C-30-Br (SERIES II)

C-28 T, °C.	c_p, cal./g./°C. (warming)	C-22-Br T, °C.	c_p, cal./g./°C. (cooling)	C-30-Br T, °C.	c_p, cal./g./°C. (warming)
20	0.46	50	0.49	10	0.42
30	.50	40.0	Freezes	20	.46
40	.56	38–32	1.15	30	.51
50	.63	30.0	Transition	40	.56
54.0	Transition	25	0.60	50	.62
55–59	1.5	10	.53	55	.67
60.7	Fusion		(warming)[a]	57.0	Transition
70	0.55	10	.40	59–65	1.15
80	.56	20	.405	66.4	Fusion
		30	.43	70	0.53
		35	0.50	80	.54
		41	1.26		
		44	Broad fusion ends[b]		
		45	0.52		
		50	.49		
		60	.50		

[a] After standing 48 hours at 0°. During this time β_1 was largely transformed to β_2. [b] The total heat input between 30 and 44° amounted to 62.8 cal./g.

of the paraffins, a detailed analysis must be deferred until more data are available on purer materials.

2. Shape of the Specific Heat Curves Near T_t and T_f.—The specific heat at constant pressure, c_p, for C-28 (Series II) is plotted in Fig. 4. The data of Garner, Van Bibber and King on C-30 (which are also typical of their results on C-22, C-26 and C-34) are shown in the same graph. The same general features are found in each case. The specific heat of the β_2-form rises with only a slightly increasing slope up to T_t where a latent[19] heat is found. The specific heat of the α-form is unusually high, and nearly constant. A definite latent heat appears at T_f.

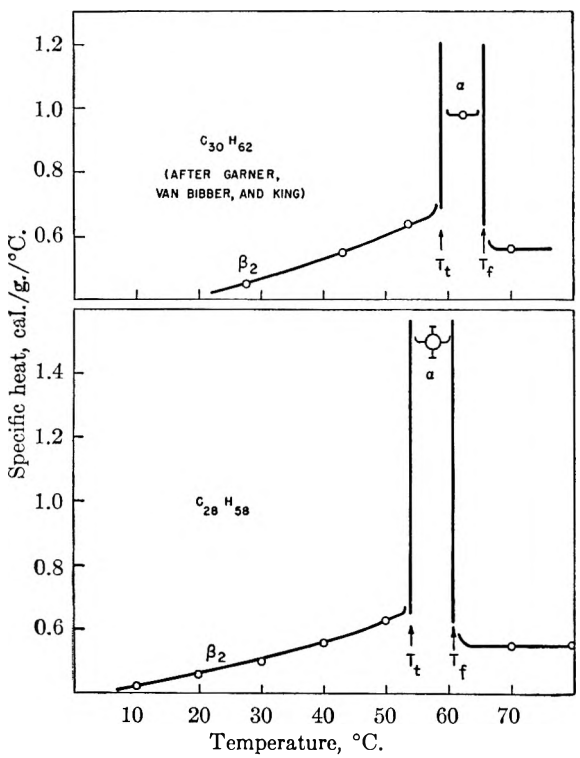

Fig. 4.—The specific heat of: $C_{30}H_{62}$, upper drawing (after Garner, Van Bibber and King); $C_{28}H_{58}$ (Series II) lower drawing. The solid vertical lines represent latent heat.

The specific heat data on C-22-Br and C-30-Br are shown in Fig. 5. The data on C-30-Br and the cooling run of C-22-Br resemble those of the hydrocarbons cited above. The anomaly in the warming run will be discussed in Sec. IV.

The shape of that part of the specific heat curves of the hydrocarbons and bromides attributable to the effects of hindered rotation is approximately that expected from previous calculations[8] of c_v. The largest discrepancy appears in the α-phase, but this is just where the largest difference between c_p and c_v is to be expected owing to the unusually large coefficient of expansion of the α-form.[18]

(19) A detailed check of the original automatically recorded time-temperature curve on which the specific heat data of C-28 are based reveals that the approximately linear increase of c_p below T_t continues to within at least 2° of T_t. Both the transition and melting point occurred over a range of 1° or less, but this is readily explained on the basis of impurities, and does not suggest that the transition and melting phenomena of pure C-28 are unsharp. Similar remarks apply to C-30-Br, and the cooling run of C-22-Br.

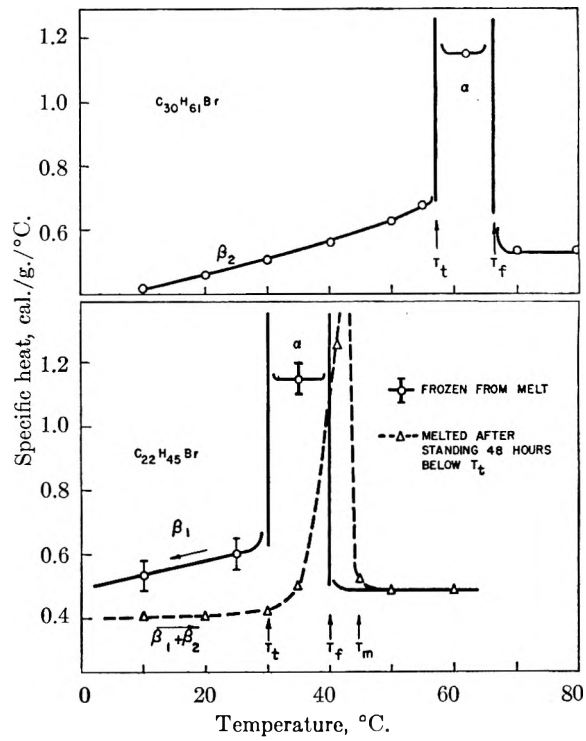

Fig. 5.—The specific heat of: $C_{30}H_{61}Br$, upper drawing; $C_{22}H_{45}Br$, lower drawing. The solid vertical lines represent latent heats. Arrows indicate direction in which the temperature was changing when the measurements were made. The warming run on $C_{22}H_{45}Br$ illustrates the effect of a β_1-β_2 transformation. Series II compounds.

3. Latent Heat of Fusion and Transition.—The latent heat of fusion of the α-phase, $\Delta H_f(\alpha)$, and the latent heat of transition, ΔH_t, of C-22-Br, C-28 and C-30-Br are entered in Table III.

TABLE III

LATENT HEATS OF FUSION AND TRANSITION, ENTROPY OF TRANSITION

Compound	Heat of transition, ΔH_t, kcal./mole	Heat of fusion of α-form $\Delta H_f(\alpha)$, kcal./mole	Entropy of transition, ΔS_t, cal./mole/°C.	Source
C-22	5.75	11.70	18.2	13
C-26	6.27	14.04	19.3	13
C-28	5.85	16.0	17.7	This work[b]
C-30	6.03	16.45	18.0	13
C-34	(7.0)[a]	19.11	(20.5)[a]	13
C-22-Br	5.53	10.75	18.2	This work[b]
C-30-Br	5.70	19.0	18.2	This work[b]

[a] Approximate values supplied by Professor Garner (see Sec. III-3). [b] Series II compounds.

It is now desired to compare our data for ΔH_t for C-28 with those of Garner, Van Bibber and King[17] who specifically recognized the presence of transitions in C-22, C-26, C-30 and C-34. In order to make the required comparison, it must first be noted that their "heat of transition," $(Q_\beta - Q_\alpha)$ is not the same as ΔH_t, which we have defined as the *latent* heat of transition. In the notation of Garner, Van Bibber and King[20]

(20) The authors gratefully acknowledge a private communication from Professor Garner regarding this difference in definitions.

$$Q_\alpha = \Delta H_f(\alpha) \qquad (2)$$

and

$$Q_\beta = \Delta H_f(\alpha) + \Delta H_t + \int_{T_t}^{T_f} c_p(\alpha)dT \qquad (3)$$

Thus, their "heat of transition" is

$$(Q_\beta - Q_\alpha) = \Delta H_t + \int_{T_t}^{T_f} c_p(\alpha)dT \qquad (4)$$

i.e., it contains the enthalpy increment between T_t and T_f as well as the latent heat of transition.[21] Since these authors give T_t, T_f and $c_p(\alpha)$ in their paper, so it is an easy matter to compute ΔH_t using eq. 4. The results are given in Table III. Q_β for C-34 appeared to be too high, so ΔH_t computed in the above manner was also too high. Professor Garner has kindly supplied us with a more reliable but still approximate value taken from the original graphs. The significance of the results is discussed below.

4. Entropy of Transition.—The values of the entropy of transition, ΔS_t calculated using the relation $\Delta H_t/T_t$ are given in Table III for the *n*-paraffins and bromides. With the possible exception of C-34, there is no increase of ΔS_t with chain length in the *n*-paraffins, and no increase whatever is apparent in the bromides. The mean value for the paraffins (excluding C-34) is 18.3 e.u., which is close to the mean value of 18.2 e.u. for the bromides. Our conclusion is that ΔS_t does not increase with chain length between 22 and 30 carbon atoms within the limits of experimental error.

An effort will now be made to estimate the configurational part of the observed entropy of transition. This may be done by subtracting the entropy of expansion,[22,23] $\Delta V\mathbf{a}/\mathbf{b}$, from the observed entropy of transition.[8] ΔV is the change of molar volume at T_t, **a** the coefficient of expansion, and **b** the compressibility. It is readily found that **a** is 60×10^{-5} deg.$^{-1}$ for the β-forms of C-22 to C-30, and ΔV is found to be 16.5 to 18 cc./mole for the same range of chain lengths.[18] Complete compressibility data are not available, but Müller[24] has found the compressibility of the β-form of C-23 to be 2.06×10^{-8} cm.^{2} g.$^{-1}$, and that of paraffin wax to be 1.7×10^{-8} cm.^{2} g.$^{-1}$. Using these data with the conversion factor 2.34×10^{-5}, it is found that the entropy of expansion is 11.8 to 14.2 e.u., the mean value being 13.0 e.u. Taking the observed entropy of transition to be 18.3 e.u., the configurational entropy of transition is found to be 5.3 ± 1.2 e.u.

It has been shown[8] that the configurational entropy of transition in long chain compounds is given (approximately) by $R \ln \Omega$ where Ω is the number of equivalent positions which a molecule may occupy in the α-phase as it rotates an angle of 2π about its long axis. One would expect Ω to depend on the shape of the molecule (viewed end-wise) and not its length if the molecules behaved as rigid rods. If the molecule twisted severely, Ω would increase markedly with increasing chain length. Taking 5.3 e.u. for the configurational entropy of transition, Ω is found to be 14. This value is close to that obtained previously by the same method,[25] and agrees with that suggested by dielectric data and considerations based on molecular models.[8]

The above calculations do not prove that Ω is constant with chain length since the compressibility data do not extend over the required chain lengths. It is still entirely reasonable, however, to assume that whatever its actual value, the compressibility is constant with chain length in the region C-22 to C-30. The use of this assumption in combination with the fact that ΔS_t does not vary with chain length still leads to the important conclusion that $R \ln \Omega$ is essentially constant between 22 and 30 carbon atoms.

5. Torsional Twisting of Chains.—It has already been shown that the rotational transition temperatures of the purified *n*-paraffins vary in a linear way with chain length, and evidence has just been presented which suggests that the configurational entropy of transition does not vary with chain length. Both of these findings are consistent with the concept that the chains do not twist severely during the rotation process in the solid state.[8]

Dielectric relaxation data may be used to detect twisting of chains. The relationship between the dielectric relaxation time τ and the activation energy U^* associated with the relaxation process is given by

$$\tau = Be^{U^*/kT} \qquad (5)$$

where B is a constant. If the molecules are rigid rods, we may write for the activation energy over which a molecule must pass to reach a new equilibrium position

$$U^* = 2U^*_{e.g} + mU^*_{CH_2} \qquad (6)$$

U^*_{eg} is the activation energy associated with each end-group, and $U^*_{CH_2}$ is the barrier associated with each $-CH_2-$ group along the chain. At constant temperature one then finds

$$\ln \tau = a + bm \qquad (7)$$

where a and b are constants. Thus, if the rigid-rod approximation (eq. 6) is reasonable, a plot of $\ln \tau$ against chain length (for data obtained at constant temperature) should be linear *provided* that no phase change intervenes.

Fröhlich[26] has pointed out that the second term on the right-hand side of eq. 6 will be of the form $\bar{m}U^*_{CH_2} \tanh (m/\bar{m})$ for the general case where chains twist. $\bar{m}$ is a constant characteristic of the stiffness of the chains; a small value of $\bar{m}$ indicates marked twisting, while substitution of $\bar{m} = \infty$ yields $mU^*_{CH_2}$, *i.e.*, the rigid-rod approximation.

(21) In cases where the transition occurs near the melting point the heat of fusion may be calculated using

$$\Delta H_t + \int_{T_t}^{T_f} [c_p(\alpha) - c_p(\beta)]dT + \Delta H_f(\alpha) = L_f \text{ (at } T_f)$$

Values of L_f calculated from the present data are not accurate enough to warrant comparison with literature values of the heat of fusion, which are usually calculated in a different way.

(22) R. A. Oriani, *J. Chem. Phys.*, **19**, 93 (1951).

(23) J. C. Slater, "Introduction to Chemical Physics," first edition, McGraw-Hill Book Co., Inc., New York, N. Y., 1939, p. 261.

(24) A. Müller, *Proc. Roy. Soc.* (*London*), **A178**, 227 (1941).

(25) A previous estimate of the entropy of expansion (ref. 8) was too low owing to the use of a low value of **a**, and the observed entropy of transition was about 3 e.u. too low. These errors were largely compensatory. Further revisions in the value of Ω are to be expected as more data become available.

(26) H. Fröhlich, *Proc. Phys. Soc.*, **54**, 422 (1942).

Using data on esters in solid solution in paraffin wax, Fröhlich found $\bar{m} = 26$ which would indicate extreme twisting. A re-examination of the data employed by Fröhlich reveals that three of the four experimental points lie on a straight line on a plot of ln τ against m, and that the curvature required to yield the value $\bar{m} = 26$ depends on the fourth point, so this estimate of $\bar{m}$ is not entirely satisfactory.

Meakins[27] has made a careful study of the dielectric relaxation times of pure samples of ketones 19 to 35 carbon atoms long in solid solution in C-26 and C-28. Pure hydrocarbon solvents are more desirable for the present purpose than paraffin wax which consists of mixed chain length hydrocarbons. Phase transitions of an expected type occur when the chain length of the ketone exceeds that of the hydrocarbon. When the ketone molecule contains 25 carbon atoms or less, however, Meakins' data fall on a straight line on a plot of ln τ against m within experimental error (his Fig. 6). This means that eq. 7 is closely obeyed for the range of chain lengths studied, and shows that $\bar{m} \gg 26$.

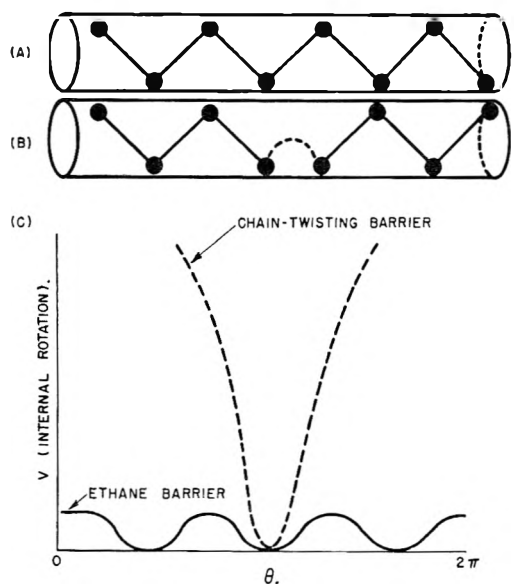

Fig. 6.—Torsional twisting of chains of molecules constrained to linear configuration by lattice forces: A, untwisted molecule; B, severely twisted molecule; C, potential energy involved in twisting of chains. Dashed line represents the potential barrier for twisting a C–C bond of a molecule constrained to a linear configuration. Solid line represents the ethane barrier appropriate to the case where the ends of the molecule may achieve any desired configuration while turning about the C–C bond.

The observed linearity in plots of ln τ and T_t with m, and the constancy of ΔS_t with m indicate that the twisting of chains in the solid state is far from pronounced. It is to be expected, however, that when a larger range of chain lengths is studied, some effects clearly attributable to chain-twisting will appear.

One reason for the stiffness of the chains is that the molecules are constrained to a linear configuration by lattice forces. This constraint (idealized) is represented by the cylindrical tube in Fig. 6a. If one attempts to twist half the molecule through an angle of π, and still restrict the molecule to the tube, the carbon–carbon bond involved must be virtually ruptured to do so (Fig. 6b). This means that internal twisting of the molecule in the tube through any given angle, θ, will require much more work than would be required for twisting the molecule to θ over an ethane-like barrier to internal rotation (Fig. 6c). The ethane-like barrier would be appropriate only if the molecule were not restricted to the tube, *i.e.*, there were no lattice forces. The above arguments do not apply, of course, to the rotation of the $-CH_3$ groups on the ends of the chain.

6. X-Ray Spacings of the α- and β-Phases of n-Paraffins.—Müller[28] has investigated the long spacing X-ray reflections of the even-carbon hydrocarbons C-6 to C-30. In general, the long spacings may be expressed by an equation of the type

$$d(\text{Å.}) = 1.25 \sin \phi(m - 1) + d_0 \qquad (8)$$

m is the number of carbon atoms, ϕ is the angle that the molecules are inclined to the plane of the end-groups, and d_0 is the effective length of the end-groups.

The α spacings quoted by Müller (his d_1) for C-24, C-26 and C-28 show that d_0 is 3.6 Å., and that ϕ is 90°, *i.e.*, the molecules are in the vertical configuration (≡|≡). Müller also reported α long spacings in C-18 and other molecules with less than 22 carbon atoms. Our thermal analyses indicate that the α-form will not appear in molecules shorter than C-22 and, accordingly, we have found no α long or short spacings in C-18 or C-20 (Series I).

Müller reported another characteristic long spacing (his d_2) in C-6 to C-20. We call the phase which gives this spacing β_2–A. The β_2–A long spacing (Table IV) appears at room temperature in C-18 through C-26, so this form has a somewhat wider range of existence than indicated by Müller. The short spacings of β_2–A (Table V) confirm the range of existence suggested by the long spacings. The present data suggest that $\phi \cong 80°$, and that d_0 is about 2.3 Å.

It is evident from the above that the transition of α to β_2–A at T_t in C-22, C-24, and C-26 involves little change in angle of tilt. A comparison of the single strong spacing of the α-form at 4.1 Å. given by Müller[1] with the numerous β_2–A short spacings given in Table V show that the greatest change at T_t must involve the lateral arrangement of the molecules. This is in accord with the assumptions used in previous calculations, and agrees with the ideas regarding molecular rotation in long chain compounds first put forward by Müller.

Both the long and short X-ray reflections of C-28 and C-30 (Tables IV and V, Fig. 7) indicate that a new stable modification, β_2–B, appears at T_t and persists to low temperatures. The data show that $\phi \cong 70°$, and that d_0 is close to 2.1 Å. The new modification is more tilted (≡/≡) than β_2–A. The change-over of β_2–A to β_2–B at C-26 was first noticed by Piper and co-workers.[29] Our values

(27) R. J. Meakins, *Australian J. Res.*, **2**, 405 (1949).

(28) A. Müller, *Proc. Roy. Soc. (London)*, **A127**, 417 (1930).

(29) S. H. Piper, A. C. Chibnall, S. J. Hopkins, A. Pollard, J. A. B. Smith and E. F. Williams, *Biochem. J.*, **25**, 130 (1931).

for T_f, and long spacings are in good agreement with theirs.

TABLE IV

LONG SPACING X-RAY REFLECTIONS[a] OF β_2-FORMS OF SERIES I *n*-PARAFFINS (~25°)

Compound	Spacing, Å.	Phase
C-18	23.2	β_2–A
C-20	25.8	β_2–A
C-22	28.1	β_2–A
C-24	30.5	β_2–A
C-26	32.9	β_2–A
C-28	33.6[b]	β_2–B
C-30	35.8[b]	β_2–B

[a] Strong reflections only. C-26, C-28 and C-30 showed weak or very weak reflections at 31.1, 37.5 and 40.6 Å., respectively. The latter two were due to supercooled α, and the former is probably due to β_2–B. [b] These spacings were observed to persist up to T_t.

TABLE V

SHORT SPACING X-RAY REFLECTIONS[a] OF β_2-FORMS OF SERIES I *n*-PARAFFINS, Å. (~25°)

Short spacings of C-18 through C-26, β_2–A form This work	Short spacings of C-8 through C-20, β_2–A form Müller	Spacings of C-28 and C-30, β_2–B form[b] This work
4.59 (S)	4.56	4.41 (M)
4.50 (S)		4.25 (M)
3.98 (M)		4.08 (S)
3.81 (S)	3.79	3.72 (S)
3.59 (S)	3.58	
3.48 (M)		

[a] S = Strong, M = Moderate intensity reflections. [b] These spacings persisted up to T_t.

The transition of α to β_2–B at T_t in C-28 and C-30 evidently involves a moderate change in angle of tilt, but the change in the short spacings is as severe as in the case of the transition of α to β_2–A in C-22 to C-26. In any event, the change of angle of tilt in the β_2–B to α-transition in C-28 and C-30 at T_t is not so large as to render untenable the assumption that the major change at the rotational transition temperature involves the lateral arrangement of the molecules. The smaller value of d_0 in the β_2–A and β_2–B phases as compared with that of α indicates that the end-groups pack more efficiently below T_t.

A surprising feature of the change-over from β_2–A to β_2–B in the room temperature X-ray data (Fig. 7) is that there is no hint of it in the plots of T_t against m, or in the approximate thermodynamic data in Table III. It is evident from this that any thermodynamical differences between β_2–A and β_2–B at T_t must be rather subtle. The appearance of a new β_2 form at C-28 may be due to small amounts of side-chains or impurities. It would be interesting to check this. No evidence has been encountered in the present study of the X-ray reflections of purified paraffins to show that either β_2–A or β_2–B undergo a slow and irreversible transformation to any other phase, even on prolonged storage.

IV. α_1–β_2 and β_1–β_2 Transformations

1. Conditions Required for Occurrence.—Evidence has been presented in Secs. III-1 and III-6 that none of the purified hydrocarbons exhibit any of the phenomena associated with the β_1–β_2 transformation; all of the phase changes in the Series I hydrocarbons are of the equilibrium type, and show complete reversibility. It is especially noted that pure C-18 and C-20 possess no α-form, and freeze directly into a stable (β_2–A) modification at T_f.

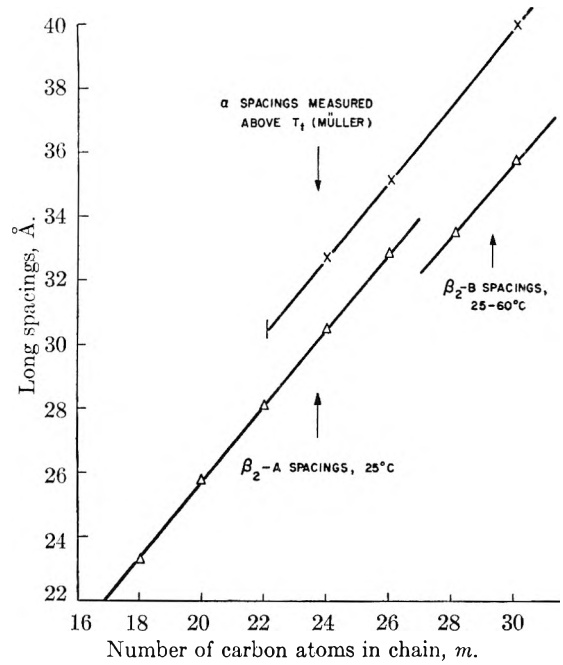

Fig. 7.—Long spacing X-ray reflections of *n*-paraffins as a function of number of carbon atoms. Only strong reflections are shown. Series I materials.

The behavior of impure (Series II) C-18 is very different from that of the pure (Series I) sample described in Sec. III-1. On cooling, impure C-18 freezes into a clear α-form at 26.5°; this form remelts at the same temperature. No clear-cut rotational transition could be found in this α-form. On storage at either 26.0 or 22.0° it was found that white nuclei of β_2 grew into the unstable α-form. On remelting after storage, the last of the stable β_2 crystals melted at 27.0°. Thus, impure C-18 exhibits a typical α_1–β_2 transformation with a concomitant increase in melting point. Comparison of the behavior of pure and impure C-18 shows that impurities are an important factor in producing the unstable or metastable phases which lead to α_1–β_2 transformations.

Another variable involved in α_1–β_2 and β_1–β_2 transformations is chain length. No signs of such transformations appear in impure C-26-Br, C-30-Br, or C-28 (Series II), but they do appear in impure C-18 and C-22-Br. Thus, the α-forms which are found near or below the chain length where α would not normally appear in pure bromides and paraffins (*i.e.*, about 22 carbon atoms) are just those which are most apt to be unstable. The α_1 and β_1 phases which appear in bromides or paraffins containing 22 or fewer carbon atoms are probably solid solutions.

The role which impurities and chain length play in α_1–β_2 and β_1–β_2 transformations in the alcohols C-14-OH to C-22-OH has not been fully elucidated. It has been noted, however, that these transformations proceed more slowly as the chain length is

increased,[4] and that increased purification sometimes raises the rotational transition temperature until α no longer appears. It would be interesting to examine the alcohols longer than C-22-OH to see if β_1–β_2 transformations were absent, and to employ extreme purification methods to see if α can be stabilized or eliminated in the region C-14-OH to C-18-OH.

2. Comment on Monophase Premelting.—Ubbelohde[30] has reported that the specific heat near the melting point of C-18 has a broad cusp-like appearance such that the *area* under the cusp in a C_p *vs.* T plot comprises a major fraction of the heat of fusion. The breadth of the specific heat "anomaly" at the melting point in Ubbelohde's sample was about 15° so that there was virtually no true *isothermal* latent heat of melting. Although Ubbelohde realized that large amounts of impurities could lead to unsharp fusion (impurity premelting), he believed that the broad anomaly he observed near the melting point of C-18 was a true bulk property of the pure material, and termed the effect "monophase" premelting.[31] Since the supposition that pure long chain compounds exhibit marked "monophase" premelting has played a significant part in some theories of melting, we believe that Ubbelohde's data on C-18 require comment.

The sample of C-18 (m.p. 28.20°) used in the present research showed no perceptible rounding off of the carefully controlled cooling curve on either side of the melting point, and exhibited a definite latent heat (to within 0.02°) over the entire range of the fusion process. Cooling curves would be rounded, and the usual flat portion indicative of a latent heat would be markedly shortened or absent if "monophase" or impurity premelting were present to the extent indicated by Ubbelohde's data on C-18. Our conclusion is that "monophase" premelting as characterized by the experiments of Ubbelohde does not appear in pure C-18 to an appreciable extent. On the same basis, no marked premelting effects appear in the other Series I hydrocarbons studied here.[32]

The sample of C-18 (m.p. 26.85–27.00°) studied by Ubbelohde melted at a substantially lower temperature than the sample studied here. The current literature value for the melting point of C-18 is 28.18° (Table I). The large premelting effect observed in this sample was undoubtedly of the impurity, and not the monophase type.

3. Heat of Transformation of β_1 to β_2 in C-22-Br.—C-22-Br freezes at 40° to a metastable α-form which undergoes a rotational transition at 30°. The resultant β-form is unstable (β_1) and rapidly transforms to stable β_2 on storage below T_t. The β_2 form remelts at about 44°. The metastable α-form will also transform to β_2 at any temperature between 30 and 40° if it is suitably nucleated. The melting process of the stable form is rather unsharp (Fig. 5). Much of the broadening of the melting point must be the result of impurity premelting, but some of it may be the result of untransformed and impurity-rich β_1 undergoing the transition to α_1 on rewarming.

The enthalpy change involved in the transformation of β_1 to β_2 in C-22-Br was estimated in an earlier publication.[8] The following data and method are revised. The total enthalpy change on cooling from 44 to 30° is

$$-\Delta h(\text{cooling}) = \int_{40}^{44} c_p(\text{liq.})dT + \Delta h_f(\alpha) + \int_{30}^{40} c_p(\alpha)dT + \Delta h_t \quad (8)$$

Using Tables II and III, this is found to be −58.8 cal./g. On warming from 30 to 44° after the β_1–β_2 transformation had proceeded during storage, the total heat input was found to be 62.8 cal./g.

$$\Delta h(\text{warming}) = \int_{30}^{44} c_p(\beta)dT \quad (9)$$

(Table II). Summing eq. 8 and 9, and taking into account the precision of the measurements, it is found that 4 ± 2 cal./g. were liberated by the spontaneous transformation of β_1 to β_2 during storage. The transformation was at least 80% complete.

V. λ-Transitions

An extrapolation of the λ-transition temperature of C-18 and C-24 reported by Parks and coworkers[14] suggests that T_λ should appear at about 0° in C-26, and at higher temperatures in C-28 and C-30. A careful thermal analysis carried out on a slow-cooled sample of C-26 (Series I) failed to reveal any thermal anomaly between −40 and 30°. Similarly, no clear evidence of a λ-transition is apparent in our thermal data of C-28 and C-30 above 15°. Parks found no λ-effect in C-16. While the present data do not preclude the presence of very small λ-transitions in the hydrocarbons considered, there is evidently room for doubt as regards their existence in unquenched samples.

Despite the fact that no clear-cut thermal evidence was found for λ-transitions in hydrocarbons in the present research, the possibility that a transition of β_2-A to β_2-B might occur was considered. X-Ray data show that both the long and short spacings of β_2-A in C-24 and C-26 (Series I) persist from room temperature to −40°; some of the short spacings were seen to undergo changes of intensity in this temperature range, but the positions of the lines did not change in a significant manner. Both the long and short spacings of β_2-B in C-28 and C-30 persist from room temperature to T_t. The results quoted above appear to eliminate the possibility that there is any rapid, equilibrium-type transition between β_2-A and β_2-B in the temperature region where λ-transitions have been reported, or might be expected.

Definite λ-transitions appear in the short odd-carbon bromides examined by Crowe and Smyth.[13]

(30) A. R. Ubbelohde, *Trans. Faraday Soc.*, **34**, 282 (1938).

(31) A. R. Ubbelohde, "An Introduction to Modern Thermodynamical Principles," 2nd edition, Oxford University Press, 1952, pp. 154–157.

(32) The onset of hindered rotation leads to experimental effects which are easily distinguished from the effects of impurity or monophase premelting. The onset of hindered rotation leads to a small increase in C_p which rises in an approximately linear way up to T_t or T_f where it breaks off sharply with the appearance of an obvious latent heat; premelting (generalized to include solid state transitions) culminates in an increasingly steep rise of C_p which tends to broaden any true latent heat.

Here, the metastable phase which undergoes the λ-transition is obtained only by rapid quenching of the liquid; the stable crystalline form shows no λ-effect whatever. The λ-transitions reported for hydrocarbons may also be the result of a transition in a metastable phase (perhaps supercooled α) induced by rapid quenching of the liquid.

The entropy of the λ-transitions in the bromides is close to R ln 2, and this indicates that some type of "two-position" theory is appropriate to these compounds. We note, however, that the extremely small change of dielectric constant at T_λ shows that the molecules develop little if any freedom to turn about the long molecular axis. This is in marked contrast to the sharp increase in dielectric constant which occurs at the rotational transition in C-22-Br and C-30-Br[8] which is a result of the onset of hindered rotation about the long axis. The λ-transitions in the short odd-carbon bromides may involve a change from an ordered head-to-head arrangement of the bromines to a random packing of the bromines. Such "longitudinal" disordering[6] would lead to the correct entropy of transition without requiring a change of dielectric constant at T_λ.

Finally, it is worth pointing out that the two strong short spacings in the β_2–B form of C-28 and C-30 at 4.08 and 3.72 Å. correspond closely with the two strong short spacings of the crystalline regions of polyethylene[33] which appear at 4.10 and 3.70 Å. It appears from this that the lateral arrangement of the molecules in the crystalline regions of polyethylene resembles that of the β_2–B form of the paraffins. (See remarks regarding β_2–B, Sec. III-6.)

Acknowledgment.—The authors wish to thank Drs. B. H. Zimm, R. W. Crowe and R. A. Oriani of this Laboratory for many stimulating conversations. Special thanks are due Professor W. E. Garner of the University, Bristol, England, for important comments and information.

(33) C. W. Bunn, *Trans. Faraday Soc.*, **35**, 482 (1945).

THE SOLUBILITY OF AMMONIUM, MAGNESIUM AND ZINC FLUOSILICATES FROM 2 TO 68°

BY EDGAR A. SIMPSON AND EDWIN M. GLOCKER

The Davison Chemical Corporation, Baltimore, Maryland

Received December 5, 1952

This study was undertaken to demonstrate a more accurate method of determining the solubility of the soluble fluosilicates. The determinations covered the range from 2 to 68°. Titration methods were found to be erratic and unreliable for most of these compounds as indicated by the references cited. A method was adapted here in which matched floats were placed in a prepared and an unknown solution and the concentration of the unknown solution adjusted to the concentration of the prepared solution. This method is particularly useful with compounds whose solutions undergo hydrolysis when analysis by titration is attempted.

Only limited information is available on the solubility of ammonium, magnesium and zinc fluosilicates. Carter[1] in 1930 published a compilation of data available at that time. These are given for one temperature only and nothing is known about the methods used. The work of Worthington and Haring[2] is also given for one temperature only. The methods that they used were (a) titrating with NaOH using phenolphthalein as the indicator with $MgSiF_6 \cdot 6H_2O$ and (b) precipitation as $ZnNH_4PO_4$ in a neutral solution, igniting and weighing as the pyrophosphate with $ZnSiF_6 \cdot 6H_2O$. Nothing is known about the method of Yatlov and Pinaevskaya.[3]

The chemical methods *versus* the physical methods for determining the solubility of these compounds have been at variance. The difficulties with several methods are discussed by Worthington and Haring[2] who point out that titrating a hot solution with NaOH, using phenolphthalein as the indicator, gave good check results with ammonium fluosilicate, but did not with magnesium or zinc fluosilicate due to hydrolysis of the last two salts during titration. This hydrolysis leads to an indefinite end-point. A satisfactory method of analysis depends upon the determination of fluorine by the method of Willard and Winter.[4] This is the method used for determining the purity of the salts used in the work reported here. It is, however, a time consuming determination, and this accounts for the attempts to substitute other methods, including titration, for analyzing fluosilicate solutions.

This paper demonstrates a method of obtaining the solubility of the more soluble salts, and gives data for the solubility of ammonium, magnesium and zinc fluosilicates between 2 and 68°.

Apparatus and Technique.—The method used is actually a specific gravity determination in which the saturated solution being studied is diluted with distilled water to the concentration of a solution of the same salt of a known concentration. The concentrations are equal when two matched floats start to rise or sink at the same time while the temperature of a bath surrounding both samples is varied slightly.

Pairs of matched floats are made out of glass. For the salts studied in this case two pairs of them are useful, one to operate at about a 15% concentration and the other at about a 28% concentration by weight.

The fluosilicates used in this study were produced by The Davison Chemical Corporation and were used without special purification. The actual purities of the various salts

(1) R. H. Carter, *Ind. Eng. Chem.*, **22**, 887 (1930).

(2) K. K. Worthington and M. M. Haring, *Ind. Eng. Chem., Anal. Ed.*, **3**, 7 (1931).

(3) V. S. Yatlov and E. M. Pinaevskaya, *J. Gen. Chem. (USSR)*, (1938).

(4) H. H. Willard and O. B. Winter, *ibid.*, **5**, 7 (1933).

as determined from fluorine analysis by the method of Willard and Winter[4] were as follows: $(NH_4)_2SiF_6$, 99.42%; $MgSiF_6 \cdot 6H_2O$, 99.61%; $ZnSiF_6 \cdot 6H_2O$, 99.04%.

A known solution of the salt in question is accurately prepared at a concentration which will activate the float at a convenient temperature, usually slightly above 40°, and introduced into a 25 × 200 mm. test-tube. In order to overcome the effect of surface tension on a float at the surface, a glass rod with a flattened end is held in a rubber stopper with the flattened end below the liquid surface. This keeps the float below the surface at all times.

A container of saturated solution, with an excess of the solid phase present, is placed in a constant temperature bath. It is introduced at a higher temperature than that of the bath itself, and several days are allowed in order for equilibrium to be established. The thermometer used in this bath was checked with a Bureau of Standards certified thermometer.

A sample of solution is then removed, and its weight and volume determined. For zinc and magnesium fluosilicates a convenient volume is 10 ml., and for ammonium fluosilicate, 25 ml. This sample of unknown solution is placed in a tube of the same size as that containing the prepared solution of known concentration and both tubes are then held in the water-bath, mentioned above as being slightly above 40°. The unknown solution is adjusted to the concentration of the known solution by the addition of distilled water (or, if necessary, by evaporation). These solutions are then at the same concentration when both matched floats are activated by a slight variation in the temperature of the bath.

A temperature variation of a fraction of a degree is sufficient to cause the floats to rise or sink slowly. It is desirable to keep this variation small in order that the direction of motion of the floats can readily be reversed several times during one determination without requiring a great amount of time. Large and rapid temperature variations amounting to several degrees would cause float motion too rapid for accurate comparison and a longer time requirement for changing the temperature of the system.

Results.—The following equation is used for calculating the concentration of the sample

$$x = SD/U$$

where x = per cent. concentration of the unknown solution, S = concentration of the prepared solution, D = weight of unknown solution after dilution to the concentration of the prepared solution, and U = weight of original sample of unknown solution.

Example: Using $MgSiF_6 \cdot 6H_2O$, a 16.66% solution at a temperature of 51° would activate the float.

13.26 g. = wt. of 10 ml. of saturated soln. at 69.4°

39.88 g. = wt. of unknown sol. at 16.66% concn.

$x = 16.66 \times 39.88/13.26 = 50.10\%$ = concn. of $MgSiF_6 \cdot 6H_2O$ at 69.4°

$(50.1/100) \times$ sp. gr. $\times 1000$ = g./l. = 664.4 g./l. at 69.4°

All calculations for magnesium and zinc fluosilicates are based on the hydrated salts which contain six moles of water of crystallization.

Table I gives the solubility of these three salts in per cent. by weight and in grams per liter of saturated solution as obtained by the float method. Each value represents the average of 3 determinations.

TABLE I

SOLUBILITY OF $(NH_4)_2SiF_6$, $MgSiF_6 \cdot 6H_2O$ AND $ZnSiF_6 \cdot 6H_2O$ FROM 1.7 TO 68.3°

	Saturated Solution					
	$(NH_4)_2SiF_6$		$MgSiF_6 \cdot 6H_2O$		$ZnSiF_6 \cdot 6H_2O$	
Temp., °C.	% by wt.	g./l.	% by wt.	g./l.	% by wt.	g./l.
1.7	11.58	126.8	34.83	430.4	51.40	731.8
10.0	14.10	157.0	37.37	464.0	52.96	769.7
18.3	16.74	187.2	39.71	498.4	54.75	795.9
26.7	19.34	217.8	41.76	530.8	56.30	815.0
35.0	21.85	247.8	43.60	560.3	57.67	851.3
43.3	24.20	278.0	45.31	588.5	58.96	879.7
51.7	26.49	307.9	46.94	613.0	60.20	906.6
60.0	28.75	337.8	48.46	637.4	61.40	934.3
68.3	30.91	369.8	49.82	660.0	62.51	962.8

For comparison with previous work the following data are given along with interpolated values from Table I shown in parentheses.

TABLE II

COMPARISON OF SOLUBILITIES REPORTED BY PREVIOUS WORKERS, %

	$(NH_4)_2SiF_6$		
		(5)	
17.5° C.		15.6	(16.48)
	$MgSiF_6 \cdot 6H_2O$		
	(2)	(3)	
0° C.		32.35	(34.31)
20	37.94	36.42	(40.12)
40		40.10	(44.63)
50		44.20	(46.61)
60		47.60	(48.46)
	$ZnSiF_6 \cdot 6H_2O$		
	(2)	(3)	
0° C.		51.35	(50.92)
20	49.94	53.50	(55.06)
40		56.25	(58.45)
60		58.50	(61.40)

Reproducibility of results was ascertained by repeating the determinations for ammonium fluosilicate at several temperatures several months after the original data were obtained. A comparison is given in Table III.

TABLE III

	Original data		Later data	
Temp., ° C.	Sol., %	Sol., g./l.	Sol., %	Sol., g./l.
68.3	30.91	369.8	31.17	368.1
60.0	28.75	337.8	28.82	337.8
26.7	19.34	217.8	19.40	218.2

Acknowledgment.—The authors wish to thank Roger K. Taylor for his suggestion of the float principle and the preparation of the floats for this experiment.

(5) Seidell and Stolba, "Solubilities," 3rd Ed., Van Nostrand Co., New York, N. Y., 1940, p. 1098.

THE THERMODYNAMICS OF IONIZED WATER IN STRONTIUM CHLORIDE SOLUTIONS FROM ELECTROMOTIVE FORCE MEASUREMENTS

BY HERBERT S. HARNED AND THOMAS R. PAXTON

Contribution from the Department of Chemistry of Yale University, New Haven, Conn.

Received December 18, 1952

From measurements of the electromotive forces of suitable cells through the temperature range of 0 to 50°, calculations have been made of: (1) the standard potential of the silver–silver chloride electrode; (2) the ionization constant of water; (3) the activity coefficient of hydrochloric acid in strontium chloride solutions; (4) the ionic activity coefficient function and ionization of water in strontium chloride solutions; (5) the relative partial molal heat content of hydrochloric acid in strontium chloride solutions; (6) the heat of ionization of water; and (7) the heat of ionization of water in strontium chloride solutions.

The ionic activity coefficients, the ionization of water and the related thermal quantities in aqueous lithium, sodium and potassium chloride from 0 to 50° have been computed from electromotive forces of cells without liquid junctions.[1] Cells of the same types

$$H_2|HCl(0.01),\ MCl_2(m)|AgCl\text{-}Ag \qquad (A)$$
$$H_2|M(OH)_2(0.005),\ MCl_2(m)|AgCl\text{-}Ag \qquad (B)$$

containing barium and strontium chloride have been measured by Vance[2] at 25°. A more thorough investigation of the barium chloride system has been carried out by Harned and Geary.[3] We have now extended these measurements to include similar cells containing hydrochloric acid–strontium chloride and strontium hydroxide–strontium chloride solutions.

Experimental Results.—The experimental procedure was carried out in cells of the type and by the method described in detail by Harned and Morrison.[4] The cells were prepared in triplicate for each concentration and used throughout the entire temperature range. The agreement between the three results was usually good. The average deviation from the mean values was 0.03 millivolt for the acid series, and the maximum deviation was 0.07 millivolt. The cells containing the hydroxide yielded somewhat less consistent results. For these, the average deviation was 0.05 millivolt and the maximum deviation was 0.15 millivolt. The cells were first measured at 25°, then at 5° intervals from 0 to 50°, and finally at 25°. The agreement between the initial, middle and final readings at 25° was excellent in the acid series. In the hydroxide series, the electromotive forces showed a tendency to decrease at temperatures above 40° and at high salt concentrations so that the final 25° readings were lower than the initial or middle ones. These discrepancies were reduced by plotting the first-order differences, $E_t - E_{(t-5)}$ against temperature and extending the plot at lower temperatures to 50°. These corrections were of the order of 0.1 to 0.2 millivolt.

The electromotive forces were corrected to one atmosphere hydrogen pressure. The relative vapor pressure lowering due to the presence of the salt is known to vary little with temperature. Therefore, by using values of the vapor pressure at 25° obtained from the isopiestic vapor pressure measurements of Stokes,[5] the standard pressure correction could be made with sufficient accuracy.

It has been shown that electromotive forces of cells of these types vary with temperature according to the quadratic equations

$$E_A = E_{A(25)} + a(t - 25) + b(t - 25)^2 \qquad (1)$$
$$E_B = E_{B(25)} + c(t - 25) + d(t - 25)^2 \qquad (2)$$

Consequently, by the use of these equations, it is possible to express the very voluminous observations in condensed form. This is done by Table I which contains values of the constants of these

TABLE I

ELECTROMOTIVE FORCES OF CELLS A AT 25° AND CONSTANTS OF EQUATION (1) AT DIFFERENT IONIC STRENGTHS

μ	$E_{A(25)}$	$a \times 10^5$	$b \times 10^6$	Δ_{max}	Δ_{ave}
0.01	0.46437	179.0	−2.89	0.04	0.02
.02	.45309	143.6	−2.86	.08	.04
.03	.44568	120.6	−2.83	.04	.02
.05	.43580	90.4	−2.75	.06	.02
.07	.42904	70.2	−2.70	.06	.03
.1	.42170	47.8	−2.64	.06	.03
.2	.40703	6.6	−2.62	.07	.03
.3	.39824	− 18.4	−2.56	.06	.02
.5	.38661	− 49.8	−2.54	.08	.03
.7	.37843	− 72.0	−2.52	.07	.04
1.	.36892	− 96.6	−2.49	.07	.04
2.	.34667	−142.8	−2.13	.07	.03
3.	.32963	−175.6	−1.81	.08	.04

ELECTROMOTIVE FORCES OF CELLS B AT 25° AND CONSTANTS OF EQUATION (2)

μ	$E_{B(25)}$	$c \times 10^6$	$d \times 10^6$	Δ_{max}	Δ_{ave}
0.02	1.07841	264.0	0.46	0.09	0.03
.03	1.05000	168.6	.45	.11	.03
.05	1.02788	93.8	.44	.12	.04
.07	1.01590	53.6	.43	.12	.04
.1	1.00422	13.0	.43	.13	.04
.2	0.98266	− 63.6	.43	.09	.04
.3	.97035	−109.0	.20	.06	.04
.5	.95459	−167.0	.11	.06	.02
.7	.94398	−202.8	.06	.09	.03
1.	.93231	−244.6	− .09	.06	.02
2.	.90741	−326.6	− .33	.03	.02
3.	.89052	−378.8	− .33	.06	.03

(1) H. S. Harned and B. B. Owen, "The Physical Chemistry of Electrolytic Solutions," Reinhold Publ. Corp., New York, N. Y., pp. 481–496, 578–579.

(2) J. E. Vance, *J. Am. Chem. Soc.*, **55**, 2729 (1933).

(3) H. S. Harned and C. G. Geary, *ibid.*, **59**, 2032 (1937).

(4) H. S. Harned and J. O. Morrison, *Am. J. Sci.*, **33**, 161 (1937).

(5) R. H. Stokes, *Trans. Faraday Soc.*, **44**, 295 (1948).

equations. The last two columns list the maximum and average values, Δ_{max}, and Δ_{ave}, of the deviations between the observed and calculated results. The ranges of validity of the equations are from 0 to 50°. The electromotive forces are given in absolute volts.

The Standard Potential of the Silver–Silver Chloride Electrode from Cells of Type A.—The equation for the electromotive force of the cells is

$$E_A = E^0 - \frac{RT}{NF}(\ln m_H m_{Cl} + \ln \gamma_H \gamma_{Cl}) \quad (3)$$

If, as suggested by Hitchcock,[6] the activity coefficient be eliminated by the Debye and Hückel limiting equation with an additional term, $B\mu$

$$\log \gamma_H \gamma_{Cl} = -\nu S\sqrt{2\mu} + B\mu \quad (4)$$

we obtain by rearrangement

$$E_A + \frac{RT}{NF} \ln 10(\log m_H m_{Cl} - \nu S\sqrt{2\mu}) = E^\circ + B'\mu \quad (5)$$

The values of the left side of this equation for the cells containing hydrochloric acid were plotted against the ionic strength, $\mu = 3m_{SrCl_2} + 0.01$ and extrapolated to zero concentration to obtain E_0. The physical constants used were those of Birge.[7] Although the large scale plot required that the extrapolation be made along a slope of appreciable magnitude, uncertainty was reduced by the fact that in nearly every case a straight line could be drawn to within 0.03 mv. of the lower six points.

TABLE II

THE STANDARD POTENTIAL OF THE CELLS AS A FUNCTION OF TEMPERATURE

t	E^0 (ref. 8)	E^0	t	E^0 (ref. 8)	E^0
0	0.23642	0.23652	30	0.21919	0.21908
5	.23400	.23405	35	.21570	.21570
10	.23134	.23137	40	.21207	.21207
15	.22854	.22849	45	.20828	.20833
20	.22558	.22549	50	.20444	.20449
25	.22246	.22239			

Ehlers[8] from the same type of cell containing hydrochloric acid and no salt. The largest difference between the two series of results is seen to be 0.1 mv. This agreement is good but since there is a discontinuity in the composition of the solutions in the present investigation, we have relied on the earlier work in fixing the values of the activity coefficient in the 0.01 M hydrochloric acid solution.

The Activity Coefficient of 0.01 M Hydrochloric Acid in Strontium Chloride Solutions.—The activity coefficient of the acid in the strontium chloride solutions has been computed relative to its value at a given temperature in 0.01 M hydrochloric acid by the well-known relation

$$\log \gamma_{\pm} = \log \gamma_{0.01} + \frac{(E_{0.01} - E_A)NF}{4.606RT} - \frac{1}{2}\log \frac{(2m + 0.01)}{0.01} \quad (6)$$

The values of $\gamma_{0.01}$ selected for this purpose agree very closely with those employed in computing the activity coefficient of hydrochloric acid in other chloride solutions.[9] Table III records these results.

The Ionization Constant of Water.—Cells B containing strontium hydroxide may be employed to determine the ionization constant of water by the following procedure. The thermodynamic mass action constant for the ionization of water, K_w, is expressed by the equation

$$K_w = m_H m_{OH} \frac{\gamma_H \gamma_{OH}}{a_{H_2O}} \quad (7)$$

Elimination of m_H between this equation and equation (3) yields

$$E_B - E^0 + \frac{RT}{NF}\ln \frac{m_{Cl}}{m_{OH}} = -\frac{RT}{NF}\left(\ln K_w + \ln \gamma_H \gamma_{Cl} - \ln \frac{\gamma_H \gamma_{OH}}{a_{H_2O}}\right) \quad (8)$$

By plotting the left side of this equation against μ, an extrapolation to zero concentration may be employed to evaluate K_w since both terms on the right containing the activity coefficients vanish at zero ionic strength. In this calculation, the values of E^0 in Table II obtained in the present investigation were employed. Our determinations of K_w are listed in Table IV where they are com-

TABLE III

THE ACTIVITY COEFFICIENT OF 0.01 M HYDROCHLORIC ACID IN STRONTIUM CHLORIDE SOLUTIONS

μ	0°	10°	20°	25°	30°	40°	50°
0.01	0.906	0.905	0.905	0.904	0.904	0.902	0.900
.02	.876	.875	.874	.874	.872	.870	.867
.03	.855	.854	.853	.852	.851	.849	.846
.05	.827	.826	.824	.824	.822	.819	.816
.07	.807	.807	.806	.805	.803	.799	.795
.1	.789	.788	.785	.785	.783	.779	.774
.2	.752	.752	.749	.746	.745	.740	.733
.3	.734	.732	.729	.726	.724	.718	.712
.5	.718	.715	.711	.708	.705	.698	.692
.7	.714	.710	.705	.702	.700	.692	.683
1.0	.721	.718	.710	.709	.705	.695	.689
2.0	.796	.788	.779	.772	.767	.752	.738
3.0	.915	.903	.889	.877	.869	.850	.829
$\Delta\gamma$	.00068	.00064	.00061	.00059	.00057	.00055	.00052

As an indication of the accuracy of these measurements values of E^0 so determined are compared in Table II with the results obtained by Harned and

(6) D. I. Hitchcock, *J. Am. Chem. Soc.*, **50**, 2076 (1928).

(7) R. T. Birge, *Rev. Modern Phys.*, **13**, 233 (1941).

(8) H. S. Harned and R. W. Ehlers, *J. Am. Chem. Soc.*, **54**, 2179 (1932).

(9) Ref. 1, p. 575.

pared with results previously obtained from cells with liquid junction containing other salts.[10] The close agreement between the two series of results over most of the temperature range confirmed our confidence in the general validity of the present series of measurements.

TABLE IV

THE IONIZATION CONSTANT OF WATER

(P = 1 ATM.)

t	$K_w \times 10^{14}$	$K_w \times 10^{14}$ (ref. 1)	t	$K_w \times 10^{14}$	$K_w \times 10^{14}$ (ref. 1)
0	0.1135	0.1139	30	1.462	1.469
5	.1847	.1846	35	2.084	2.089
10	.2923	.2920	40	2.918	2.919
15	.4521	.4505	45	4.012	4.018
20	.6808	.6809	50	5.450	5.474
25	1.008	1.008			

The Ionic Activity Coefficient Function of Water in Strontium Chloride Solutions.—Rearrangement of equation (8) yields

$$E_B - E^0 + \frac{RT}{NF}\left(\ln \frac{m_{Cl}}{m_{OH}} + \ln K_w + \ln \gamma_H^\circ \gamma_{Cl}^\circ\right) = \frac{RT}{NF} \ln \frac{\gamma_H \gamma_{OH}}{a_{H_2O}} \quad (9)$$

which may be employed to compute the ionic activity coefficient function of water, $\gamma_H\gamma_{OH}/a_{H_2O}$, in the strontium chloride solutions. In this equation $\gamma_H^\circ\gamma_C^\circ$ represents the activity coefficient of hydrochloric acid at zero concentration in a strontium chloride solution of ionic strength, μ. Since the logarithm of the activity coefficient of the acid varies linearly with its concentration in these solution mixtures of constant total ionic strength,[11] the values of the mean activity coefficient γ^0 at zero concentration may be calculated by the equation

$$\frac{1}{2}\log \gamma_H^0\gamma_{Cl}^0 = \log \gamma^0 = \log \gamma_{0.0} - \frac{0.01}{\mu - 0.01}(\log \gamma_\mu - \log \gamma_{0.01}) = \log \gamma_{0.01} - \Delta\gamma \quad (10)$$

where γ_μ applies to pure hydrochloric acid at the concentration μ, and log $\gamma_{0.01}$ (Table III) and log γ^0 apply to hydrochloric acid in the salt solutions of the same ionic strength. The values of $\Delta\gamma$ are given at the bottom of Table III.

For this calculation we have employed the values of E_B computed by equation (2), $\gamma_H{}^0\gamma_{Cl}{}^0$ calculated from the data in Table III by equation (10) E^0 (ref. 8) from Table II and K_w (ref. 1) from Table IV. The results are recorded in Table V.

From these results the dissociation of water, $(m_H m_{OH})^{1/2}$, in strontium chloride solutions may be readily calculated by means of equation (7).

The Relative Partial Molal Heat Content of Hydrochloric Acid in Strontium Chloride Solutions.—The temperature variation of the electromotive forces of the acid cells (A) may be used to calculate the partial molal heat content of 0.01 M hydrochloric acid in the salt solutions relative to its value in the absence of salt by calculating the temperature derivative of the voltage difference $E_A(\mu) - E_A(0.01)$, followed by substitution in the

(10) Ref. 1, p. 485.

(11) Ref. 1, p. 457ff.

TABLE V

THE IONIC ACTIVITY COEFFICIENT FUNCTION OF WATER IN STRONTIUM CHLORIDE SOLUTIONS

μ	0°	10°	20°	25°	30°	40°	50°
0.02	0.755	0.749	0.746	0.744	0.748	0.740	0.737
.03	.714	.709	.705	.704	.706	.698	.695
.05	.660	.654	.650	.648	.650	.642	.637
.07	.622	.616	.611	.610	.611	.603	.597
.1	.581	.574	.573	.569	.568	.560	.554
.2	.499	.493	.489	.484	.484	.475	.466
.3	.452	.447	.442	.436	.437	.425	.416
.5	.400	.394	.388	.384	.381	.368	.360
.7	.370	.363	.357	.353	.349	.338	.328
1.0	.343	.339	.331	.328	.324	.311	.301
2.0	.317	.312	.304	.298	.294	.278	.264
3.0	.323	.316	.307	.301	.295	.277	.261

Gibbs–Helmholtz equation. In terms of the quantities in equation (1)

$$\frac{\Delta H}{NF} = [298.16(a(\mu) - a(0.01)) - (E^\mu_{A(25)} - E^{0.01}_{A(25)})] + 596.32(b(\mu) - b(0.01)) - (b(\mu) - b(0.01))(t - 25)^2 \quad (11)$$

is obtained which reduces to the form

$$\bar{H}_\mu - \bar{H}_{0.01} = \bar{L} = \bar{L}_{(25)} + \alpha(t - 25) + \beta(t - 25)^2 \quad (12)$$

The constants of this equation at designated values of the ionic strength are compiled in Table VI.

TABLE VI

THE RELATIVE PARTIAL MOLAL HEAT CONTENT OF 0.01 M HYDROCHLORIC ACID IN STRONTIUM CHLORIDE SOLUTIONS

$$\bar{L} = \bar{L}_{(25)} + \alpha(t - 25) + \beta(t - 25)^2$$

μ	$\bar{L}_{(25)}$, cal.	α	$\beta \times 10^3$
0.02	16.8	0.4	0.7
.03	29.5	0.8	1.4
.05	49.3	1.8	3.0
.07	66.4	2.3	3.9
.1	81.6	3.0	5.1
.2	136.5	3.9	6.5
.3	167.2	4.4	7.4
.5	219.5	4.8	8.1
.7	255.3	5.2	8.8
1.0	305.5	5.9	9.9
2.0	500.6	10.0	16.8
3.0	668.0	15.3	25.6

The Heat of Ionization of Water in Strontium Chloride Solutions.—The heat of ionization of pure water, ΔH_i^0, may be obtained from values of its ionization constant by the van't Hoff equation

$$\Delta H_i^0 = RT^2 \frac{\partial \ln K_w}{\partial T} \quad (13)$$

The partial molal heat content of ionized water in the salt solutions relative to its value in pure water may be derived from the expression

$$\bar{L}_{H^+,OH^+} = -RT^2 \frac{\partial \ln \gamma_H \gamma_{OH}}{\partial T} \quad (14)$$

Also, the partial molal heat content of the undissociated water in the chloride solutions relative to its value in the absence of salt is given by

$$\Delta\bar{H}_w = -RT^2 \frac{\partial \ln a_w}{\partial T} \quad (15)$$

By combining the last three equations, the total

heat of ionization in the salt solutions, ΔH_i, may be expressed by the equation

$$\Delta H_i = RT^2\left(\frac{\partial \ln K_w}{\partial T} - \frac{\partial \ln \gamma_H\gamma_{OH}}{\partial T} + \frac{\partial \ln a_w}{\partial T}\right) \quad (16)$$

If equations (3) and (8) are combined

$$E_B - E_A = -\frac{RT}{NF}(\ln K_w - \ln\frac{\gamma_H\gamma_{OH}}{a_w} - \ln m_H m_{Cl}\frac{m_{OH}}{m_{Cl}} - \ln \gamma_H^0\gamma_{Cl}^0 - \ln \gamma_{H(0.01)}\gamma_{Cl(0.01)}) \quad (17)$$

which upon substitution in the Gibbs–Helmholtz equation becomes

$$\Delta H_i = RT^2\left(\frac{\partial \ln K_w}{\partial T} - \frac{\partial \ln \gamma_H\gamma_{OH}/a_w}{\partial T} + 2\frac{\partial \Delta\gamma}{\partial T}\right) \quad (18)$$

where $\Delta\gamma$ has the significance assigned to it in equation (10). From the values in Table III this latter quantity may be expressed by

$$\Delta\gamma = 0.00068 - 3.2 \times 10^{-6}t \quad (19)$$

The corresponding contribution to ΔH_i is about four calories which may be considered negligible. Therefore equation (18) reduces to equation (16).

According to equations (1) and (2) and the fundamental thermodynamic expression

$$\Delta H_i = -NFT^2\frac{\partial(E_B - E_A)/T}{\partial T} \quad (20)$$

$$\Delta H_i = \Delta H_{i(25)} + A(t - 25) + B(t - 25)^2 \quad (21)$$

in which

$$\Delta H_{i(25)} + NF[E_{B(25)} - E_{A(25)} - 298.16(c - a)] \quad (22)$$

$$A = -596.32(d - b)(t - 25) \quad (23)$$

$$B = -(d - b) \quad (24)$$

in terms of constants in Table I. Values of $\Delta H_{i(25)}$, A and B at various salt concentrations are recorded in Table VII.

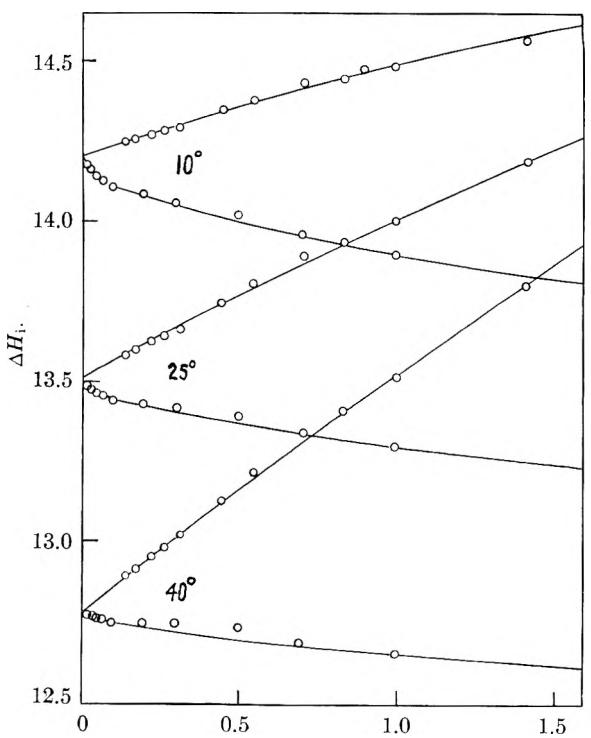

Fig. 1.—The heat of ionization of water in kilocalories in strontium chloride solutions at 10, 25 and 40°. Upper curves represent plots of ΔH_i computed by equation (21), *versus* $\mu^{1/2}$. Lower curves represent plots of the left side of equation (27) *versus* μ.

TABLE VII

THE HEAT OF IONIZATION OF WATER IN STRONTIUM CHLORIDE SOLUTIONS ACCORDING TO EQUATION (21)

μ	$\Delta H_{i(25)}$	$-A$	$-B$
0.02	13588 (cal)	45.7	0.077
.03	13601	45.1	.076
.05	13626	44.1	.074
.07	13643	43.5	.073
.1	13667	42.6	.071
.2	13752	40.7	.068
.3	13811	38.9	.065
.5	13899	36.6	.061
.7	13936	34.9	.059
1.0	14005	32.6	.055
2.0	14190	25.6	.043
3.0	14327	19.3	.032

In Fig. 1, the heat of ionization calculated by equation (21) is plotted against the square root of the ionic strength at 10, 25 and 40°. The heat of ionization of pure water ΔH_i^0 is the intercept at zero concentration.

An alternative extrapolation may be derived from the limiting equation of the Debye and Hückel theory plus a linear term

$$\Delta\overline{H}_i = S\mu^{1/2} + k\mu \quad (25)$$

Upon substitution in the equation for the total heat of ionization

$$\Delta H_i = \Delta H_i^0 + \Delta\overline{H}_i \quad (26)$$

the equation

$$(\Delta H_i - S\mu^{1/2}) = \Delta H_i^0 + k\mu \quad (27)$$

is obtained. The lower curves in Fig. 1 represent the plot of the left side of this equation against the ionic strength.

The two methods of extrapolation supplement each other, for at high temperatures where the slope obtained by the square-root plot is greatest, the plot of equation (27) is the least and, on the other hand, at low temperatures, the square-root plot is the more reliable. The values of the heat of ionization of pure water ΔH_i^0 (in calories) obtained from these extrapolations, are listed in Table VIII. The differences between these results and

TABLE VIII

THE HEAT OF IONIZATION OF PURE WATER IN CALORIES

$\Delta = \Delta H_i^0$ (obs.) $- \Delta H_i^0$ (calcd. by eq. (28)).

t	ΔH_i^0	Δ
0	14645	− 9
5	14435	+ 6
10	14198	− 4
15	13980	+ 7
20	13744	+ 2
25	13520	+11
30	13272	− 2
35	13025	−12
40	12768	−31
45	12525	−33
50	12275	−41

those calculated by the equation of Harned and Robinson[12]

$$\Delta H_i^0 = 23984.15 - 23.4977T - 0.039025T^2 \quad (28)$$

(12) H. S. Harned and R. A. Robinson, *Trans. Faraday Soc.*, **36**, 973 (1940). See also H. S. Harned and B. B. Owen, ref. (1), p. 492.

are shown by the table. Throughout the entire range of temperatures the agreement is good, and from 0 to 35° where the electrodes were found to be most stable, the deviations are less than 0.1%. This fact is excellent confirmation of the accuracy and consistency of the present results as well as the earlier determinations by means of cells without liquid junctions containing hydrochloric, hydrobromic acids and other alkali and alkaline earth halides.

NEUTRON DIFFRACTION STUDIES ON SCANDIUM ORTHOVANADATE AND SCANDIUM OXIDE[1]

BY W. O. MILLIGAN,[2] AND L. W. VERNON

The Rice Institute, Houston, Texas

H. A. LEVY AND S. W. PETERSON

Chemistry Division, Oak Ridge National Laboratory, Oak Ridge, Tenn.

Received December 19, 1952

Examination of $ScVO_4$ and Sc_2O_3 by neutron diffraction confirms that these crystals possess the zircon and thallic oxide structures, respectively, and yield the following values for neutron scattering properties of scandium: $f = (1.18 \pm 0.05) \times 10^{-12}$ cm., $\sigma_{coh} = 17.5 \pm 1.5$ barns, $\sigma_s = 24 \pm 2$ barns.

Introduction

Recent X-ray studies[3] on scandium orthovanadate suggest that it possesses the zircon structure and is isomorphous with rare earth orthovanadates,[4] the tetragonal unit cell containing four molecules of $ScVO_4$ with $a_0 = 6.78$ Å. and $c_0 = 6.12$ Å. The oxygen tetrahedra are elongated in the direction of the c-axis with parameters $x = 0.20 \pm 0.01$ and $z = 0.32 \pm 0.01$. In addition to the systematic extinctions characteristic of space group $D_{4h}^{19} - I4/amd$, the X-ray diffraction pattern exhibited a pseudo-extinction in that many reflections with l odd were missing. These pseudo-extinctions were explained by noting that the X-ray scattering amplitudes of V^{5+} and Sc^{3+} are approximately equal; since for l odd the wave diffracted by scandium is out of phase with that diffracted by vanadium, reflections with l odd depend primarily on oxygen scattering and in some cases their intensity is unobservably small.

Since neutron scattering amplitudes are in general quite different from the corresponding X-ray scattering amplitudes, one may expect to detect the missing reflections in neutron diffraction.[5] The coherent neutron amplitude of oxygen is relatively large,[5] 0.58×10^{-12} cm., while that of vanadium is small,[6] -0.048×10^{-12} cm. A value of the coherent neutron amplitude of scandium, not previously reported, is derived in the present study of $ScVO_4$ and is confirmed from data on Sc_2O_3.

Scandium oxide, Sc_2O_3, has been reported to be isotypic with cubic thallic oxide with a lattice constant of 9.79 Å. This structure, belonging to space group $T_h^7 - Ia3$, is described with one parameter u for scandium and three, xyz, for oxygen which are not accurately known for any single oxide possessing this structure. However, the mixed oxide bixbyite, $(Fe, Mn)_2O_3$, has been studied[7] in detail and the parameter values found, $u = -0.030$, $x = 0.385$, $y = 0.145$, $z = 0.380$, lead to reasonable oxygen–oxygen and cation–oxygen distances.

Experimental

The apparatus employed is a neutron diffraction spectrometer similar to that described by Wollan and Shull.[8] In the present work, a monochromatic beam of neutrons of wave length 1.15 A. was obtained by reflection from the (111) face of a single crystal of copper. The wave length and incident beam intensity were determined from the angle and intensity of diffraction from pure nickel powder ($a_0 = 3.517$ Å., coherent scattering cross-section $\sigma_{Ni} = 13.4$ barns, temperature factor from Debye characteristic temperature, 400°K.). The diffracted neutrons were detected by a boron trifluoride proportional counter whose pulses activated a calibrated linear count-rate meter, and the output of the latter was recorded by a Brown potentiometer. The scanning rate was in some measurements 5° per hour and in others 4° per hour. Reproductions of representative observed neutron patterns are given in Figs. 1 and 2. The horizontal trace at the top represents the intensity of the primary monochromatized neutron beam as recorded by means of a separate monitor circuit.

The sample of scandium orthovanadate was prepared as previously described.[3] That of scandium oxide was prepared by ion-exchange methods by Dr. G. E. Boyd and Mr. D. H. Harris of Oak Ridge National Laboratory, and was kindly furnished for this study. The oxide sample was spectroscopically pure. Total neutron cross-sections of both samples were measured by the transmission method.

The total number of diffracted neutrons E_{hkl} in each Bragg reflection was obtained by measuring the areas of the peaks on the chart record with a planimeter. Observed crystal structure amplitudes $|F_{hkl}|$ were obtained by means of the equation

$$E_{hkl} = \left(\frac{I_0 \epsilon l w \lambda^3 V}{8\pi r^2 \omega}\right) \frac{\rho'}{\rho} \frac{N^2}{\sin\theta \sin 2\theta} A j |F_{hkl}|^2$$

in which I_0 represents the incident intensity, ϵ the counting yield of the detector, l, w, ω and r the height, width, angular

(1) Work done in part under the auspices of the AEC.

(2) Research Participant, Oak Ridge Institute of Nuclear Studies.

(3) W. O. Milligan and L. W. Vernon, THIS JOURNAL, **56**, 345 (1952).

(4) W. O. Milligan, L. Merten Watt and H. H. Rachford, Jr., *ibid.*, **53**, 227 (1949).

(5) C. G. Shull and E. O. Wollan, *Phys. Rev.*, **81**, 527 (1951).

(6) S. W. Peterson and H. A. Levy, *ibid.*, **87**, 462 (1952).

(7) L. Pauling and M. D. Shappell, *Z. Krist.*, **75**, 128 (1930).

(8) E. O. Wollan and C. G. Shull, *Phys. Rev.*, **73**, 830 (1948).

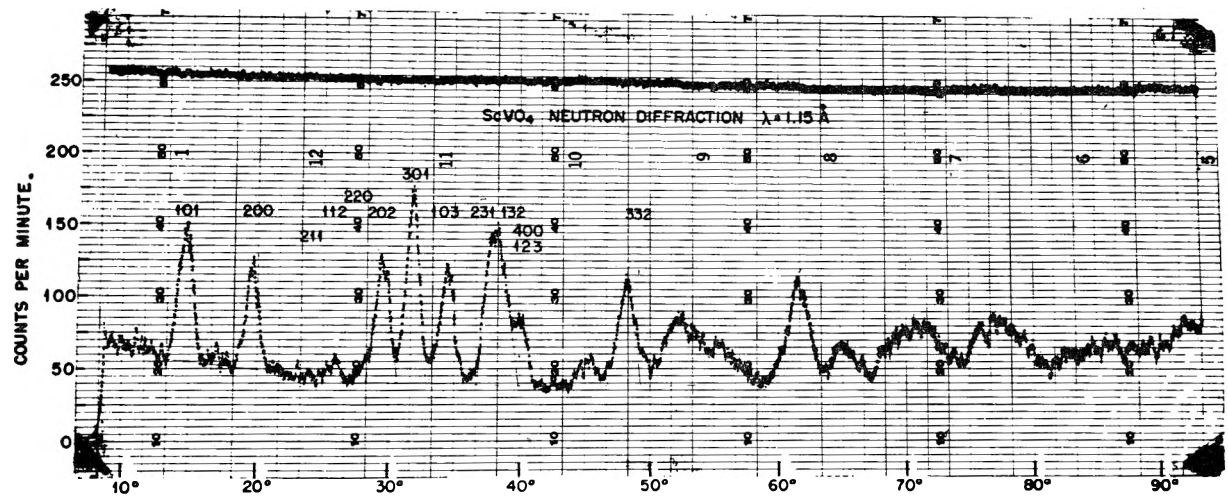

Fig. 1.—Typical neutron diffraction pattern from $ScVO_4$.

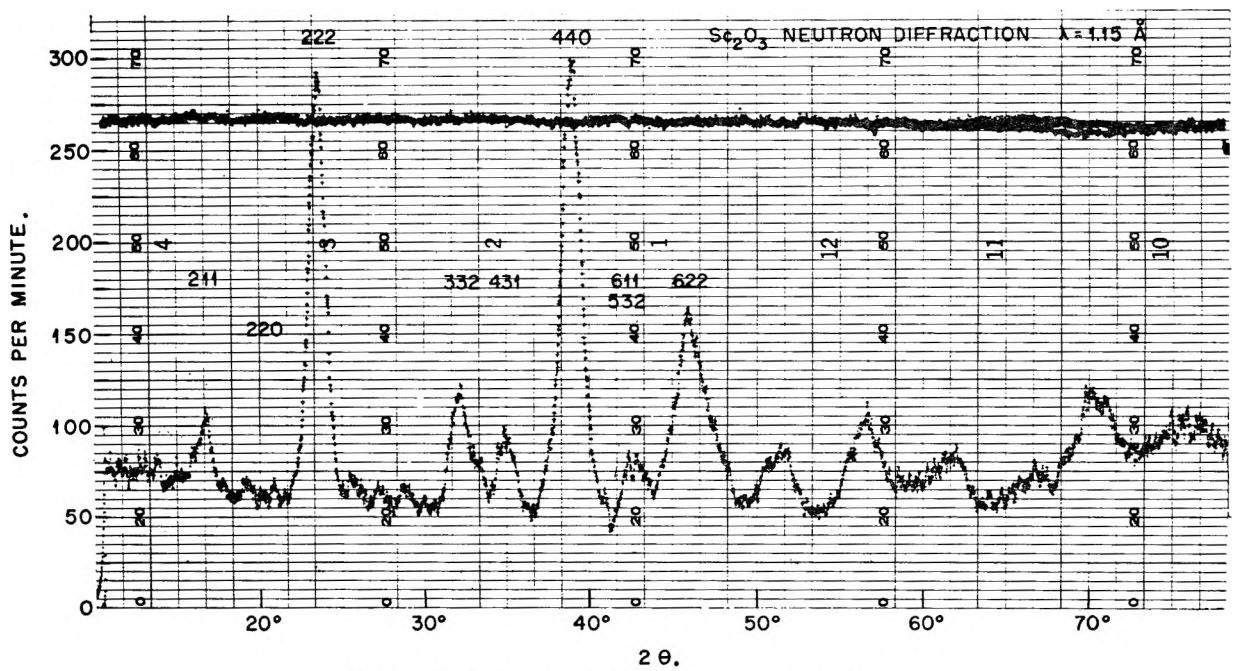

Fig. 2.—Typical neutron diffraction pattern from Sc_2O_3.

velocity and radius travel of the counter slit, V the irradiated volume of the cylindrical sample, ρ' and ρ, respectively, the apparent powder density and crystal density, N the number of unit cells per unit volume of crystal, θ the Bragg angle, A the absorption correction factor and j the multiplicity of the reflection. The quantity in parentheses was determined from the calibration pattern of nickel. Calculated structure amplitudes were given by the equation

$$F_{hkl} = \sum_i f_i \exp(-B \sin^2\theta/\lambda^2) \exp 2\pi i(hx_i + ky_i + lz_i)$$

in which f_i is the scattering amplitude of atom i, $x_iy_iz_i$ are its parameters and B is the Debye–Waller temperature factor coefficient. The amplitude f is related to the coherent scattering cross-section σ_{coh} by the expression $\sigma_{coh} = 4\pi f^2$.

Results and Conclusion

Scandium Orthovanadate.—The total cross-section of the sample was measured to be 78.8 barns; this value was used to determine the absorption correction. Subtraction from this value of the sum of scattering cross-sections of vanadium (5.1) and oxygen (4.2 × 4) and the capture cross-sections for scandium[9] and vanadium (15.0 and 2.9 at λ = 1.15 Å.) leaves 39.0 barns. Of this quantity about 24 barns is shown by the oxide data below to be attributable to total scattering by scandium. The remainder, 15 barns, is probably due to absorption by rare earth impurities; if these are present in the same relative amounts[10] as in natural rare earth deposits, thus value corresponds to about 0.3 atomic per cent.

The diffraction pattern of $ScVO_4$ for neutrons, unlike that for X-rays shows many reflections with l odd. The reflection (202) is strong and well re-

(9) H. S. Pomerance, private communication, has remeasured the capture cross-section of Sc and finds 24 barns. An earlier lower value is believed to be in error.

(10) D. M. Yost, H. Russell and C. S. Garner, "The Rare-Earth Elements and Their Compounds," John Wiley and Sons, Inc., New York, N. Y., 1947.

solved in the pattern, and its intensity is independent of the amplitudes of scandium and vanadium. Its structure amplitude, together with the known scattering amplitude for oxygen and the previously determined oxygen positions, yields the temperature dependence of the oxygen scattering factor. Values of the scattering amplitudes of scandium were then computed from the observed $|F|$ values for the (101), (200), (301) and (103) reflections. It was found that a slight revision of the oxygen parameter x from 0.20 to 0.195 gave improved consistency among the f_{Sc} values; since this is not in disagreement with the X-ray determination this value was used in the final calculations. Figure 3 shows the derived values of the scandium scattering amplitude plotted logarithmically against $\sin^2\theta$. The consistency is seen to be excellent, and the angle dependence, which corresponds to a Debye temperature factor coefficient $B = 0.5$ Å.^{2}, is essentially the same as that of the oxygen scattering. Extrapolation of the best straight line through the data to zero angle yields the values $f_{Sc} = 1.18 \times 10^{-12}$ cm., corresponding to a coherent cross-section of 17.5 barns. The sign of the scandium amplitude is positive, since the scandium and oxygen amplitudes are of like sign. Table I presents observed and calculated squared structure amplitudes; in the latter, temperature corrected oxygen contributions, but uncorrected scandium contributions were used. The satisfactory agreement shows that the structure derived from X-ray data is confirmed. With the revised parameter, the V–O distance is 1.72 Å. and O–O distances within the tetrahedron are 2.64 and 2.89 Å.

TABLE I

NEUTRON DIFFRACTION DATA FROM $ScVO_4$

Indices	$\|F\|^2$, obs.	F^2, calcd.	f_{Sc}
101	12.5 ± 0.3	12.6	1.17
200	30.4 ± 0.7	31.5	1.15
211	1.0 ± 0.5	0.6	
112	6.3 ± 1.4	6.5	
220	8.8 ± 4.0	6.8	
202	38.2 ± 2.5	40.0	
301	73.8 ± 5.5	77.4	1.16
103	63.7 ± 4.3	68.0	1.14

TABLE II

NEUTRON DIFFRACTION DATA FROM Sc_2O_3

Indices	$\|F\|^2$, obs.	F^2, calcd.[a]
211	36 ± 6	36.8
220	2 ± 10	0.2
222	1175 ± 46	1202.0
332	190 ± 29	145.5
431	78 ± 13	56.3
440	2720 ± 94	2820.0

[a] Values include a Debye–Waller temperature correction; see text.

Scandium Oxide.—The total cross-section of the scandium oxide sample was measured to be 90.5 barns; this value was used to correct the diffraction data for absorption. The capture cross-section of the sample was measured by H. S. Pomerance using the pile oscillator method[11] and proved to correspond to 47.8 barns per Sc_2O_3; correction of this value to a neutron wave length of 1.15 Å. yields 30 barns. Subtraction of this value and the scattering cross-section for 3 oxygen atoms (3×4.2) from the total 90.5 leaves 47.9 barns attributable to the scattering cross-section for 2 Sc, or 24.0 barns per atom. Evidently the spin-incoherent scattering cross-section of scandium is about 6 barns.

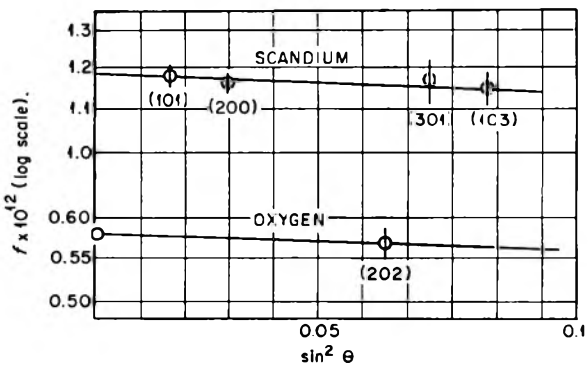

Fig. 3.—Determination of the neutron scattering amplitude of scandium from $ScVO_4$ diffraction data.

Several of the best-resolved neutron diffraction peaks were satisfactorily indexed on the basis of the cubic unit. Packing considerations suggest that the three oxygen parameter values reported for bixbyite should prevail in scandium oxide. Structure amplitudes were calculated for various values of the scandium parameter u and for the scandium coherent scattering amplitude f_{Sc}. Best agreement was found for $u = -0.03 \pm 0.01$, $f_{Sc} = 1.18 \times 10^{-12}$ cm. and the bixbyite oxygen parameters. These parameters lead to reasonable interatomic distances in scandium oxide, the shortest oxygen–oxygen distance being 2.62 Å. and the scandium oxygen distances 2.10 and 2.11 Å. The sum of the crystal ionic radii is 2.15 Å. (Goldschmidt) or 2.21 Å. (Pauling).

A Debye–Waller temperature correction was determined which gave best agreement throughout the pattern; the value of B (see equation 2) is 0.9 Å^2. A comparison of observed and calculated squared structure amplitudes is presented in Table II.

From the results of the two studies, we report the coherent neutron scattering amplitude of scandium to be $(1.18 \pm 0.05) \times 10^{-12}$ cm., positive phase, the corresponding coherent cross-section to be 17.5 ± 1.5 barns, and the total scattering cross-section of scandium to be 24 ± 2 barns.

(11) J. I. Hoover, W. H. Jordan, C. D. Moak, L. Pardue, H. S. Pomerance, J. D. Strong and E. O. Wollan, *Phys. Rev.*, **74**, 864 (1948).

THE DIPOLE MOMENTS OF HYDROCARBONS

BY AUBREY P. ALTSCHULLER

Contributed from the National Advisory Committee for Aeronautics, Lewis Flight Propulsion Laboratory, Cleveland, Ohio

Received December 29, 1952

The dipole moments of some slightly polar aliphatic and aromatic hydrocarbons are calculated by means of the Onsager Equation and a simplified equation. The results are compared with the moments calculated from solution and gas measurements. The agreement among the moments calculated by the Onsager Equation, the simplified equation and from solution measurements is generally satisfactory. The values calculated from gas measurements are higher than those found by the other methods. The ease of application of the simplified equation recommends it for calculation of the moments of hydrocarbons.

Several investigators[1] have calculated the dipole moments of organic liquids by use of the Onsager Equation[2] which may be written in the form

$$\mu_l^2 = \frac{9kT}{4\pi N}\frac{M}{d}\frac{(D - n_\infty^2)(2D + n_\infty^2)}{D(n_\infty^2 + 2)^2} \qquad (1)$$

where μ_l is the dipole moment of the molecule in the liquid state; k is the Boltzmann constant; T is the absolute temperature; N is Avogadro's number; D is the static dielectric constant; n_∞ is the refractive index at infinite wave length; M is the molecular weight; and d is the density.

Böttcher[1a] has suggested that the Onsager Equation might prove useful in calculating the dipole moments of slightly polar liquids where $\mu < 1$ Debye unit. The slightly polar hydrocarbons form a class of compounds which would serve to test Böttcher's suggestion. Calculations of μ for hydrocarbons from the Onsager Equation do not appear to have been made in the literature. One purpose of this investigation is to make such calculations and to compare them with values of the dipole moment calculated by the use of data obtained from solution and gas measurements. While making these calculations it was noted that the expression $[9kTM(2D + n_\infty^2)/4\pi NdD(n_\infty^2 + 2)^2]^{1/2}$ which appears in the Onsager Equation is nearly equal to 1×10^{-18} for hydrocarbons around room temperature; and consequently the simple equation

$$\mu = (D - n^2)^{1/2} \times 10^{-18} \qquad (2)$$

could be employed. The second purpose of this paper is to calculate μ from equation (2) and to compare the values found with equation (1) and the values calculated from the solution and gas measurements.

The quantity most difficult to evaluate in the Onsager Equation and equation (2) is the refractive index. The value of n_∞ as usually evaluated involves the extrapolation of n_∞ from the visible region to infinite wave length. Even when sufficient data at various wave lengths are available, the results of these extrapolations usually include the electronic contributions to the refractive index at infinite wave length,[3] but not the contributions from vibrational modes in the infrared. While these vibrational contributions are of negligible importance when $D \gg n_\infty^2$, they become important when D and n_∞^2 are nearly equal. On the other hand, if the refractive index of the sodium D line is employed, partial allowance is made for contributions from the infrared.[4] Furthermore, the value of n_D is usually the only refractive index available for a compound. It has also been found by the present investigator that when a n which included only electronic contributions was used, the dipole moments calculated for hydrocarbons are too large. In view of these considerations, n_D would appear to more closely approximate n_∞ than would a value of n found by an extrapolation from the visible region to infinite wave length; consequently, n_D has been employed in making calculations from both the Onsager Equation and equation (2).

It can be shown that the moments calculated by means of equation (2) are zero for some completely non-polar compounds, if the dielectric constants measured by Smyth and his co-workers[5,6] for a number of straight and branched-chain alkanes are employed along with the appropriate refractive indices.[7,8]

The probable error in Smyth's dielectric constant measurements is given as $\pm 0.2\%$ or 0.004 of a dielectric constant unit for these hydrocarbons. The values of $D - n^2$ (some of the μ are slightly negative) scatter about zero to about this same magnitude. The straight chain alkanes show an average deviation of 0.003 of a unit, while the branched chain alkanes show an average deviation of 0.004 of a unit. These results indicate that within the experimental error $D - n_D^2$ is zero for these compounds.

The dipole moment as calculated by the Onsager Equation μ_1, the dipole moment calculated from equation (2) μ_2, the dipole moment in solution $\mu_{sol.}$, and in the gas state η_{gas}, are compared in Table I for some aliphatic alkenes and in Table II for some aromatic hydrocarbons. The refractive indices and densities are NBS values[7] except for

(1) (a) C. J. F. Böttcher, *Physica*, **6**, 59 (1939); (b) W. M. Heston, Jr., E. J. Hennelly and C. P. Smyth, *J. Am. Chem. Soc.*, **72**, 2071 (1950); (c) T. L. Jacobs, J. D. Roberts and W. G. MacMillan, *ibid.*, **66**, 656 (1944); (d) S. R. Phadke, S. D. Gokhale, N. C. Phalniker and B. V. Bhide, *J. Indian Chem. Soc.*, **12**, 235 (1945).

(2) L. Onsager, *J. Am. Chem. Soc.*, **58**, 1486 (1936).

(3) A. Weissburger, "Physical Methods of Organic Chemistry," Vol. I, Part II, Second Edition, Interscience Publishers Inc., New York, N. Y., 1949, p. 1150.

(4) *Ibid.*, p. 1623.

(5) R. W. Dornte and C. P. Smyth, *J. Am. Chem. Soc.*, **52**, 3546 (1930).

(6) C. P. Smyth and W. N. Stoops, *ibid.*, **50**, 1883 (1929).

(7) National Bureau of Standards, "Selected Values of Properties of Hydrocarbons," American Petroleum Project 44, NBS Circular C461, United States Government Printing Office, Washington, D. C., 1947.

(8) G. Egloff, "Physical Constants of Hydrocarbons," Vol. I-IV, Reinhold Publ. Corp., New York, N. Y.

the values of pentadiene-1,3 and *p-t*-butyltoluene which come from Egloff[8] and NACA.[9]

The dielectric constants used to calculate the dipole moments μ_1 and μ_2 came in the case of pentene-1 and hexene-1 from the International Critical Tables,[10] while the remainder of the values are given by Farmer and Warren.[11]

TABLE I

DIPOLE MOMENTS OF ALIPHATIC ALKENES

Compound	μ_1, D.	μ_2, D.	$\mu_{sol.}$, D.	μ_{gas}, D.
Pentene-1	0.44	0.44	...	...
Hexene-1	.34	.32	...	...
Pentadiene-1,3	.51	.55	0.50[12]	0.68 ± 0.05[13]
2-Methylbutadiene-1,3	.28	.29	.15[12]	0.38 ± 0.1[13]
2-Methylpentadiene-1,3	.58	.58	.59[12]	...
3-Methylpentadiene-1,3	.56	.57	.53[12]	...
4-Methylpentadiene-1,3	.70	.69	.52[12]	...
2,3-Dimethylbutadiene-1,3	.20	.20	.00[12]	.52 ± 0.07[13]

Good agreement of μ_1 and μ_2 with $\mu_{sol.}$ is found for three of the alkenes listed above. The value of $\mu_{sol.}$ for 4-methylpentadiene-1,3 is much lower than μ_1 or μ_2. The values of μ_1 and μ_2 may be close to the dipole moment of the molecule in the gaseous state. The values of μ_1 and μ_2 for 2-methylbutadiene-1,3 are, within the error due to uncertainty in atomic polarization, equal to the gas value of the moment. The situation in the case of 2,3-dimethylbutadiene-1,3 is curious. The solution value is reported to be zero[12] and both μ_1 and μ_2 are not too far from zero; however, the gas moment[13] is definitely quite far removed from zero. Hannay and Smyth[13] argue that their moment indicates that 2,3-dimethylbutadiene-1,3 is in a *cis* hyperconjugated form with respect to the central double bond. A redetermination of the solution and gas moments of a highly purified sample of this compound would be of interest.

The sources of the densities and refractive indices employed to calculate μ_1 and μ_2 in Table II have already been given.[6,7] The dielectric constant of 1,3,5-trimethylbenzene is given by Müller,[14] while the dielectric constants of 1-methyl-4-ethylbenzene, 1-methyl-4-isopropylbenzene and *p-t*-butylbenzene are taken from an investigation of Le Fèvre, Le Fèvre and Robertson.[15] The remainder of the dielectric constants used in calculating μ_1 and μ_2 come from the International Critical Tables.[10]

The dipole moments calculated by the Onsager Equation and the simplified equation for benzene are in the range from 0.1 to 0.2 Debye unit. On the other hand, the complete symmetry of benzene and the zero moment calculated from measurements in the gas state[6] indicate that benzene is non-polar. Cancellation of dipoles in *p*-xylene and 1,3,5-trimethylbenzene would result in zero moments for these molecules also. The solution moment,[17] μ_1 and μ_2 for these two hydrocarbons have values of 0.1 to 0.2 *D*, while the gas moment for *p*-xylene[18] has been found equal to zero. A difference between *D* and n^2 of only 0.01 unit results in a moment of 0.1*D* by the Onsager Equation or equation (2); consequently, it is quite difficult to distinguish between a moment of zero and one of 0.1 to 0.2 *D*. This is a result of the difficulty in choosing a wholly satisfactory value of n. It is also very hard to tell whether a solution moment is zero or really finite and less than 0.2 *D*. Gas measurements appear to be somewhat more precise although Smyth[19] has stated that even measurements in the vapor state are scarcely capable of distinguishing between 0.0 and 0.1 *D*. The moments of between 0.1 and 0.2 *D*, found by solution measurements and from μ_1 and μ_2 for 1-methyl-4-ethylbenzene and 1-methyl-4-isopropylbenzene combined with the moments of between 0.2–0.3 *D* resulting from the gas measurements indicate that these two molecules may have very small but finite moments. The moments found by the four different methods are in good agreement for *p-t*-butylbenzene with values ranging between 0.35 to 0.40 *D* show that appreciable differences in alkyl group moments may exist.

TABLE II

DIPOLE MOMENTS OF AROMATIC HYDROCARBONS

Compound	μ_1, D.	μ_2, D.	$\mu_{sol.}$, D.	μ_{gas}, D.
Benzene	0.15	0.18	0.0–0.1[16]	0.0[16]
Toluene	.35	.38	.34[15]	.37[17]
Ethylbenzene	.48	.49	...	.58[17]
p-Xylene	.13	.13	.12[16]	.0[18]
o-Xylene	.53	.56	.58[16]	.62[18]
m-Xylene	.36	.36	.39[16]	...
n-Propylbenzene	.39	.37	...	...
Isopropylbenzene	.44	.42	...	.65[16]
1,2,4-Trimethylbenzene	.41	.40	...	...
1,3,5-Trimethylbenzene	.20	.18	...	...
1-Methyl-4-ethylbenzene	.12	.11	.15[15]	.21[17]
1-Methyl-4-isopropylbenzene	.15	.13	.15[15]	.28[17]
t-Butylbenzene	.44	.40	.53[15]	.70[17]
p-t-Butyltoluene	.38	.34	.35[15]	.39[17]

The moments calculated for toluene and *m*-xylene by the various methods employed are in good agreement. The values of μ_1 and μ_2 and the solution moment for *o*-xylene indicate an ortho effect, but the gas value[18] reveals no appreciable effect. If one employs the values of μ_1 and μ_2 for the moments of toluene and *o*-xylene, the moment calculated for 1,2,4-trimethylbenzene is between 0.28 and 0.30 *D*. If the methyl groups in the one

(9) K. T. Serijan, H. F. Hipsher and L. C. Gibbons, *J. Am. Chem. Soc.*, **71**, 873 (1949).

(10) "International Critical Tables," Vol. VI, John Wiley and Sons, Inc., New York, N. Y.

(11) E. H. Farmer and F. L. Warren, *J. Chem. Soc.*, 1297 (1933).

(12) E. H. Farmer and F. L. Warren, *ibid.*, 1303 (1933).

(13) N. B. Hannay and C. P. Smyth, *J. Am. Chem. Soc.*, **65**, 1931 (1943).

(14) F. H. Müller, *Physik Z.*, **38**, 283 (1937).

(15) C. G. Le Fèvre, R. J. W. Le Fèvre and K. W. Robertson, *J. Chem. Soc.*, 480 (1935).

(16) *Trans. Faraday Soc.*, **30** (1934), Appendix A—Table of Dipole Moments, following p. 904.

(17) J. W. Baker and L. G. Groves, *J. Chem. Soc.*, 1144 (1939).

(18) E. C. Hurdis and C. P. Smyth, *J. Am. Chem. Soc.*, **64**, 2212 (1942).

(19) W. M. Heston, Jr., and C. P. Smyth, *ibid.*, **72**, 99 (1950).

and four positions are assumed to cancel each other out, the moment of 1,2,4-trimethylbenzene would be equal to that of toluene 0.35 to 0.38 *D*. The moment found for 1,2,4-trimethylbenzene of 0.40–0.41 *D* agrees better with the result of the second method of calculation. It may well be, however, that the dielectric constant of 1,2,4-trimethylbenzene which was used in the calculations is somewhat higher than the correct value.

The moments calculated from the results of gas measurements show a progressive increase in the series toluene, ethylbenzene, isopropylbenzene and *t*-butylbenzene. The moments resulting from the application of the Onsager Equation or equation (2) are erratic. The moments calculated for the series by means of the Onsager Equation are 0.35, 0.48, 0.44, 0.44 *D* units. While the other moments are greater than the methyl group moment, no further conclusions may be drawn about them, except to note that the moments of ethylbenzene, isopropylbenzene and *t*-butylbenzene are from 0.1 to 0.25 *D* less than those derived from the gas measurements. The dipole moment of ethylbenzene may be anomalously high owing to an incorrect value for the dielectric constant of ethylbenzene.

The average difference between the solution moments and the moments calculated by both the Onsager Equation and equation (2) is 0.07 *D*. All of the other moments are generally lower than the gas moments. The moment calculated by the Onsager Equation or equation (2) is certainly as accurate as the solution moment. Equation (2) gives the moment for hydrocarbons with much less experimental work and calculation than is necessary in order to obtain the moment from solution or gas measurements.

The lower value of the Onsager moment compared to the gas moment may be attributed to the crude approximation of the reaction field given by the Onsager theory and to dipole association.[20] The estimation of the correct value for the reaction field is difficult.[20] The dipole association may take the form of contra-association in the case of the polar hydrocarbons. Hoffman[21] has proposed that the use of an extrapolation of μ_1's found at various temperatures to $1/T = 0$ would give better agreement with the gas moment. He gave some proof of this argument by employing data for alkyl and aryl halides which also show contra-association.[20] Better agreement between the Onsager moment and the gas moment may possibly be obtained for polar hydrocarbons also by this method. Unfortunately, the necessary data over a wide temperature range are not available for hydrocarbons.

(20) J. N. Wilson, *Chem. Revs.*, **25**, 377 (1939).
(21) J. D. Hoffman, *J. Chem. Phys.*, **20**, 740 (1952).

APPARATUS FOR MEASUREMENT OF ELECTRICAL PROPERTIES OF COLLOIDAL SUSPENSIONS IN OILS

BY C. J. PENTHER AND A. BONDI

Shell Development Company, Emeryville, California

Received January 2, 1953

A capacitor cell with rotating inner electrode and sensitive conductimeter are used for measurement of flocculation and deflocculation in non-aqueous systems. The speed of the electrode is controlled steplessly and held constant by a thyratron circuit. The motor load current is proportional to torque and is therefore a measure of viscosity. Conventional oscillator, bridge and null detector are used for dielectric constant and loss measurements over the range 20 c./sec. to 100 kc./sec.

Introduction.—In the development of lubricating oils and greases the need arose to measure the degree of flocculation or deflocculation of colloidal dispersions by a simple, reproducible method. The method used and results obtained are described elsewhere.[1]

Rotary Cell.—Design requirements called for a cell clearance of 0.5 mm., operating temperatures from 30 to 180°, maximum viscosity of 2000 poises at 5 r.p.m. and 500 poises at 500 r.p.m. with shear rates of 5 to 1000 sec.$^{-1}$.

The rotating electrode is 2 cm. in diameter by 10 cm. long and runs in adjustable preloaded ball bearings. The stationary electrode provides a 0.5 mm. clearance and is insulated from the rotor and mounting with a Mycalex flanged hub and four Mycalex skirted washers for the clamping screws.

The cell assembly and drive motor are made as an integral unit. A hub, having an enlarged end to accommodate the stator insulation, is surmounted by a large circular flange which serves to secure the assembly to the bath top and support the motor base plate.

Constant Temperature Bath.—The bath tank is 12.5 in. × 14.5 in. × 9 in. high and is constructed of 16 gage Monel. Three Lo-lag heaters are provided, 200 w. control, 30 w. steady and 500 w. "quick" heat.

The thermoregulator, similar to several described in the literature, uses a nickel resistance thermometer as the temperature sensitive element in an a.-c. bridge circuit having two fixed arms and one variable arm which permits selection of any one of four operating temperatures.

The bridge unbalance voltage is amplified by a two stage amplifier and applied to the grid of a 3D22 thyratron. Throttling control is obtained by applying a quadrature signal obtained by connecting a small capacity (selected by trial) between the thyratron filament and grid.

Drive Motor Speed Control.—This circuit follows the general design of Tuttle[2] and provides a rotor speed range from 5 to 500 r.p.m. Speed is continuously variable through two small panel controls, a coarse and fine adjustment, and is indicated on a meter calibrated in ranges of 0–50 r.p.m. and 0–500 r.p.m. The drop in speed with increasing torque ranges from 3% at maximum speed to 10% at minimum speed over the range no load to full load.

Torque Meter.—By incorporating a milliammeter in the common thyratron anode lead and arranging a local battery circuit so that the no-load current can be "bucked out," the motor control current for different loads can be determined. For this application, for the particular range of

(1) A. Bondi and C. J. Penther, THIS JOURNAL, **57**, 72 (1953).
(2) W. N. Tuttle, *Electronics*, **21**, 106 (1948).

viscosity of the oils under test, the 1/8 h.p. motor was replaced with 1/30 h.p. Bodine Type NSE-11R, 115V AC-DC, 0.43 ampere, 5000 r.p.m., 10:1 gear reduction. While not highly precise, the method serves for a rough check of viscosity. Table A is a listing of anode load current for torques of 640, 1600 and 2400 g. cm. over the speed range 25 to 500 r.p.m. Table B shows the stability of the no-load current over a period of 1.5 hours for the same speed range.

Electronic Multimeter.—Because of the high conductance of the carbon blacks used it was found more convenient to measure the d.c. resistance than dielectric loss factor and this was done with a general purpose multimeter. This instrument is similar to many commercial test instruments but has a range of 0.3 ohm to 50,000 megohms in resistance measurement, from 5×10^{-4} microampere to 5.0 microamperes for current measurement, and from 0.5 to 500 volts for potential measurements. An additional voltage range of 0.5 volt is provided which draws less than 5×10^{-12} ampere in current for use in electrokinetic and in glass-electrode potential measurements.

TABLE A

THYRATRON ANODE LOAD CURRENT, MA.

Speed, r.p.m.	Torque, g. cm. 640	1600	2400
25	16.0	40.0	60
50	16.0	40.0	61.5
100	14.5	39.8	58.5
200	15.3	37.5	56.5
300	14.5	35.3	52.5
400	14.0	35.0	...
500	13.3	34.8	...

TABLE B

THYRATRON NO-LOAD CURRENT, MA.

Speed, r.p.m.	Time, min. 30	60	90
25	26.0	27.0	25.0
50	29.5	28.0	26.8
100	30.5	31.0	28.0
200	33.8	33.8	31.5
300	36.5	...	35.5
400	40.0	37.0	...
500	42.8	40.8	...

FREEZING POINT DIAGRAM AND LIQUID–LIQUID SOLUBILITIES OF THE SYSTEM URANIUM HEXAFLUORIDE–HYDROGEN FLUORIDE[1]

BY GENE P. RUTLEDGE, ROGER L. JARRY AND WALLACE DAVIS, JR.

Carbide and Carbon Chemicals Company, Union Carbide and Carbon Corporation, K-25 Laboratory Division, Oak Ridge, Tennessee

Received January 10, 1953

The complete freezing point diagram for the system uranium hexafluoride–hydrogen fluoride has been determined. In addition, liquid–liquid solubilities of these compounds have been measured up to the consolute temperature of 101°. A miscibility gap starts at 61.2° and extends over the composition range 10 to 80 formula % UF_6. The eutectic temperature of this binary system is −85°. There is no indication of compound formation.

Hydrogen fluoride is a frequent, and sometimes a major, impurity in uranium hexafluoride, either as a result of the method of preparing the latter or as a result of its reaction with water. As described by Katz and Rabinowitch,[2] much effort has been devoted to studies of methods of removing hydrogen fluoride from uranium hexafluoride and to the use of getters that would keep the latter free of the former. These studies, as well as others devoted to methods of analysis of hydrogen fluoride impurity,[2] were not designed to provide complete knowledge of phase equilibria in the binary system uranium hexafluoride–hydrogen fluoride.

The present paper is the first of two designed to present solid–liquid, liquid–liquid and liquid–vapor equilibria of this system over the full composition range and over the temperature range −85° (*i.e.*, the eutectic temperature) to 105° (*i.e.*, above the consolute temperature of 101°). Solid–liquid and liquid–liquid equilibria are presented below. Since previous work on this system has been fragmentary only a few comparisons with the present work are justified.

Experimental

Apparatus.—Three types of apparatus have been used in this study: (1) filter cell; (2) freezing point cell; (3) transparent Fluorothene tube. The filter cell was used to measure solubilities at temperatures of −5 to 25°, in which range thermal effects in the freezing point cell could not be measured. The freezing point cell (Fig. 1), developed from modifications of apparatus of Skau[3] by W. S. Wendolkowski and E. J. Barber of this Laboratory, was used to determine the freezing point diagram of solutions containing 7 to 100 formula % UF_6. The Fluorothene tube used in investigations of liquid–liquid equilibrium was a test-tube type unit, connected to a metal valve through flare fittings and fitted with a thermocouple well extending nearly to its base. This type of tube was also used with solutions containing 2 to 10 formula % UF_6, a range overlapped by the other two units. The filter cell was composed of two Fluorothene tubes connected by Crane HGP valves through a porous nickel filter disc.

Materials.—Uranium hexafluoride used in this work contained less than 0.015 weight % impurity. The vapor pressure[4] at various temperatures was determined frequently to detect any leaks or volatile impurities.

The middle fraction of a commercial tank of hydrogen fluoride was used. This fraction was further purified by the method described by Jarry and Davis.[5] The resulting hydrogen fluoride contained 0.04 ± 0.02 mole % impurity as determined by the procedure of partial melting in an adiabatic calorimeter.[6] A routine check on the dryness of hydrogen fluoride was obtained by condensing some of this material into a Fluorothene tube and then adding a small quantity of uranium hexafluoride. The presence of even minute quantities of water resulted in the formation of a yellow precipitate.

Procedure.—One of the tubes of the filter cell assembly was charged by condensation with a synthetic mixture of hydrogen fluoride and uranium hexafluoride, containing an excess of the latter. The unit was mounted in a low temperature thermostat and rotated overnight at a controlled temperature. An average of several Beckman thermometer readings, taken the last hour before filtering, was used as a measure of the solution temperature. Fluctuations in temperature in the thermostat were less than ±0.05°. After stopping the thermostat rotor so that the charged tube was

(1) This document is based on work performed for the Atomic Energy Commission by Union Carbide and Carbon Corporation at Oak Ridge, Tennessee. Presented at the 123rd National Meeting of the American Chemical Society, Los Angeles, Calif., March 13–19, 1953.

(2) J. J. Katz and E. Rabinowitch, "The Chemistry of Uranium," Part I, "The Element, Its Binary and Related Compounds," McGraw-Hill Book Co., Inc., New York, N. Y., 1951.

(3) E. L. Skau, *Proc. Am. Acad. Arts Sci.*, **67**, 551 (1933).

(4) G. D. Oliver, H. T. Milton and J. W. Grisard, *J. Am. Chem. Soc.*, **75**, in press (1953).

(5) R. L. Jarry and W. Davis, Jr., THIS JOURNAL, **57**, in press (1953).

(6) J. W. Grisard, H. A. Bernhardt and G. D. Oliver, *J. Am. Chem. Soc.*, **73**, 5725 (1951).

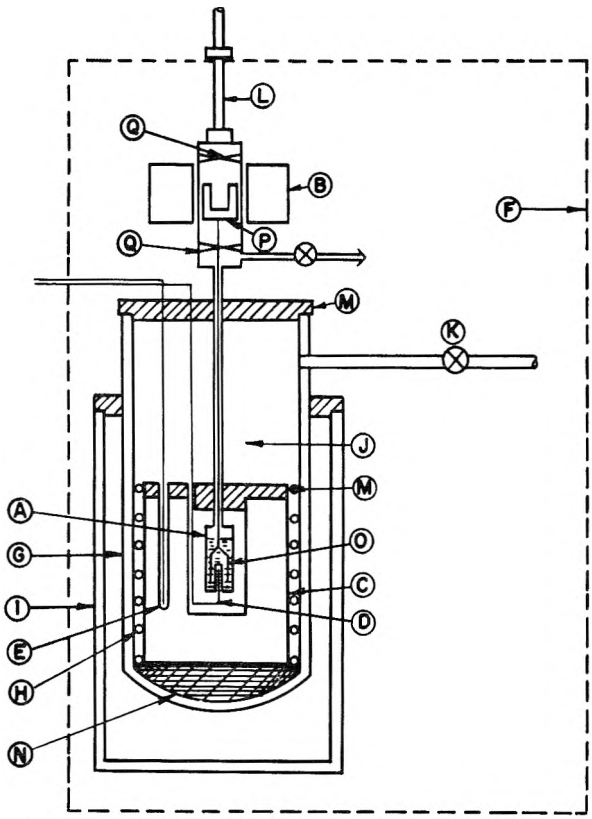

Fig. 1.—Freezing point cell with auxiliary equipment: A, freezing point cell; B, solenoid; C, copper shield; D, cell thermocouple; E, shield thermocouple; F, air thermostat; G, glass dewar; H, nichrome heater coil; I, metal dewar; J, glass wool insulation; K, stopcock leading to vacuum pump; L, cell anchor; M, plastic lids; N, firebrick shield base; O, UF_6 + HF mixture; P, piston of stirrer; Q, nickel rod piston stops.

in an inverted position (the empty one therefore being upright), the valve on this tube was opened to allow solution to pass through the filter disk and into the empty tube. This filtrate was weighed and then analyzed for uranium.

The freezing point cell (Fig. 1) was loaded under vacuum conditions with uranium hexafluoride and the weight determined, using an analytical balance, with an accuracy of ±2 mg. Enough hydrogen fluoride was then added, by liquid nitrogen condensation, to give the desired synthetic mixture. The melting point of a sample of carefully purified uranium hexafluoride was used as a primary standard after the absolute correction of the copper–constantan thermocouple was found to be only about 0.1°. This fixed point temperature was measured by Oliver, Milton and Grisard[4] as 64.02 ± 0.05°. Above 7 formula % UF_6 all freezing temperature measurements were within 5 degrees of this melting temperature.

The melting point of hydrogen fluoride at −83.6° was used as a calibration point for measurements of the uranium hexafluoride–hydrogen fluoride eutectic temperature, which was less than two degrees from this melting temperature. White double and K-2 potentiometers were used in conjunction with the freezing point cell.

In order to determine the temperature at which two liquid layers disappear, forming one homogeneous solution, it was necessary to use a transparent Fluorothene tube. This tube was partially filled with weighed quantities of the two chemicals and heated in an air thermostat, with manual shaking of the mixture, until the two layers disappeared. Temperature was measured by use of a calibrated copper–constantan thermocouple and a K-2 potentiometer. The major source of error arose from the difficulty of seeing exactly when the two layers disappeared or reappeared. Errors involved in this method amount to as much as ±2°.

Results and Discussion

The data obtained are given in Table I and are plotted in Fig. 2. The inset in Fig. 2 gives in more detail the region of low hydrogen fluoride concentration which is of value for analytical determinations. It should be kept in mind that all of this work was done in the absence of foreign gases and

TABLE I

EXPERIMENTAL DATA FOR THE FREEZING POINT DIAGRAM AND LIQUID–LIQUID SOLUBILITIES OF THE SYSTEM URANIUM HEXAFLUORIDE–HYDROGEN FLUORIDE[a]

Formula % UF_6	Eutectic t, °C.	Freezing t, °C.	Miscibility gap t, °C.	Formula % UF_6	Eutectic t, °C.	Freezing t, °C.	Miscibility gap t, °C.
0.00		−83.6		10.38			69
.16		− 5.0		11.92		60.96	
.24		− 5.1		12.20			78
.27		− 5.0		16.29			83
.32		− 5.2		19.85			87.9
.41		− 5.0		23.39			90.3
.45		0.0		24.52		61.16	
.48		− 0.1		28.58			97.2
.781		5.0		29.13			93.2
.98		25.0		39.38			98.8+
1.593		26.5		49.97			100.5
3.04		44.3		53.14			99.9
3.93		50		53.53	−85.13		
4.20		52		55.02		61.14	
5.39		55		55.40			95.7
6.24		55		56.77		61.25	
6.67		59.12		57.09			95
6.90	−84.18			58.45			98
7.95		58		61.35			90.5
8.32		60.25		62.03			93.5
8.51		59		64.49			87.5
9.45		60.55		65.21	−85.06		
10.28			69	66.70			83

TABLE I (*Continued*)

Formula % UF_6	Eutectic *t*, °C.	Freezing *t*, °C.	Miscibility gap *t*, °C.	Formula % UF_6	Eutectic *t*, °C.	Freezing *t*, °C.	Miscibility gap *t*, °C.
67.13			84.0	91.09		62.3	
69.35			79.5	94.15		62.45	
70.44		61.18		95.06	−85.10		
72.54		61.25		95.77		62.51	
72.96			76	96.47		62.39	
81.56		61.32		96.47		62.53	
82.03	−85.10			98.45		63.09	
83.06	−84.99			99.63		63.76	
87.73		61.56		100.00		64.02	
90.46		61.95					

[a] Experimental information on the individual measurements may be obtained by using this table with Fig. 1.

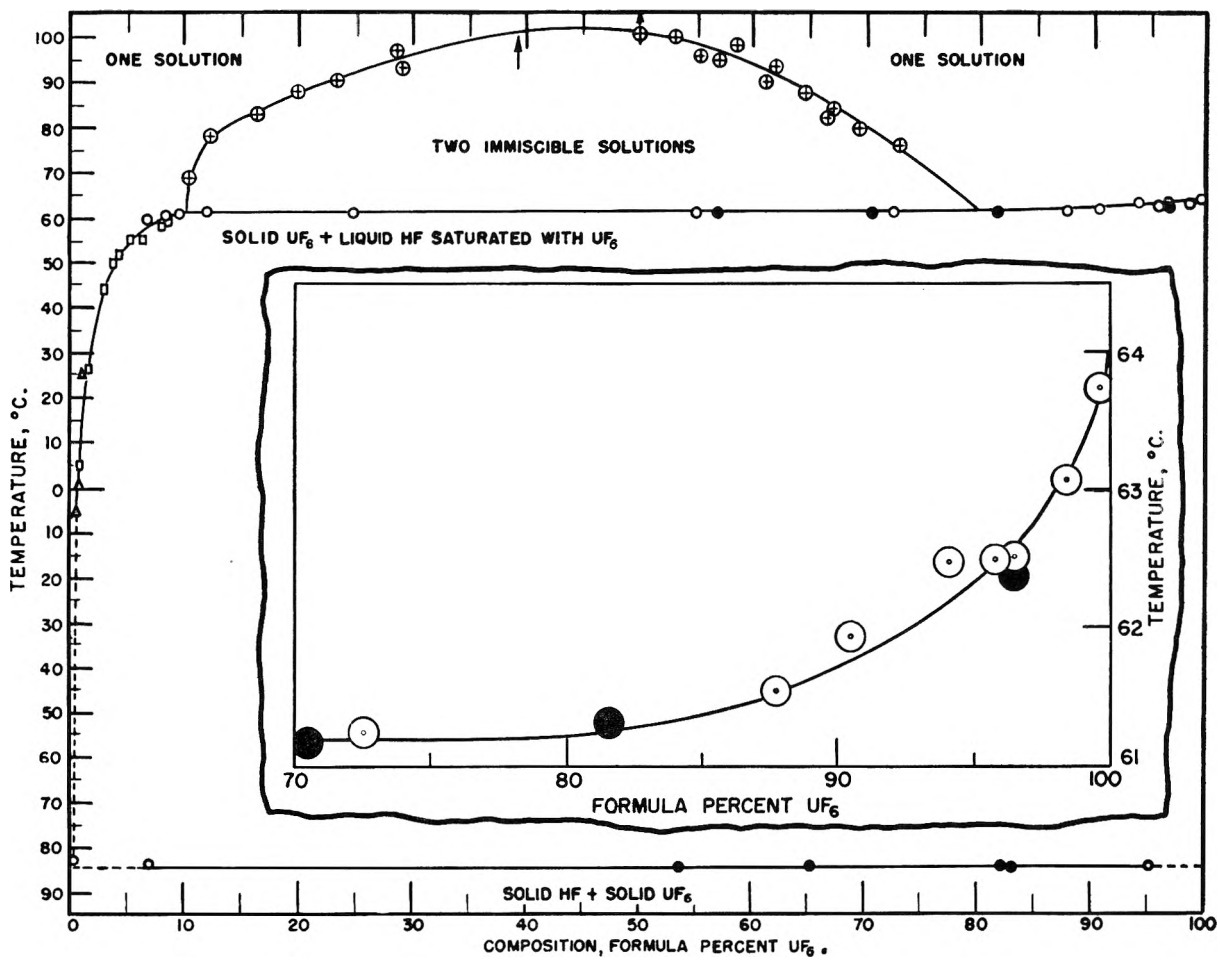

Fig. 2.—Phase diagram of the binary system: UF_6–HF. ⊕, visual observation of disappearance of two liquid layers; □, visual observation of precipitation of solid UF_6; Δ, filter cell; ○, freezing point cell—K-2 Potentiometer; ● freezing point cell—White Potentiometer; ↑, rupture of Fluorothene tube.

that pressures were not atmospheric, but the normal vapor pressures of the binary mixtures at given temperatures.

It should be noted that data are presented in terms of formula %; the term "mole %" cannot be used since the variation of the degree of polymerization of hydrogen fluoride in these solutions was not determined. In addition, differences in liquid and vapor compositions necessitated correction of some synthetic composition values. These corrections were important in the present work only in the region 80 to 100 formula % UF_6 and were made by use of data soon to be published.[7]

Katz and Rabinowitch[2] have reported, from Manhattan Project literature, a cryoscopic constant of 0.065° per 0.01 mole % hydrogen fluoride, as contrasted with an ideal value of 0.0839°. Within experimental error, the present data indicate ideal solubility from 0–2.5 formula % hydrogen fluoride. From recent vapor pressure data[4] on uranium hexa-

(7) R. L. Jarry, F. D. Rosen, C. F. Hale and W. Davis, Jr., THIS JOURNAL, unpublished.

fluoride, a cryoscopic constant of 0.0828° per 0.01 formula % hydrogen fluoride may be calculated.

In contrast to earlier statements,[2] it should be noted from Fig. 2 that hydrogen fluoride is very soluble in uranium hexafluoride, to the extent of about 20 formula % at 61.2° (at one end of the miscibility gap), or even 90 formula % (if uranium hexafluoride is considered as solvent at the other end of the miscibility gap). As the solution temperature is increased to 101° complete miscibility is obtained.

Calculations of activity coefficients indicate large positive deviations from ideality as the concentration of hydrogen fluoride increases above 2.5 formula %. Below 61.2° solubilities are much lower than ideal values, evidently as a result of large difference in the "cohesive energy densities" of the two compounds. Above the four phase invariant temperature of 61.2° uranium hexafluoride and hydrogen fluoride exhibit a miscibility gap with a consolute temperature of about 101°. At about 100° and, therefore, over 10 atmospheres pressure Fluorothene tubes begin to get soft; in two experiments they ruptured. As a result few measurements were made above 98°. Although no experiment was performed with a mixture having the maximum temperature of incomplete miscibility, it is probable that the interpolated value of the consolute temperature 101° is accurate within ±2°. Compositions of the two immiscible solutions at 61.2° are approximately 10 and 80 formula % uranium hexafluoride. Measurements over the composition range 6.9 to 95 formula % uranium hexafluoride have shown a single binary eutectic at −85°.

Acknowledgments.—Grateful acknowledgment is given to E. J. Barber for his many helpful comments and suggestions during the course of this work, to G. D. Oliver and J. W. Grisard for determining the purity and triple point of hydrogen fluoride, and to W. S. Wendolkowski for loan and aid in use of the White double potentiometer and auxiliary apparatus.